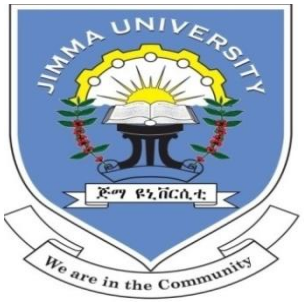

JIMMA UNIVERSITY
SCHOOL OF GRADUATE STUDIES
JIMMA INSTITUTE OF TECHNOLOGY

FACULTY OF CIVIL AND ENVIRONMENTAL ENGINEERING
CHAIR OF HYDROLOGY AND HYDRAULIC ENGINEERING

Impact of Climate Change on Flood Frequency of Guder Watershed, Upper Abay River Basin, Ethiopia

By: Girma Wagi Gobote

A Thesis submitted to the School of Graduate Studies of Jimma University, Jimma Institute of Technology in Partial Fulfillment of the requirements for the Degree of Masters of Science in Hydraulic Engineering

October, 2021

Jimma, Ethiopia

JIMMA UNIVERSITY
SCHOOL OF GRADUATE STUDIES
JIMMA INSTITUTE OF TECHNOLOGY
FACULTY OF CIVIL AND ENVIRONMENTAL ENGINEERING
CHAIR OF HYDROLOGY AND HYDRAULIC ENGINEERING

Impact of Climate Change on Flood Frequency of Guder Watershed, Abay River Basin, Ethiopia

By: Girma Wagi Gobote

A Thesis submitted to the School of Graduate Studies of Jimma University, Jimma Institute of Technology in Partial Fulfillment of the requirements for the Degree of Masters of Science in Hydraulic Engineering

Main advisor: Dr. Dawud Temam (Ph.D.)
Co-advisor: Mr. Seife Belete (MSc.)

October, 2021
Jimma, Ethiopia

DECLARATION

I hereby declare that I am the sole author of this thesis on the Impact of Climate Change on Flood Frequency of Guder Watershed is entirely original work and all other materials are duly acknowledged. This work has not been submitted for any academic degree award at any University.

Girma Wagi _____ _____

Signature Date

This thesis has been submitted for examination with our approval as thesis advisor.

Advisor: Dr. Dawud Temam (Ph.D.)

_____ _____

Signature Date

Co-advisor: Mr. Seife Belete (MSc.)

_____ _____

Signature Date

APPROVAL

The thesis entitled "**Impact of Climate Change on Flood Frequency of Guder Watershed, Upper Abay River Basin, Ethiopia**" submitted by Girma Wagi Gobote is approved and accepted as a Partial Fulfillment of the Requirements for the Degree of Masters of Science in Hydraulic Engineering at Jimma Institute of Technology.

	Signature	Date
Dr. Dawud Temam (Ph.D.) (Main Advisor)	_____	_____
Mr. Seife Belete (MSc.) (Co-advisor)	_____	_____

As members of the Examining board of MSc. thesis, we certify that we have read and evaluated the thesis prepared by Girma Wagi Gobote. We recommend that the thesis could be accepted as a Partial Fulfillment of the Requirements for the Degree of Masters of Science in Hydraulic Engineering.

		Signature	Date
External Examiner	Dr. Adane Ababe(Ph.D.)	_____	_____
Internal Examiner	Tadele Shiferaw (MSc.)	_____	_____
Chairman	Walabuma Oli (MSc.)	_____	_____
Chair holder	Nasir Gebi (MSc.)	_____	_____

ABSTRACT

Climate change is a global concern as one of the most challenging and threatening issues of the 21st century to the world devastating natural hazards, which can significantly damage human lives and properties. This study examined the Impact of Climate change on Flood frequency in the Guder watershed in upper Abay river basin of Ethiopia. For the future, CORDEX-Africa data output of three RCMs under RCP 4.5 and RCP 8.5 climate scenarios were predicted for two horizons time (2041-2070) and (2071-2100) as the mid-term and the long-term respectively with a baseline period of (1971-2000). The three RCMs model performances were evaluated in terms of BIAS, RMSE and R^2 evaluation criteria, how the RCMs perform in simulating the rainfall. In terms of BIAS, and RMSE the RCA4 model performed best whereas the CCLM4-8 model performed poorest. The biases of climate variables were removed by Delta change and Variance Scaling for precipitation and temperature respectively. Non-parametric Mann-Kendall test was carried out to detect trends of observed and future projected climate variables. The result of MK test shows; the future precipitation shows increase trend. HEC-HMS Model was used to simulate future daily stream flow data in both time horizons to checking model performance. The R^2 and Nash- Sutcliffe Efficiency (NSE) values for the Watershed were 0.76 and 0.73 for calibration and 0.79 and 0.76 for the validation respectively shows good performance of the model. Flood frequency analysis considering the GEV distribution, AM data series, and the Maximum likelihood method for parameter estimation was selected based on goodness of fit. The future flood in different time horizons under dominant RCP's will expected to increase for 2, 5, 10, 25, 50, 100, 200 and 1000 return periods. The quantile estimated from observed and simulated discharge for three RCMs in both terms of Guder watershed indicated that RACMO22T for both terms of RCP4.5 and RCP8.5 revealed high quantile estimates. In the future, the change of flood magnitude for CCLM4-8 and RACMO22T in AM series by GEV show increasing in all return periods under RCP4.5 and RCP8.5 of both terms by 1.2 %and 1.4% respectively. But RCA4_RCP8.5 mid-term of return period shows decrease with magnitude of -0.3% while RCA4_RCP4.5 long-term is increased. The magnitude change of analysis shows increasing future Flood frequency in dominant RCP scenarios for both mid-term and long-term periods.

Keywords: Climate Change; CORDEX; Guder Watershed, HEC-HMS; RCMs; Flood frequency

ACKNOWDLEGMENT

Beyond all, I would like to thank the Almighty God for giving me his priceless help, without his assistance, everything is impossible. With great pleasure and a deep sense of indebtedness, I extend my gratitude and appreciation to my advisors Dr. Dawud Temam and Mr. Seife Belete (MSc.) for their persistent, support, constructive guidance and advice throughout the work.

I would like to gratefully acknowledge to Jimma Institute of Technology, Faculty of Civil and Environmental Engineering for providing me the opportunity to study this MSc. Program and the support made to carry out my work. I also thank all my staff members of Hydraulic and Water Resources Engineering Department for the services provided. Finally, yet importantly, I would like to express my very profound gratitude to all my family and friends for providing me with nonstop encouragement throughout my studies.

TABLE OF CONTENTS

LIST OF TABLES

LIST OF FIGURES

ABBREVIATIONS AND ACRONYMS

AMS	Annual Maximum Series
CMhyd	Climate model data for hydrologic modeling
CMIP5	Coupled Model Inter-comparison Project Phase 5
CORDEX	Coordinated Regional Downscaling Experiment
DEM	Digital Elevation Method
FFA	Flood Frequency Analysis
GCM	Global Circulation Model
GHG	Greenhouse gas
GIS	Geographical Information System
GDP	Growth Development Percent
GEV	Generalized Extreme Value
GPD	Generalized Pareto Distribution
HadGEM2-ES	Hadley Center Global Environment Model2 Earth System
HRUs	Hydraulic Reponses Units
HEC-GeoHMS	Hydrologic Engineering Center's Geospatial Hydrological Modeling System
HEC-HMS	Hydrological Engineering Cycle for Hydrological Model Simulation
ITCZ	Inter-Tropical Convergence Zone
IPCC	Inter-Governmental Panel on Climate Change
NAP-ETH	National Adaptation Plan of Ethiopia
POT	Peaks-Over Threshold
RCM	Regional Climate Model
RCP	Representative Concentration pathway
SCS	Soil Conservation Service

1. INTRODUCTION

1.1. Background

Climate change is a global concern as one of the biggest challenges of the 21st century to the whole world will face cause enormous suffering economic and catastrophic environmental damage throughout the world (Yanjuan Wu et al., 2021). The result is increased variability in rainfall intensity in the future, leading to more frequent flooding a substantial loss of lives and it affects many aspects of (Ye Bai et al., 2019). Climate change is the variation in the statistical distribution of average weather conditions over a prolonged period and statistically significant change of climate elements, such as precipitation, temperature, and pressure sustained over several decades or longer in any region of the world (Ibe Go & Amikuzuno J, 2019). Thus, Climate change will result in global warming leads to many changes in climatic conditions which cause extreme weather events like floods and droughts to become more frequent & severe (Ahmad I. et al., 2019).

Global warming is one of the most immediate caused by anthropogenic increases of greenhouse gases concentrations in the atmosphere is associated with climate change around the world (Maikel et al., 2020),would be the changes in the local and regional water availability, extreme weather events since the climate system is interactive with hydrological cycle (Ibe Go & Amikuzuno J, 2019). The hydrological regime change can induce the acceleration of water the cycle, which can consequently affect the frequency and intensity of future storm events. The entire globe has been experiencing surface warming and the evidence for this warming comes from multiple climate system (Ionela Gabriela Bucse et al., 2019).

Greenhouse gases have played a great role in changing the climate change at global as well as regional level causes subsequent global warming and changes the Earth's hydrologic cycle in multiple ways (Shrestha S & Sharma S, 2021). The Earth warming and as global temperatures increase the hydrological cycle is becoming more vigorous (Mahmood Azari et al., 2016)and global average temperature would rise between 1.4 and 5.8°C by 2100 with the doubling of the CO2 concentration in the atmosphere which consequence of rising global temperature (Abeba et al., 2017). This is expected to have a potential impact on level rise, change in precipitation pattern, and change in other different socio-economic sectors (IPCC, 2018).

In the 19th century, progress in science and technology led to the Industrial Revolution. Starting in Great-Britain, industrialization spread first to Europe and then worldwide. Alongside expansion in the industry, transportation, and agriculture, the global population grew rapidly due to progress in urban growth, hygiene and medicine. Together, these factors led to a rapid increase in fossil fuel consumption, and consequently, global greenhouse gas emission and water resource related problems will be of utmost significance throughout the next decades (IPCC Special Report of Global Warming, 2018).

Today, the environmental issue become the biggest concern of mankind because of the increasing of the concentration of greenhouse gas in the atmospheric and the climate change of the earth and recently at global scale temperature is increasing probably cause changes in the region's weather patterns hydrological cycle (Muhammad Shahid Iqbal, 2018). Under the effect of global warming and climate change, there will be more water vapor in the atmosphere, increased capacity of air to accommodate rainfall intensities, intensified hydrological cycle, resulting in increasing the frequency and cause future extreme storm events to occur more frequently (Singh R. et al., 2016).

Climate change is expected to amplify existing stresses on water availability, agriculture and will affect public health (Rangecroft al et., 2018) and manifests itself on different time-scales: through changes like single, short-lived extreme weather events, hurricanes, and through incremental changes that build up over decades, such as sea level rise. These can interact and reinforce one another of extensive flooding due to a storm surge in addition to long-term sea level rise. The intensification of the global water cycle generally causes dry areas to become drier due to increased evaporation and wet areas to become wetter (IPCC Special Report of Global Warming, 2018).

Africa is highly vulnerable continent expose to impacts of climate change has an extensive effect on already daunting challenges facing sustainable development, especially in Sub-Saharan Africa (Ibe Go & Amikuzuno J, 2019) and on water resources in particular of high significance due to the dependence on agriculture as well as their poor financial, technical, and institutional capacity to adapt (Oladayo N.A. and Jonathan T., 2017). Ethiopia is often cited as one of the most vulnerable and with the least capacity to respond and adapt. The direct impact of climate change can be a varied and changing pattern of water resources availability, influence water supply system, power generation, and hydrological extreme events such as floods frequency and the occurrence will lead to severe water shortages or flooding (Belay & Getaneh, 2016).

For a country like Ethiopia, which is vulnerable to climate change and the unpredictability of climate variability is imperative to implement coordinated adaptation measures (Ethiopia's Climate Resilient Green Economy, NAP-ETH, 2019).The Impact may be worse for developing countries like Ethiopia because their economies are strongly dependent on basic forms of natural resources mainly on agriculture and their economic structure is less flexible to adjust to such drastic changes. Agriculture is one of the sectors, which is sensitive to climate change of global warming, most farmers make low crop yields due to the incidents of extreme weather conditions such as high fluctuating rainfall patterns, flooding, droughts, high temperature, and other disparaging weather conditions (Ibe Go & Amikuzuno J, 2019).

Climate change affects multiple deleterious consequences in all regions around the world. The negative effects of climate change on water systems aggravate the impact of other changes expected by specialists such as population growth, changing economic activity, changing land use and urbanization expansion (Fikru et al, 2018). Besides the impact on water availability, climate change also affects the operation of existing water infrastructure (hydropower, hydraulic structures for flood defenses, drainage and irrigation systems) as well as water management practice at local and regional scales under changing climate is a major challenge (M. Caian et.al., 2021).

Generally, the impacts of climate change on water resource availability and the regime of hydrologic extremes have will be alterations in major climate variables changes in stream flow, Flood frequency, and timing of extreme events are one of the most significant consequences of climate change. It is expected that future climate change may exacerbate the level of water stress or increase the water resource across the basin and it is therefore important to assess and manage the potential effects of such changes in the Guder watershed.

1.2. Statement of the Problems

Abay River Basin is critically significant in Ethiopia in terms of large population coverage, massive resources and high potential developments of different projects. One of the basin which has been affected by climate change, as well as catchment characteristics alteration due to the natural or anthropogenic activities, which may lead to extreme event such as flood (Shimelis, 2017). Accordingly, the number of studies that were conducted on the Guder Watershed has the Climate change impact on flow volume was analyzed on a monthly, seasonal and annual basis. The response of the water resources of the river catchment to the scenarios of projected climate

change an annual and seasonal increase in inflow volume in the future periods for the next 90 years up to 35% may be an average (Fikru et al., 2018).The projected increase in annual Potential Evapotranspiration in the sub-basin will vary on an annual average in the catchment will also increase up to 25% (Fikru et al., 2018). The incidence of severe precipitation promotes increased amounts of surface runoff causing a higher flood frequency (Joonghyeok Hoe, 2018).

Climate-driven changes in flood frequency exhibit a huge complexity that depends on the generating mechanisms. Changes in Earth's climate system can disrupt the delicate balance of hydrologic cycle and can eventually lead to increased occurrence of extreme events such runoff, increases in the frequency and intensity of heavy rainfall would contribute to increases in rain-generated local floods, and spring peak flows fed rivers are expected to flood magnitudes are rise. Extreme rainfall events and the resulting floods usually could cause significant damage to agriculture, causing huge economic losses (C. Hu, et al, 2019) and ecology, infrastructure, loss of lives and negative impact on environmental issues (Biniyam Y. & Abdella K., 2017).

But in the past finding does not consider the impact of climate change that has on the flood frequency in the Guder Watershed. The impact of climate change is expected to increase the challenges for water and flood management in the 21st century. The frequency and magnitude of hydrological extreme events caused by rising temperatures and heavy rainfall such as floods and drought are on the rise and are expected to continue to increase as a consequence of climate change through the world (Dawit T. G & Hatim O. S, 2021). Therefore, the potential impacts of such variations in the future climate need to be taken into consideration by policy and decision-makers when managing water resources and making plans for the future. It is extremely important to conduct a research on the impacts of climate change on hydrological regimes so that people and society can foresee and respond to the tentative future challenges either by mitigating the worst condition that likely to happen in the future or at least be well prepared and resilient to face the possible challenges. Potential future increases in flooding due to climate change should be taken into account when designing flood protection devices or planning new infrastructure or subdivisions (A.L. Kay et al., 2021).

1.3. Objectives

1.3.1. General Objective

The general objective of this study is to evaluate the impact of climate changes on flood frequency of Guder Watershed

1.3.2. Specific Objective

1. To assess the future trends climatic variables of rainfall and temperature in Guder watershed
2. To evaluate the performance of regional climate model simulations over study area
3. To analyze the impact of climate change on the future flood frequency and magnitude in the study area.

1.4. Research Questions

This study will address the following research questions:

1. What will be the trends of climate variables in the future in Guder watershed?
2. Which CORDEX-Regional Climate Model Performance is best over the Study area?
3. Is that the future climate change impact on the flood frequency over the study area?

1.5. Significance of the study

This study is expected to become valuable on the prediction of flood frequency under the changing climate for various return periods provides important and valuable information for the proper management and planning of water resources, management of flood disasters or Flood risk estimation, economic evaluation of flood control projects, design of water resources management options on the study area. Therefore, the information will contribute to future planning as well as managing the current water resource use in an adaptive way and the effect of climate change on extreme flood events. In addition, it will use as an input for anyone who likes to work and avoid or minimize the adverse impact of climate change on flood frequency of Guder watershed.

This study analyzed the flood flow, generated the future stream flow for the projected climate by using a selected hydrological model, and quantified the impact of climate change on flood frequency over Guder catchment. Hence, it may enable the government and NGOs to recognize the impact of climate change and work together towards finding lasting solutions that will help to reduce the risk of extreme flood events in the study area. And also, facilitate various policy

decision makers and stakeholders while deciding mitigation and adaptation strategies ahead of time, and any further investigation that will undertake on the Guder Watershed.

1.6. Scope of the study

The domain of the study is the Guder Watershed, which is a sub-basin of the upper Abay basin located in the Oromia Region, Northwest of Ethiopia. The downscaled regional climate data from the HadGEM2-ES output of CORDEX-Africa with recently developed RCPs (RCP 4.5 and RCP 8.5) scenarios were used to indicate future projections in mid-term (2041-2070) and long-term (2071-2100) two periods with respect to the baseline period (1971-2000). The HEC-HMS model was applied to simulate future streamflow of the basin for both terms. Further to this, Hydrologic and climatic variabilities trends were investigated in the watershed using MK trend test. The flood frequency was analyzed for observed and two horizons time employed AM time series and Generalize Extreme Value distribution in Guder watershed using the simulated streamflow and compared it with the observed flood frequency. In this study, the impact of climate change was assessed by assuming the land cover will remain the same at future time horizons.

2. LITERATURAL REVIEW

2.1. Global Climate Change Overview

Climate change refers synthesis of atmospheric conditions characteristic of a particular place in the state of the climate that can be identified by changes in the mean or the variability of its properties and that persists for a long period (G. Gelete et al., 2019). Natural climate variability maybe happens because of external factors forcing persistent anthropological induced activity; mainly due to fossil fuel burning, deforestation, and internal variability climate system like volcano irruption, earthquake (Belay & Getaneh, 2016). Global atmospheric and oceanic perturbations and local weather variability induced factors highly alter the rainfall pattern (Negash & Marie, 2016).

Climate change will have a significant impact on water cycle and will lead to severe environmental problems, disaster (Yamamoto et al., 2021) and the various challenges being faced by the world have different impact on Water resources, especially flood frequency (Demissie et al., 2016) and is expected to exacerbate in future; becoming an increasingly important issue that threatens the imperiled (Singh R. et al., 2016). In recent decades, the dramatic development of industrial activities, leads to increasing greenhouse gases, causes a climatic imbalance on the earth. An increase of atmospheric greenhouse gases results in climate changes, causing rapidly rising sea levels and an increased frequency of extreme climatic events; this includes intense storms, heavy rainfall and droughts. Global climate and water stress are serious problems, including loss of native biodiversity and risks to ecosystems and humans, from increased flooding or water shortages (Ionela Gabriela Bucse et al., 2019).

The consequences of climate change are unpredictable weather patterns, Droughts and extreme flooding can be triggered by weather instability (Sharu, 2021). The devastation caused by floods in different parts of the world in addition to the challenges currently being posed by uncertainties occasioned by climate change phenomenon has made the reliable estimation of rainfall events more imperative (G. D. Akpen et al., 2018). Climate change has influenced the recurrence of extreme rainfall events resulting to destructive soil erosion, flooding, landslides triggered by poor land conservation (R.C.C. Puno, et al., 2019) and may lead to unexpected impacts on the characteristics of watershed hydrology like evaporation, streamflow and sedimentation (A. N. Hilo et al, 2019).

2.2. Climate Change of Africa

African countries are more affected by climate change inducing climate-relate to natural disasters such as droughts and floods, because of their macroeconomic reliance on agriculture as well as their lower financial, technical, and institutional capacity to adapt (Jessie R.G. et.al.). Agriculture is considered as the largest main economic activities about 80% are rural dwellers engaged in rain-fed agriculture in Africa (Gebreegziabher et al., 2016) and it provides employment approximately 60 % of the African population, and more than 50 % of GDP in some countries (Oladayo N.A. and Jonathan T., 2017). A growing consensus in the scientific community indicates that climate change will reduce crop yields in developing countries and multiplier of existing threats to food security (T. Alemu and A. Mengistu, 2019).

The rise in average global surface temperature is attributed to the accelerated human activities and an increase in the concentration of greenhouse gasses in the atmosphere over the last century (Schardong & Simonovic, 2019). Temperatures in Africa are forecasted to rise faster than the global average during the 21st Century, with temperature extremes breaching levels experienced today by 2°C by 2050 and 4°C-6°C. Changes to rainfall regimes are more uncertain, but indications from global climate modeling exercises are that southern African will become drier, and eastern and western Africa will become wetter, with rain falling more intensely and bringing an increase in the risk of floods. These broad directional changes mask variability on a smaller scale; for example, modeling results in Ethiopia indicate a wide range of rainfall pattern changes (Climate Change Adaptation in Africa, 2018).

2.3. Impact of Climate change in Ethiopia

Climate change poses a huge challenge to Ethiopia and its people faced with increasingly unpredictable rains, floods, landslides, and in some years the complete failure of seasonal rains occurrences that are linked to climate change (Climate Change Profile: Ethiopia, 2018). Ethiopia is most vulnerable to climate risks to current variability and there are also indications that climate change will increase rainfall variability which will likely increase losses from heavy dependence on rain-fed, subsistence agriculture (Belay & Getaneh, 2016).

Climate change will make the prospect of economic development harder for Ethiopia in at least two ways: first, by reducing agricultural production and output in sectors linked to agriculture, which is likely to reduce Ethiopia's GDP by about 10% from its benchmark level; and second, by raising the degree of income inequality which is likely to further decrease economic growth (Ethiopia Climate Action Report, 2016). Ethiopia is a country where about 80% of the population is engaged in the agricultural sector and the main source of income for rural communities. Climate change will be increasingly intense rainfall will bring increased floods and soil erosion, which is the main cause of sediments and pollutants in freshwater bodies. Soil erosion is a serious problem in Ethiopia every year, 1.5 billion metric tons of topsoil erodes from the highlands into streams and rivers, thus increasing sediments, pollutants (Ethiopia Climate Action Report, 2016) Consequently, agricultural and livestock production, people's livelihoods, and food security depend strongly on weather conditions mainly on rainfall patterns such as amounts and timing.

The increment of greenhouse gas concentration in the atmosphere results in changing of global climate, increasing of temperature, excessive deforestation during the last century and a half has increased concentration of carbon dioxide in Earth's atmosphere and alteration of the amount and distribution of precipitation (Biniyam Y. & Abdella K., 2017). According to the IPCC, an increase in global warming, extreme climate events like drought, and flooding occur more frequently. Climate change increases uncertainty in water availability which negatively affects agricultural production, threatens the environment, and results in a socio-economic problem (IPCC Special Report of Global Warming, 2018).

2.4. Climate Change and Flood Events

Climate change is expected to alter average temperature and precipitation values in the frequency and intensity of flooding events may produce serious impacts on society, such as enormous economic, societal and environmental damage, including loss of lives and disrupting livelihoods throughout the world (Badri Bhakta Shrestha et al., 2019). Climate change can increase the likelihood of occurrence and strength of extreme weather such as extreme precipitation events, which might lead to cause more flooding in some regions (R.C.C. Puno, et al., 2019). Floods are due to natural factors such as heavy rainfall, the glaciers melt and ocean levels are rising and high tides, (Ionela Gabriela Bucse et al., 2019) and human factors such as blocking of channels or

aggravation of drainage channels, improper land use and deforestation in headwater regions (Aicha Saad et al., 2019).

The occurrence of extreme events is more frequent due to a variety of natural global climatic phenomena (Lauro C et al., 2018) and anthropogenic factors are the most common environmental hazard affecting people globally leading cause of natural disaster deaths worldwide (M.S. Bhat et al., 2019). ` The World Disaster Report reveals that flooding is the leading disaster accounting for around 55% of all the natural disasters. Flood magnitude and frequency are essential for both hydraulic structures and flood risk management but it will change as climate changes (J.G. Duan et al., 2017). The probability of extreme weather events increases with rising temperatures from global climate change and a possible cause of extreme hydrologic events such as flood, drought, snowmelt, heat-waves, and variability (Ye Bai et al., 2019).

2.5. Climate change modeling approach

To capture the range of possible changes in flood magnitude under a future climate change, an ensemble methodology is applied here in which data several GMC/RCM combinations are used for hydrological modeling of climate change impacts on floods, based on the different global scenarios for technological change. The GCM/RCM predictions are employed to derive recommendations for policymakers by Statistical and dynamic downscaling methods are applied to cope with this issue and provide for bias correction of the dataset series from the climate models to the observation records at the catchment levels (Schardong & Simonovic, 2019).The climate downscaling technique is used to bridge the gap between the higher resolution GCMs and the local climatic process, which is broadly classified as statistical or dynamical downscaling (Muhammad Noor et al., 2018). The outputs from GCMs are typically defined at 150–300 km coarse grids, while regional climate models resolutions are about 12–50km (Ashish Shrestha et al., 2017).

Statistical Downscaling: It is widely used for assessing climate change on local scales due to simplicity of use, lower computational cost, representations can be generated quickly and flexibility, without compromising on downscaling accuracy (Muhammad Noor et al., 2018). Statistical downscaling is based on coarse resolution predictors that lead to high-resolution predictions for temperature and precipitation.

Dynamic Downscaling: The use of finer-scale Regional Climate Models (RCMs) that produce output series with a spatial resolution (Schardong & Simonovic, 2019) and improving spatial resolution typically by the factor of five-ten times as compared to the host GCMs (P. Ganguli & P. Coulibaly, 2019). Dynamic downscaling requires a large amount of computational and data storage resources. Dynamical downscaling is physically based regional climate models (RCMs) driven by conditions provided by a GCM and techniques transfer information from GCMs to produced finer scales output by applying higher resolution RCMs over a limited area with initial boundary conditions taken from a driving GCM (Maikel et al., 2020).

2.5.1. Global Climate Model/General Circulation Model (GCM)

General Climate Models (GCMs) are developed to represent the dynamics within the Earth's atmosphere to understand current and future climatic conditions (Schardong & Simonovic, 2019). It is the physically-based models that provide information of current and future climate conditions, are typically designed to simulate large-scale atmospheric processes (large scale models; horizontal grid spacing of 150-300 km) (P. Ganguli & P. Coulibaly, 2019), can serve as the basic input for climate change impact studies on water resources (Nkululeko Simeon Dlamini et al, 2017). Virtually all published estimates of how are the climate could change in the future are produced climate by the computer models of the earth's climate system. To estimate the impacts of anthropogenic emissions on climate, a mathematical model has to be constructed of the complete climate system, which must include the atmosphere, oceans, land, glaciers and ice sheets.

GCMs are the prime tools used for simulating present climate and projecting future climate change impacts (Myo, H. T. et al ., 2020) and physically based on derived scenarios of climate change used for predicting climates condition (Melke and Abegaz , 2017), typically designed to simulate large-scale atmospheric processes (P. Ganguli & P. Coulibaly, 2019). This model is a mathematical description of the earth's climate system, firstly broken down into layers (both above and below sea level) and then each grid is broken down into boxes or cells. The GCMs are designed to predict the climatic variables based on greenhouse gas emissions as the primary variable for generating future conditions. However, other variables such as land-use, energy production, global and regional economy, and population growth (Schardong & Simonovic, 2019). The outputs of GCMs, at various spatial resolutions, can be used as the inputs to hydrological model simulations to assess the impact of climate change on hydrology and water resources (Myo, H. T. et al ., 2020).

2.5.2. Regional Climate Models (RCMs)

Regional Climate Model can sit within a global model to provide more detailed information for a particular location and ability to provide additional climate change signals that are not resolved in the coarser-resolution GCMs (Maikel et al., 2020). It relies on the observed climate as a basis for driving future projections. Local topographical features, such as mountains, influence no doubt local climate change significantly. RCMs are more reliable at reproducing relevant patterns of local precipitation, atmospheric processes so that the topographic effects on precipitation can be much better represented at a regional scale and future projections of precipitation have extensively been used to assess the impact of climate change on various water resources systems (Maikel et al., 2020).

2.5.3. CORDEX Dataset and Emission Scenario

CORDEX data project formed under the World Climate Research Center to improve the Regional Climate Model of the world and it's the most recent provided. These models were run using different emission scenarios of Representative Concentration Pathways which provide different assumptions of greenhouse gas emission pathways (Batablinle et al., 2018). The Coordinated Regional Downscaling Experiment aims is to provide coordinated sets of high-resolution regional climate projections worldwide climate information produced by different dynamical and statistical downscaling techniques. Recently, various studies had been conducted globally using ensembles of high-resolution regional climate projections generated by Regional Climate Models (RCMs) within the CORDEX (Negash et.al., 2020). CORDEX focused on the GCM experiments using emission scenarios known as RCP2.6, RCP4.5, RCP 6.0 and RCP8.5 which represent Low, mid and high-level emission scenarios respectively.

The RCPs represent the range of Greenhouse gas emissions, Out of four alternative emission scenarios of a stringent mitigation scenario RCP 2.6, two intermediate Scenarios (RCP 4.5 and RCP 6.0), and one scenario with very high GHG emissions RCP8.5 (Myo, H. T. et al ., 2020). But, Regional climate model data from the ensemble of CORDEX Africa models performed well in simulating rainfall over east Africa and predicted high variation both run under RCP 4.5 and 8.5 (Negash et.al., 2020). CORDEX-Africa RCMs generate an ensemble of high resolution historical and future climate projections at regional scale by downscaling different GCMs forced by RCPs.

2.3.4. Uncertainty of Climate Modeling

There are several sources of uncertainty in the generation of climate change information associated with alternative scenarios of future emissions and their radiative effects. The dynamically or statistically downscaled projections within these two distinct approaches to downscaling, uncertainty arises in the resulting ensemble for different reasons. In dynamically downscaled ensembles, structural uncertainty arises from the choice of regional and global climate model pairing, while in statistically downscaled ensembles, the statistical technique of bias correction and spatial downscaling (Wootten et al ., 2017).

The motivation behind the use of multiple models in climate change research is to cover different sources of uncertainties, for more details (R. A .I. Wilcke and L.Barring, 2016). The CORDEX after applying on an ensemble RCMs for multiple GCMs produced high resolution downscaled historical and future climate data based on CMIP5 simulations used for impact and adaptation studies (Fikru et al, 2018). Uncertainty can be inherited from GCMs due to factors such as internal variability, modeling assumptions, greenhouse gas emissions scenarios, and the spatial resolution of the RCM used in impact assessment; but can addressed by using an ensemble of multiple models (Lauren M. Cook, et al., 2020).

2.5.5. Hydrologic Modeling

Hydrological modeling is a tool generally used to estimate the hydrological response of the basin due to rainfall (Mokhtari E.H. et al., 2016). Deterministic hydrological models ignore the uncertainty or randomness involved in the hydrologic variables widely applied in research and decision-making processes (L. Ammann et al., 2019). Models can also be used to simulate information in both space and time when measurements are limited, not available (e.g. regarding the future) (Rangecroft al et., 2018) and process with its output being close to exactly what happened in the real system consists of a set of simultaneous equations or a logical set of operations contained within a computer program. Hydrological model is, Quantifying expression of observation analysis and prediction of the interaction of the various hydrological processes which vary in time and over space i.e. Rainfall, infiltration, evaporation, and streamflow. Hydrological models are simplified, conceptual representations of the hydrologic cycle. They are primarily used

for hydrologic prediction, understanding of hydrologic processes and also considered to be mathematical formulations to simulate natural hydrologic phenomena.

2.5.6. Type of Hydrologic Modelling

Hydrological Models are classified as Physical based, conceptual and empirical depending on the degree of complexity and physical completeness in the information of the structures. Modes are further classified as Lumped, semi-distributed and distributed depending on the degree of decentralization when describing the terrain in the basin. This type of model is routinely used to evaluate the hydrological behavior of watersheds in several applications, such as river flows forecasting, water availability assessment, and its dependence on external factors like climate or land-use change (F. Mendonça dos Santos al et., 2018).

2.5.6.1. Lumped Model

Parameters of lumped models assume spatially uniform watershed Characteristics within the basin (F. Mendonça dos Santos al et., 2018) and thus, basin response is evaluated only at the outlet, without explicitly counting for the response of individual sub-basins. Parameters of lumped models often do not represent physical features of hydrologic processes. The impact of spatial variability on the model parameters is evaluated by using certain procedures for calculating effective values for the entire basin. The lumped models simulate runoff while considering the whole catchment as a single unit irrespective of the spatial variation in rainfall and land use, the outputs generated can potentially vary widely when compared to the observed flows (Proloy Deb et al., 2018).

2.5.6.2. Distributed and Semi Distributed Model

Parameters of distributed models are adjusted each model cell independently allowed to vary in space at a resolution usually chosen by the user and approach attempts to incorporate data concerning the spatial distribution of parameter variations together with computational algorithms. Distributed models generally require large amounts of data for parameterization and which consider the spatial distribution of rainfall, evapotranspiration and watershed characteristics at a resolution normally selected by the modeler to reflect the spatial-temporal variability of runoff (Ambrose M.et.al., 2021).

Semi-distributed models have been widely used to simulate catchment specific hydrological processes in environmental studies strategies in the areas of land use, runoff processes, factors influencing hydrological processes, and climate change impact assessments (I. Kása et al., 2017). Parameters of semi-distributed models are adjusted in a few spots over a river basin partially allowed to vary in space by dividing the basin into many smaller sub-basins and can be accomplished based on varies catchment characteristics such as topography, elevation, soil type and land use. The main advantage of semi-distributed model is more physically based structure than that of lumped models, and the lesser amount of input data than fully distributed models. HEC-HMS is in the domain of semi-distributed hydrological model rainfall-runoff widely applied in operation for applications such as the impact of climate change and flood forecasting (M. Dal Molin et al., 2020).

2.5.7. Hydrological Model Selection

Model selection is challenging for practicing a hydrologist for the reason of complex, patterns of the hydrologic data and which models are the right ones for their purposes (I. Kása et al., 2017). Validation of hydrological models against measurements could help the researchers to select the best model for their purpose. However, the model section is based the availability of input data, on the characteristics of the problem under analysis, nature and type of hydrologic process needed to be simulated and nature of data handling mechanisms (F. Mendonça dos Santos al et., 2018) for this study the semi-distributed model HEC-HMS is selected to calibrate the streamflow data of the Guder Watershed.

2.5.7.1. Hydrologic Modeling System (HEC-HMS)

Hydrologic Modeling System is a rainfall-runoff simulation model used to simulate peak river discharge values for current and future conditions to calibrated and validated based on the observed river discharge data (A. Rafiei Emam et al., 2016). HEC-HMS is one of those models significantly used in different parts of the world used to predict the hydrologic response of the basin to the climate changes scenarios (Mokhtari E.H. et al., 2016), the GCM outputs were bias-corrected at the selected HRUs and fed to the calibrated HEC-HMS model and the future water resource was assessed (Proloy Deb et al., 2018). HEC-HMS has become very popular and adopted in many hydrological research institute because of its ability to simulate and run in both short and long time events (Sharu, 2021)

HEC-HMS is developed by the US Army Corps of Engineers Hydrologic Engineering Centre, which is designed to simulate the precipitation runoff processes within a wide range of geographic areas, such as large river basins and a rainfall-runoff simulation model. HEC-HMS has become very popular and been adopted in many hydrological studies to the simulation of runoff volume in integrated water resources and watershed management projects and for estimating flood peaks in flood forecasting (M. Dal Molin et al., 2020). A special extension programmed of the HEC-GeoHMS in ArcGIS has been applied in some of the studies and allowed researchers to generate relevant spatial data to terrain characteristics which cloud be used as input data for the HEC-HMS model. Hence, choosing a particular model structure for a particular application is one of the challenges of the model user suggested four criterions for selecting model structures.

1. Consider models which are readily available and whose investment of time and money appeared worthwhile.

2. Decide whether the model under the consideration will produce the outputs needed to meet the aims of a particular project.

3. Prepare a list of assumptions made the model and check the assumptions likely to be limiting in terms of what is known about the response of the catchment. This assessment will generally be a relative one, or at best a screen to project those models that are obviously based on the incorporate representation of the catchment process.

4. Make a list of the inputs required by the model and decide whether all the information required by the model can be provided within the time and cost constraints of the project. Considering the above four criterions into account the better performance model for this study is event based HEC-HMS hydrological model is selected. Based on the model selection suggestions criterions Arc GIS, Arc-Hydro, HEC-GeoHMS and HEC-HMS were selected.

2.5.7.2. Arc GIS

For hydrological modeling, GIS, especially through their powerful capabilities to process DEM data, has provided modelers with new platforms for data management, visualization and have made extra efforts to improve the analytical and modeling capabilities of their products (Aicha Saad et al., 2019). For all GIS-related tasks, the Environmental Systems Research Institute´s (ESRI) ArcMap software, version 10.1 was used in this study. ArcMap is the main component of ESRI´s

ArcGIS suite of geospatial processing software. Most of the GIS tasks were performed based on the functionality of the ArcMap extensions Arc-Hydro and HEC-GeoHMS.

2.5.7.3. Arc-Hydro

Arc-Hydro is an extension of different Arc GIS versions, which is developed in the Esri water resource team to support water resources applications. The availability of DEM and GIS tools, watershed properties can be extracted by using compatible version of Arc-Hydro automatically. It simplifies the process of delineating watershed, sub-watersheds, stream network, and some other watershed characteristics that collectively describe the drainage patterns of a basin. Arc Hydro tools can be used to create input files for hydrologic models (HEC-GeoHMS).

2.5.7.4. HEC-GeoHMS

Hydrologic Engineering Center's Geospatial Modeling System has been developed as a geospatial hydrology tool kit for engineers and hydrologists allows users to visualize spatial information, water shade characteristics, perform spatial analysis, delineate sub-basins and streams, and construct inputs to hydrologic models (Demissie et al., 2016). Analyzing digital terrain information, HEC-GeoHMS transforms the drainage paths and watershed boundaries into a hydrologic data structure that represents the watershed response to Rainfall. ArcGIS uses HEC-GeoHMS Version 10.1 and Spatial Analyst to develop many hydrological model inputs. Concerning hydrologic parameter estimation, HEC-GeoHMS contains tools to assist the user in estimating initial values of some hydrologic parameters. The program allows users to visualize spatial information, document watershed characteristics, perform spatial analysis, delineate sub-basins and streams, construct inputs to hydrologic models, and assist with report preparation.

HEC-Geo HMS is used to create hydrologic inputs that can be use directly with the HEC-HMS, it creates background map files, basin model files, meteorology model files, and a grid cell parameter file, digital elevation model, soil types, land use information and meteorology model (Demissie et al., 2016). The HEC-GeoHMS program features illustrate functionality and ease use of Data management, terrain preprocessing, basin processing, hydrologic parameter estimation and HMS model support. These features perform administrative tasks, terrain preprocessing and sub-basin delineation in either a systematic fashion or batch mode. In addition to these, it computes the Curve Number (CN) and other loss rate parameters based on various soil and land use databases,

watershed and channel characteristics. The outputs obtained from HEC-GeoHMS were used as input for the HEC-HMS model to set up (Proloy Deb et al., 2018).

2.5.7.5. Advantages HEC-HMS

HEC-HMS has merits to simulate the flow in the outlet of the watershed, and then provide data that help manager and decision makers to adopt the plausible management strategies, the future enhancements in progress and help the ecosystems to build a strong resilience capacity against climate change and natural hazard risks (Ismail Elhassnaoui et al., 2019). Additionally, it is in the public domain and peer-reviewed and available to download free of charge from HEC's web site. Therefore, the model applicability and efficiency to simulate rainfall stream flow was done in various regions of the world, the model widely applied in Abay river basin in Ethiopia more recently. The suggested criterions are; freely the model availability, the model efficiency to meet the target objective of the study, the model representations of assumed process in the catchment, and availability of all information required by the model within time and cost constraints.

2.6. Bias correction

Bias correction methods are used to minimize the discrepancy between observed and simulated climate variables of precipitation and temperature projections given by climate models in the control period usually do not fit the observations in the same period exactly from a statistical point of view (Enrique S. et al., 2018).The bias correction of the daily RCM precipitations and temperatures is therefore necessary to produce seasonal and regional hydrological variability, and extremes, that are in line with the observations of the control period (Noora Veijalainen et al., 2017). For applying bias correction to climate model simulated rainfall, different options are available to be applied entire time series, annual mean precipitation (P. Ganguli & P. Coulibaly, 2019) Bias correction is the adjustment of biased simulated data to observations and it is the systematic deviation between an observed or computed value (Maikel et al., 2020)

The Bias correction should be applied to compensate for any tendency to overestimate or underestimate the mean of downscaled variables. Often, the outputs of RCMs/GCMs cannot be directly used for impact assessment as the computed variables may differ systematically from the observed ones. Bias correction is the differences in observed climatological mean values between downscaled GCM and observations for historical reference period used to “correct” future

downscaled GCM simulations, to compensate for any tendency to overestimate or underestimate the mean of the downscaled variables (Zhe Yuan et al., 2018).

There are several bias correction methods which have been developed to adjust meteorological variables: Delta change, Variance Scaling Linear scaling, local intensity scaling, power transformation, and distribution mapping are among the bias correction methods applied for many studies yet. The delta-change method generates climate scenarios by adding the future change signal (anomalies) from GCM-RCM simulations for a perturbation of the observational datasets (Maikel et al., 2020) and conventional way to construct precipitation time series for a projected future climate change (Yèkambèssoun N'Tcha M'Po, et.al., 2016). For temperature correction methods including linear scaling, variance scaling and are used for many studies. The Variance scaling method was developed to correct both the mean and variance of normally distributed variables of temperature while the linear scaling method aims to perfectly match the long-term monthly mean of corrected values with those of observed values (Maikel et al., 2020).

2.7. Streamflow data Transfer to ungauged watershed

Streamflow is one of the crucial data for practical hydrological applications in such as basin management, the design of flood control infrastructure, water resource system planning and management, disaster risk management, and environmental impact assessment (Xiao et al, 2017). The stream flow prediction are very important for ungauged or poorly gauged river basins to characterizing the hydrological behavior in response to climate change in growing economies countries like Ethiopia; because, there are a limited number of stations in the streamflow gauging network (Mustafa U. Y. & Bihrat O., 2020).

There are different regionalization techniques to transfer information from gauged sites to ungauged sites (target station) through the use of catchment physical characteristics should be hydrologically reasonable (B. Choubin, et al., 2019), in order to make reliable predictions in ungauged basins. Regionalization is a statistical process of transferring information, which aims to estimate streamflow at ungauged basins or interest site (B. Choubin, et al., 2019). There are many methods used for parameter regionalization statistical process that are used to predict streamflow at target station.

i. **Drainage Area Ratio Method** : The most common and oldest information transferring method appealing as it requires no additional information other than the streamflow values at the donor station, the drainage areas of the donor and target stations., making it the easiest possible method that one could consider (F. Saka &H. T.Babacan, 2019). Parameter set of gauged watershed are transferred to un gauged watershed of comparable area based on the assumption that watershed area was the dominant factor for controlling the volume of water that can be generated from the rainfall and gauged watershed that is located nearest to the ungauged watershed of interest is identified as stream flow values are transferred from gauged to ungauged watershed. Model parameter sets of gauged catchments are transferred to ungauged catchments by catchment size comparison. The method is a simple approximation, which works best when the gauging station is close to the respective outlet and the area ratio gauged to ungauged is 1 to 1.5 intervals

ii. Spatial proximity: The transfer parameters approach is based on the geographical distance between catchment centroids or catchment outlets, between the catchments may be an appropriate measure of similarity when selecting the donor catchment to receiver catchments, but the accuracy of results depend upon the density of gauged catchment networks (J.B. Swain & K.C. Patra , 2017).

iii. Inverse Similarity Weighted (ISW) Method: It is the most Sophisticated method has capability to transfer from Multiple donor gauged catchment to ungauged catchment; which based physical similarity approach, to determines appropriate donor basins by considering similarities between gauged and ungauged basin (T. Razavi and P. Coulibaly, 2016). The similarity coefficient is used to define the physical similarity between the target station and the donor station. Drainage area, elevation, annual mean total precipitation, annual mean temperature, basin slope, channel length, latitude, and longitude were considered as the basin characteristics in order to measure the physical similarity between the donor station and the target station (Mustafa U. Y. & Bihrat O., 2020). In this method, the parameters set from the most physically similar the donor catchment is transferred to the target site using similarity indices (X. Yang et al, 2018).

2.8. Flood frequency Analysis

The flood frequency analysis is one of the important studies of river hydrology and crucial parameter to determine the extended flooding for the different return periods (Ery Suhartanto et al., 2018). To describe the flood frequency at a particular site, the choice of an appropriate probability distribution and parameter estimation methods are immense importance to identify underlying probability model of flood peaks which can then be used to perform risk-based design and flood risk assessment. (Mahmood Ul Hassan et al., 2019). It attempts to quantify the flood peak discharge as a function of the probability of exceeding a discharge and essential to interpreting the record of flood events to evaluate future possibilities of such occurrences (M. L. Kavvas, et al., 2017). The magnitude and probable frequency of such recurrence are also required for proper design and location of hydraulic structures and other allied studies.

Flood frequency analysis is the determination of the magnitude of flood flows extreme events to their probability distribution at different frequency or recurrence interval (Usman A. I. et.al, 2016)and a technique used by hydrologists to predict flow values corresponding to specific return periods or probabilities along with river floods of high magnitude for larger return periods (Ahmad I. et al., 2019). Classic flood frequency analysis fits a probability distribution to annual maximum flow series which is caused by Climate change that can result in changes in the mean or the variability of floods that persists for an extended period, decades or longer (Xin Yu et al., 2018). A return period is a recurrence interval which is an estimate of the interval of time between events flood or river discharge flow of a certain intensity. Flood frequency analysis has been mainly aimed at frequency estimations at the design level, and to make adaptation plans against recent devastating flood disasters and climate change, the rational estimation of extreme floods over the design level is also crucial (Tomohiro Tanaka et al., 2016).

Flood frequency analysis is the procedure to extract information from a flow record data to estimate the relationship between flows (Noor S. R & Zulkifli Y., 2017) and return periods of a hydrological event such as flood, using observed annual peak flow discharge data as a function of recurrence interval. In flood frequency modeling, there are problems related to the Choice of model type, distribution to be used, method of a parameter, and quantile estimation. The impact of climate change on flood frequency is analyzed using the extreme discharge series extracted using two main model types of data series available.

i**) Annual maximum series (AMS)**

Flood frequency analysis by using annual maximum instantaneous streamflow records are required to reduce the uncertainty due to time resolution of the sampling model approach and the most frequently used, which is composed of the single maximum streamflow for each year of the record (T.T. Hailegeorgis & K. Alfredsen, 2017).The main advantages of using the annual maximum series: there is a high probability that flood events are independent; the series is easily and unambiguously extracted, and the form of the frequency distribution of annual floods generally conform to theoretical distributions (S.Malik & S.Chandra Pal, 2021). The major disadvantage of using the annual series is that because only one flood is included from each year of the stream-flow record, the annual series may exclude significantly large floods if several occur in a single year and may include small annual maximums for some years.

ii) Partial duration series

Peaks over threshold is also called the partial duration series approach and defined by all peak values that lie above a certain truncation level. In POT method, the derived series provide a more complete description of flood behavior than annual maximum series and well-defined peaks above a specified threshold value. The POT series model replaces the continuous hydrograph of flows by a series of randomly spaced spikes on the time axis. Major difficulties in using the POT method are assuring the independence of the data series and choosing an appropriate threshold value.

2.8.1. Probability Distribution

To describe the flood frequency at a particular site, the choice of an appropriate probability distribution and parameter estimation methods are immense importance (Mahmood Ul Hassan et al., 2019). The most common technique used for the at-site estimation of flood recurrence magnitude and the four most commonly used distribution methods (Muhammad Farooq elt al., 2018), the number of probability distribution models viz., Weibull, gamma (Pearson type 3), generalized extreme value (GEV), lognormal, Gumbel, and normal are in use in the hydrologic frequency analysis of floods. The use of probabilistic approaches to fit and select the best fitting probability model to a set of observed data has lately gained currency among researchers (Philip Kibet Langat et al., 2019). Within probabilistic models, the two most popular are Gumbel maximum value and Log Pearson type III distribution (Vikas Kamal et al., 2017).

After obtaining the data series, it is essential to determine the proper statistical distribution families fit most AM flood data that is able to describe the time series data fit best model amongst these distributions. Two distribution families are suggested as reasonable to choice for AM series, namely the GEV and LP3 but, GEV distribution is frequently used for AMS data (Firdaus M.H. et.al., 2021). The GEV model fits the AM series well and the GPD model fits the POT series well (Zhanling Li et.al., 2016).

2.8.1. Parameters of Flood Estimation Methods

One of the biggest challenges for hydrologists is the reliable estimation of extreme flood events (Igor Lešcešen and Dragan Dolinaj, 2019). Accurate estimation of maximum flood discharges is very crucial to assign hydraulic structures dimensions design and operation of flood control structures (dams, retaining basins) of infrastructures such as flood defenses, bridges, roads and dams, as well for flood risk management, planning, and diversion canals for increases safety of the performance the hydraulic structures (Fevzi Onen and Tamer Bagatur, 2017). The nature of most hydrological events such as rainfall is erratic and varies with time and space, it is commonly possible to predict return periods using various probability distributions (Wan Husna Aini Wan Deraman et al., 2017). The most commonly used methods for estimation of flood frequency analysis are the maximum likelihood estimation method, the method of moments, the L-moments (LM) method and the probability-weighted moments method (Mahmood Ul Hassan et al., 2019).

i) Maximum likelihood Method

The method of maximum likelihood (MML) is considered to be the most accurate method, especially for large datasets since it leads to efficient parameter estimators with Gaussian asymptotic distributions. are consistent, reliable, and unbiased (Tegegne G.et.al., 2020). It provides the smallest variance of the estimated parameters, and hence of the estimated quintiles, compared to other methods. The ML method is one of the most applied methods for parameter estimation of probability distributions obtained by maximizing the likelihood function or log-likelihood function of the probability distribution (Kousar S et al., 2020).

ii) Method of moment

Method of moment (MOM) is relatively easy and is more commonly used methods of estimating parameters of a probability distribution. It can also be used to obtain starting values for numerical procedures involved in MML estimation. However, MOM estimates are generally not as efficient as the MML estimates. Especially for distributions with a large number of parameters, as higher order moments are more likely be used to obtain starting values for numerical procedure involved in MML estimation and to be highly biased for relatively small samples. The method of moments is based on observation, noting that the parameters of probability destitution can be estimated using sample statistics. Afterwards, the parameters of the distribution can be calculated using the relation between the parameters and the moments (Hasan, 2020).

iii) L-Moment method

The most popularized method to frequency analysis in recent time is L-moment approach which is widely used for developing regional flood frequency relationships (Vikas Kamal et al., 2017), able to characterize a wider range of distributions, they are less subject to bias in estimation and more robust to the presence of the data outliers (Igor Lešcešen and Dragan Dolinaj, 2019). Linear moment method offers small bias, which is an advantage over all other parameter estimation methods developed methodology in statistics and probability FFA (Muhammad Rizwan et al., 2018). L-moments are alternative to the conventional moments can be directly interpreted as a measure of the scale and shape of the distribution , but computed from linear combinations of order statistics (Mahmood Ul Hassan et al., 2019) .

iv) Probability-weighted moments method

Probability-weighted moments (PWM) are useful in the deriving expression for the parameters of distributions can be explicitly defined. Methods of parameter estimation obtained in this method are by equating moment of the distribution with the corresponding sample moment of observed data. For a distribution with a parameter, the first sample moments are set equal to the corresponding population moments. The resulting equation then solved simultaneously for the unknown parameters. PWM are often considered to be higher than standard moment-based estimates and may be useful in the absence of maximum likelihood estimates or if they are difficult to compute (Philip Kibet Langat et al., 2019).Parameter estimation by PWM, which is relatively new is as easy to apply as ordinary moments is usually unbiased and is almost as efficient as MML.

3. MATERIALS AND METHODS

3.1. Description of the Study Area

3.1.1. Location

Ethiopia has twelve river basins among them, the Abay river basin is the largest catchment area hydropower development potential and runoff. It has the major sub-basins of Anger, Beles, Dabus, Debre Markos, Didesa, Fincha, Guder, Jemma, Lake Tana, Mota, and Muger. Guder Watershed found in the Northwest of Ethiopia; in the Southeastern part of the Abay River Basin approximately between 7º30' to 9º30' N latitude and 37º00' to 39º00'E longitude. The Guder River originates from the mountainous area of the southern towns of Ambo and Guder at an elevation of 3000masl. The river flows from the south to the north and has its outlet to the Abay River.

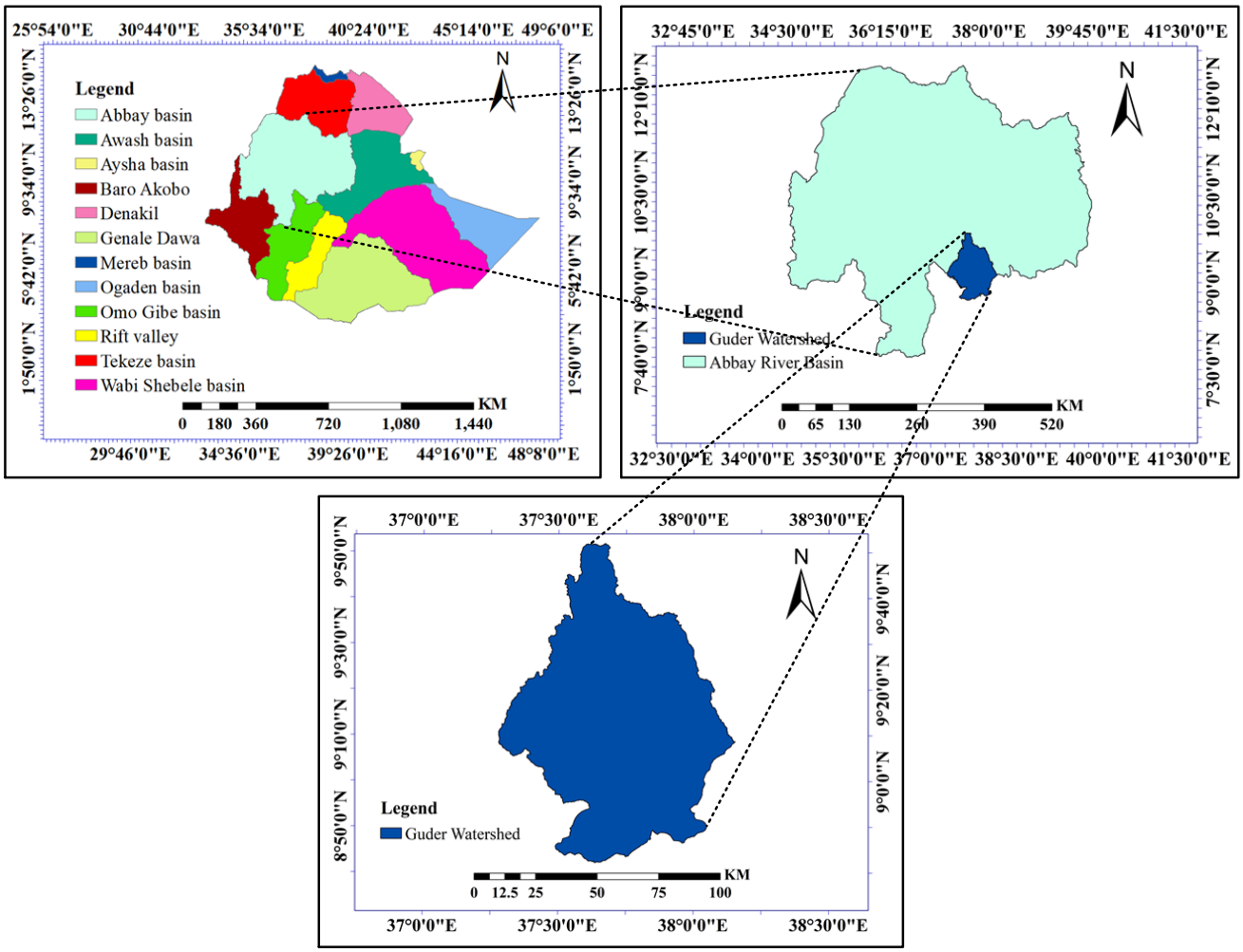

Figure 3.1 Map of Guder Watershed

Guder is a river of central Ethiopia which is a tributary of the Abay or Blue Nile on the left side; tributaries of the Guder include the Dabissa and the Taranta. The Guder Watershed has a total area approximately about 6758 square kilometers in size.

3.1.2. Climate

The movement of the intertropical convergence zone primarily regulates the distribution of precipitation in the Upper Blue Nile basin which is conditioned by the convergence of trade winds of the northern and southern hemispheres and the associated atmospheric circulation. The annual climate may be divided into a rainy and dry season. The main rainy season is from June to September, above 75-90% of the total rainfall occurs and in Belg season from March to May small rainfall occurs. The mean daily temperature of the watershed ranges between 17.3^0C and 23.4^0C. Lower annual rainfall less than 1600 mm in the major sub basin and higher rainfall greater than 1600 mm in same high lands of catchment.

3.1.3. Topography

The response of a catchment to flood is primarily influenced by the morphological characteristics and climatic elements. The elevation of Guder Watershed varies from 1500 to 3000masl. The higher elevation ranges are located on the mountainous area at the South of the town of Ambo and Guder. To cope the adverse effect of climate change, a sound understanding of hydrologic processes is very important. Stream networks originate from southern, eastern and western parts of the catchment and confluence at central part where they form Guder River.

3.1.4. Land Cover and Land Use

Climatic changes can influence land use changes plays an important role in the environment, as it partitions rainfall into the components of the hydrological cycle such as evaporation, runoff and groundwater land use changes thus change the balance between the components of the hydrological cycle, which can lead to several challenges in water resources and environmental management. The combined effects of climate change and land use changes on hydrology and the environment can lead to severe water resources and environmental problems at the local scale. Adaptation through land use planning, flood mapping, flood risk management and changes in regulation rules and practices can help diminish potential increases in flood damages (Noora Veijalainen et al., 2017).

The majority of the catchments are dominated by Agricultural areas and state farms. Forest are also used in the catchment with Woodlands in some parts of the watershed. However, Bushland, water, grassland and state farmland uses practiced in the watershed. The reasons provided for the increased frequency and magnitude of the flood events were attributed to land-use change (deforestation and over cultivation) and climate change in the area. The land cover of the Guder Watershed essentially follows the divide between highland and lowland. The high land around the Ambo and Guder mountainous areas were once dominantly covered with forests. However, these sub-humid tropical forests have been reduced to remnants, having been converted to cultivation and grazing. The spatial distribution and land use type in these sub-basins and watershed used for deciding the loss model in HEC-HMS model and also for better understanding of the study area. The land use types in each subdivision and its area have been used for initial estimation of loss and transform parameters in loss and transform method in HEC-HMS.

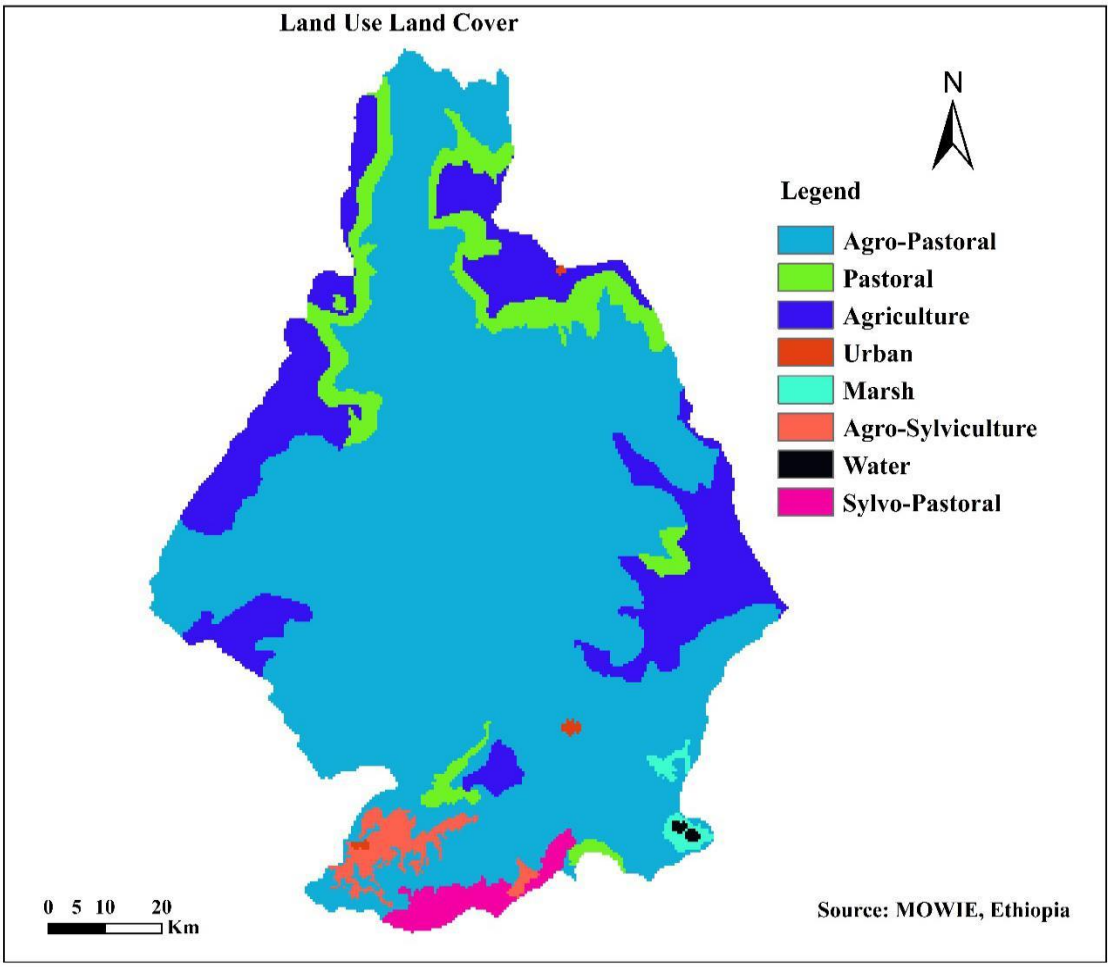

Figure 3. 2: Land use Land cover of Guder Watershed

3.1.5. Geology and Soil

Guder Sub-Basin lies in a large structural basin surrounded by volcanic mountains composed mostly of Quaternary volcanic rocks on the mountainous area of south of the towns of Ambo and Guder and Mesozoic sedimentary rock on the lower part of the river. Corresponding to the variation in landscape and other soil forming factors such as climate and vegetation, the soils of the Guder sub-basin are also highly variable.

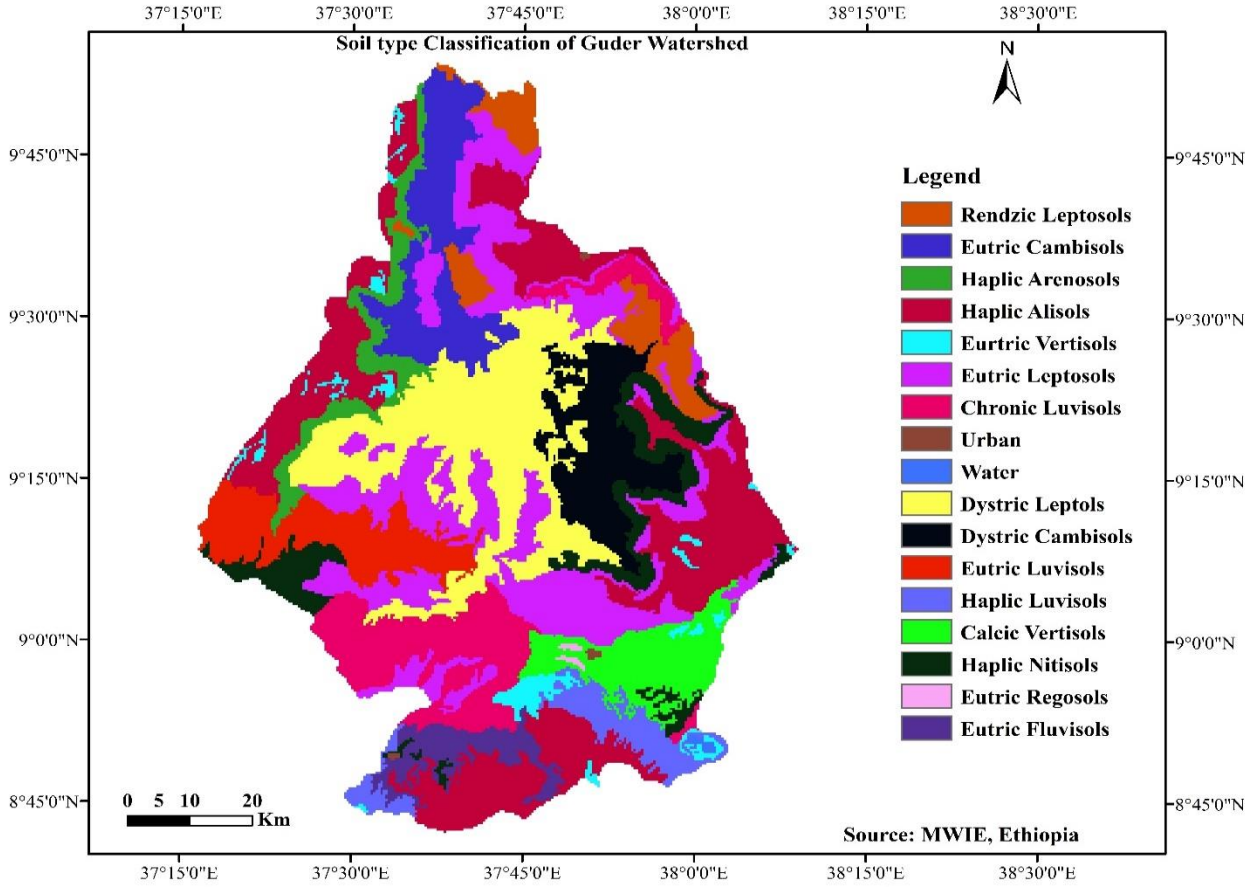

Figure 3.3:Map of the soil type classification of Guder watershed

3.2. Data types and Sources

The data used for this research is varies in types and sources. Daily climate variables of Rainfall, maximum and minimum temperature were sourced from National Meteorological Service Agency of Ethiopia (NMSA). Regional climate model data from Coordinated Regional Downscaling Experiment (CORDEX) were downloaded via the download node (https://esgf-data.dkrz.de/search/cordexdkrz).

3.2.1. Spatial data

NASA's Earth Observing System Data and Information System is the data distribution system facilitated with NASA's Distributed Active Archive Centers (DAACs). Alaska Satellite Facility is one of the DAAC providing various data sources that offer worldwide coverage of void filled data at a resolution of 12.5m Alos Palsar DEM and provide open distribution of this high-resolution global dataset. For hydrologic model development, the watershed was delineated from the same Digital Elevation Model (DEM) spatial data. Creation of radio metrically terrain corrected (RTC) products is a project of the Alaska Satellite Facility that makes SAR data accessible to a broader community of users, https//vertex.daac.asf.alaska.edu. The project corrects synthetic aperture radar geometry and radiometry, and presents the data in the GIS-friendly GeoTiff format.

A) Meteorological Data

Daily data like Rainfall, T_{Max} and T_{Min} data required for input to the HEC-HMS model, collect from Ethiopian National Meteorological Service Agency at Head Office. The meteorological variables collected vary from station to station depending on the class of the stations.

Table 3. 1:Location of selected Meteorological stations of study area:

S No	Stations	Latitude	Longitude	Elevation	% of missed data
1	Ambo Agr.	8.986	37.83967	2068	1.67
2	Combolcha	9.504	37.477	2341	3.4
3	Fincha	9.572	37.373	2262	2.5
4	Gedo	9.024	37.463	2520	2
5	Jeldu	9.257	38.086	2951	2.4
6	Kachise	9.608	37.861	2557	2

B) Hydrological Data

The hydrological data required for calibration and validation of the model results, the daily streamflow records of gauge stations found in the Gudar Watershed can be collected from the Ministry of Water, Irrigation Energy office, and hydrology department. Four river gauging stations named Bello, Fatto, Guder, and Indris data for 24years (1986-2009) record period are available.

Table 3. 2:Hydrological data Gauging station of Guder watershed

River	Latitude	Longitude	Area (km^2)	Elevation	Missed data Daily (%)
Belo	8°52'N	37°40'E	290	2509	5
Fatto	8°52'N	37°43'E	96	2551	3
Guder	8°57'N	37°45'E	524	2518	1.1
Indris	8°56'N	37°45'E	111	2520	4.5

C) Potential Evapotranspiration (ET)

Evapotranspiration is responsible for significant water losses from a watershed and defined as the evapotranspiration that would occur with specified weather and vegetative cover conditions and unlimited soil moisture. It is one of the major inputs into flood forecasting models. In this study, the potential ET was calculated using the Hargreaves method. This method is selected as the method gives reasonable estimates of evaporation despite its low demand for input data. To estimate potential ET using this method input data like TMax and TMin air temperature, latitude coordinate of the station, and altitude (elevation) are required. Since only little meteorological time series data is available in the study area, evapotranspiration for the baseline period (1971-2000) and future time horizons (2041-2100) was also calculated by Hargreaves's method.

$$ET = 0.0023(T_{maen} + 17.8)\,(T_{max}-T_{min})^{0.5}Ra \quad \ldots\ldots (1)$$

Where: ET is the potential evapotranspiration by the Hargreaves method (mm/day), Ra is the extraterrestrial radiation (mm/day); Tmean is the average temperature (°C);T_{Max} and T_{Min} are the maximum and minimum temperature respectively.

D) CORDEX-RCP climate data

The Coordinated Regional Climate Downscaling Experiment provides a means to evaluate model performance, assess downscaling, and provide a more solid scientific basis for impact assessments and other uses of downscaled climate information (Ye Bai et al., 2019). In this study, the results of CORDEX-Africa ensemble RCMs simulations for the historical and future climate projections downscaled from GCMs under RCP4.5 and RCP8.5 with a spatial resolution of 50km is used. The

climate data contains daily values of Precipitation, Maximum, and Minimum Temperature but the other climate variables were assumed to be constant for the future time. Climate change time series will be deriving for two RCP scenarios using downscaled GCM and analyze for two 30-year periods, representing mid-century (2041–2070) and near to end-century (2071-2100) conditions. Changes in temperature and precipitation under the different RCPs projected by three RCMs in the two time horizons were compared to those in the reference period (1971–2000).

3.2.2. Filling missing data

Incomplete records of hydro metrological data sometimes occur possibly due to absence of observer, instrumental failure or equipment malfunction further the personal to take readings are either too few or unreliable this the problem to many developing countries. In such a case, before using any data for analysis, one can estimate and fill the missing data by varies methods based on their needs and accuracy. For this study, XLSTAT2021 was employed for each station to estimate the meteorological and hydrological gauging station missing data.

3.3. Checking consistency of the data

The most common method of checking for the inconsistency of recorded data is Double Mass Curve analysis. After all, the meteorological and hydrological input data is filled in missing data, their consistency is checked, and the data is prepared as per the standard format for each type of the selected model. Double-mass curve analysis is a graphical method for identifying or adjusting inconsistencies in a station record by comparing its time trend with those of other stations. If significant change in the regime of the curve is observed, it should be corrected by using the equation (2). The trend of the RF records at a station may slightly change after some years. Due to a change in the environment (or exposure) of a station either due to the coming of a new building, fence, planting of trees or cutting of forest nearby, overgrazing, which affects the catchment of the gage due to change in the wind pattern or exposure.

$$Px' = \frac{M\prime}{M} * Px \quad \ldots\ldots\ldots\ldots\ldots\ldots\ldots\ldots\ldots\ldots\ldots\ldots\ldots\ldots\ldots\ldots\ldots\ldots \text{(2)}$$

Where: Px'= corrected precipitation at station x

Px =original recorded precipitation at station x

M’ =corrected slope of the double mass curve

M= original slope of the double mass curve.

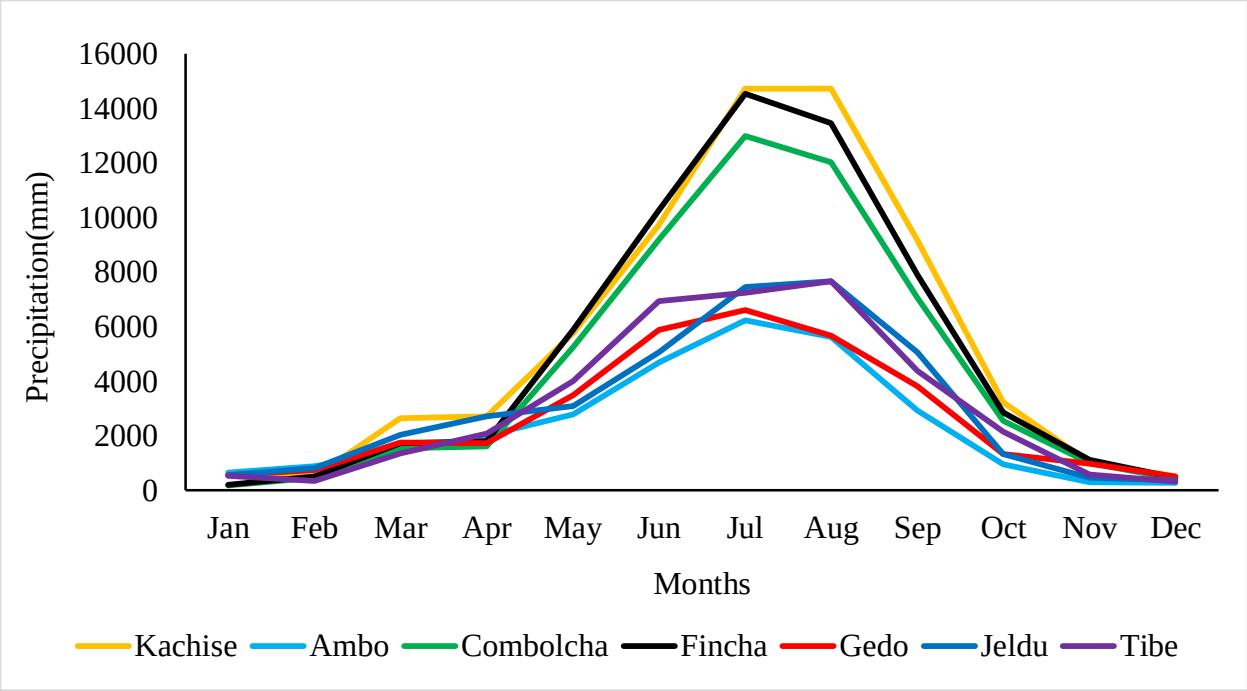

Figure 3. 4:Precipitation Consistency test of Meteorological stations (Monthly Cumulative)

3.3.1. Rainbow Homogeneity Test

Rainbow software is the popular one which offers to check the homogeneity of Rainfall data. Homogeneity analysis is employed to identify a change in the statistical properties of the time series data. In RAINBOW, the test for homogeneity based on the cumulative deviation from the mean. The cause's non homogeneity can be either natural or man-made, these include alterations to land use and relocation of the observation station. Therefore, to select the representative meteorological station for the analysis of areal rainfall estimation, checking homogeneity of group stations is essential, the homogeneity of the selected gauging stations. The data recorded in the selected stations of the study area are cheeked and plotted for comparison with each other, which characterized by unimodal types of rainfall regime. It notifies that the monthly rainfall distribution and rainfall pattern of the basin is monomodial in which the basin gets only one peak rainfall season (June to September). The basin gets high amount of seasonal rainfall during the Kiremt season is that due to the migration of ITCZ RF & PET(mm) (bundle of cloud) to the north western Ethiopia in this season.

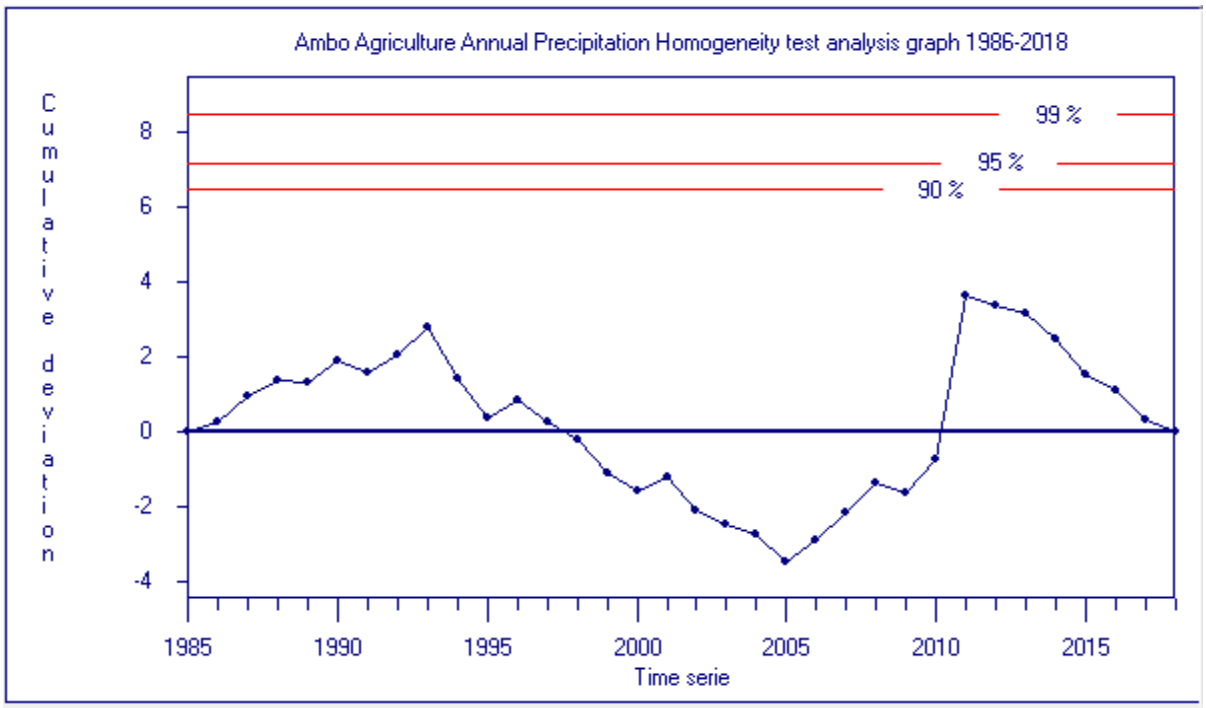

Description Ambo Agriculture Annual Precipitation Homogeneity test analysis

Restrictions

Homogeneity test

Probability of rejecting homogeneity

statistic	rejected ? 90 %	95 %	99 %
Range of Cumulative deviation	No	No	No
Maximum of Cumulative deviation	No	No	No

Figure 3. 5: Homogeneity test of Ambo Agriculture station

The figure 3.5 shows the homogeneity test of Ambo Agriculture station. Probability of rejecting homogeneity test is accepted at all significance levels (90, 95, and 99 %) for both range of cumulative deviation and maximum of cumulative deviation. Appendix: A shows other stations homogeneity test of annual rainfall.

3.4. Estimation of Areal rainfall

The observed and future rainfall stations are used for this study to drive time series of areal rainfall spatial distribution for the sub-basin in Guder watershed. A rainfall measurement is a point observation and may not be used as representative values for some large catchment areas under consideration. Therefore, time point measurements have to be averaged over the area. In this study, the Thiessen polygon method was used to estimate the areal rainfall. The method assumes that the recorded rainfall in gauge is representative for the areal half-way to the adjacent gauge. Thiessen polygon method is best suited for finding out the mean rainfall of the catchment concerned. Thiessen polygon are formed around each precipitation station by drawing perpendicular bisectors of the lines join adjacent stations, if there are 'n' number of stations and 'n' polygons, the average depth of the precipitation over the total area A is given by

$$P = \frac{1}{A}\sum_{i=1}^{n} Ai * Pi \quad \text{.....(3)}$$

Where, P = Areal mean RF,

Pi = RF measured at sub-region,

Ai= Area of sub-region and

A = total area of sub-regions.

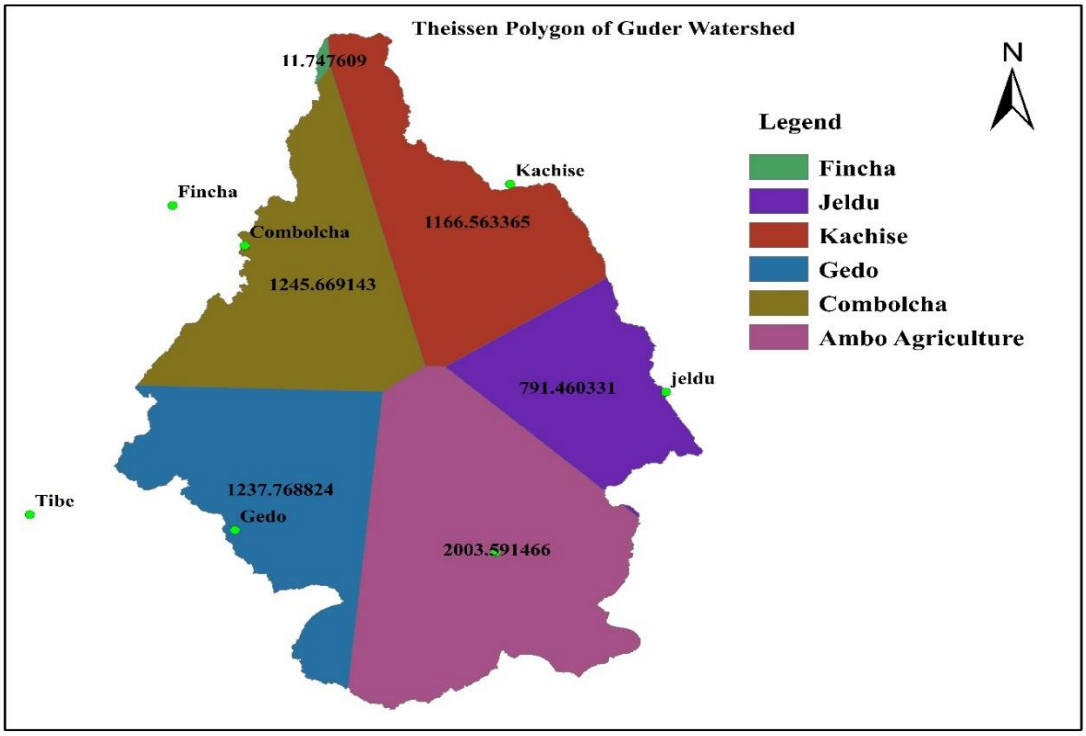

Figure 3. 6:Thiessen polygon of Guder watershed

3.5. Regional Climate Model Data Analysis

The study focuses on HADGEM2-ES climate model outputs (RCP4.5 and RCP 8.5) within three RCM families of CCLM4-8, RCA4 and RCAMO22T. Representative concentration pathways (RCPs) of CORDEX climate model output stands for a pathway in order to provide time-dependent projections of atmospheric greenhouse gas (GHG) concentrations. This study uses the results for the most extreme RCP8.5 and moderate RCP4.5 emission scenarios. The RCP4.5 is a stabilization scenario where total radioactive forcing is stabilized before 2100 by employing technologies and strategies to reduce greenhouse gas emissions, whereas RCP8.5 characterized by increasing greenhouse gas emissions that lead to high greenhouse gas concentrations over time.

Hence, this study used HadGEM2-ES United Kingdom Met Office Hadley Center, Uk of climate model, the reason is that the earth system components of this model compare well with observations and with other models. Therefore, the HadGEM2-ES models is a valuable tool for predicting future climate and understanding the climate feedbacks within the earth system. The downscaled climate data has been obtained from CORDEX-Africa database of the Africa domain AFR-44 has a 0.44-degree spatial resolution in daily time frequency base from 1951-2100. The climate data download simulated daily maximum and minimum temperatures and daily amounts of precipitation from CORDEX project (Coordinated Regional Climate Downscaling Experiment) at spatial grid resolution of 0.44^0 (~50 Km) (http://esgfdata.dkrz.de/login/?next=http://esgf-data.dkrz.de/search/cordex-dkrz/)

3.6. Grid Point Selection for RCM data

The grid point selection data have been based on Ethio-CORDEX of their grid location between latitude and longitude ($8^0$30’ -10^0 0’ & $37^0$10’-38^0 20’) respectively. After grid point selection, create thiessen polygon for both RCM and Meteorological coordinate by union and intersection area of sub-basins can be obtained, bias correction has been computed for three RCMs from areal rainfall. There are 6 grid points within the catchment for the study area is cover by thiessen polygon created by using selected grid points that the RCM data was extract by using R-Studio Programming language.

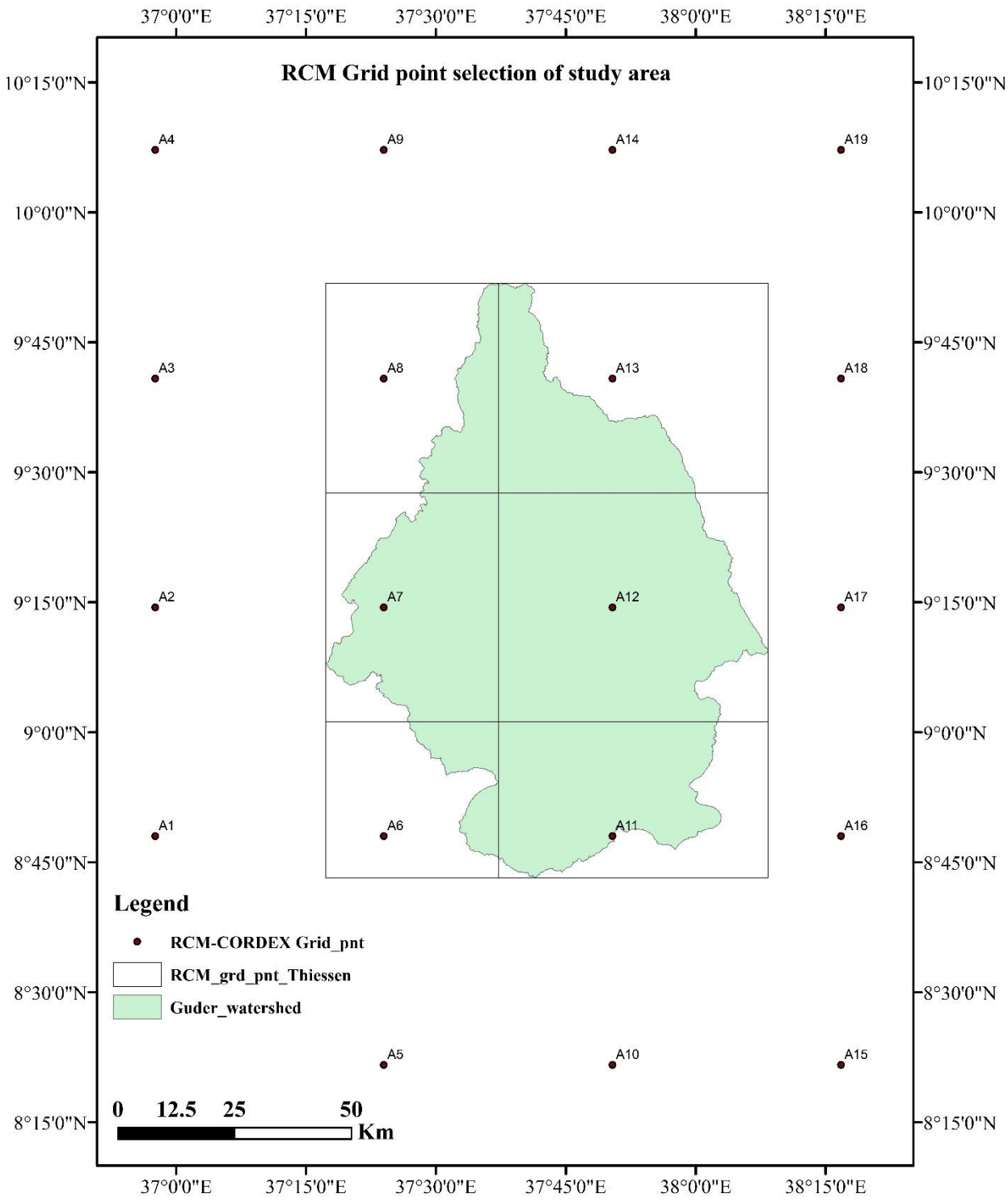

Figure 3. 7:RCMs Grid point selection of Guder watershed

3.7. Bias correction method of climate data

Bias correction is the adjustment of biased simulated data to observations which is always applied within Climate impact studies to correct the climate input data provided by General Circulation Models (GCMs) or regional climate models (RCMs) for systematic statistical deviations from observational data. Bias correction is the differences in observed climatological mean values between downscaled RCM and observations for historical reference period used to "correct" future downscaled RCM simulations. The out puts of RCMs/GCMs cannot be directly used for impact assessment as the computed variables may differ systematically from the observed ones. Bias correction methods are assumed to be stationary, i.e., the correction algorithm and its parameterization for current climate conditions are also valid for future conditions.

Climate model data for hydrologic modeling (CMhyd) is a tool that can be used to extract and bias-correct data obtained from global and regional climate models by adjusting climate model output. CMhyd was designed to provide simulated climate data that can be considered representative for the location of the gauges used in a watershed model setup. The tool has been tested using the CORDEX archive, which is a reliable source for regional climate models. The precipitation extracted from three RCMs by R-studio simulated were bias corrected using CMhyd tool. The Delta Change Correction bias removal approach is selected which is Conventional way to construct precipitation time series for a future climate is to perturb an observed data series and Variance Scaling for Temperature with a projected future climate change.

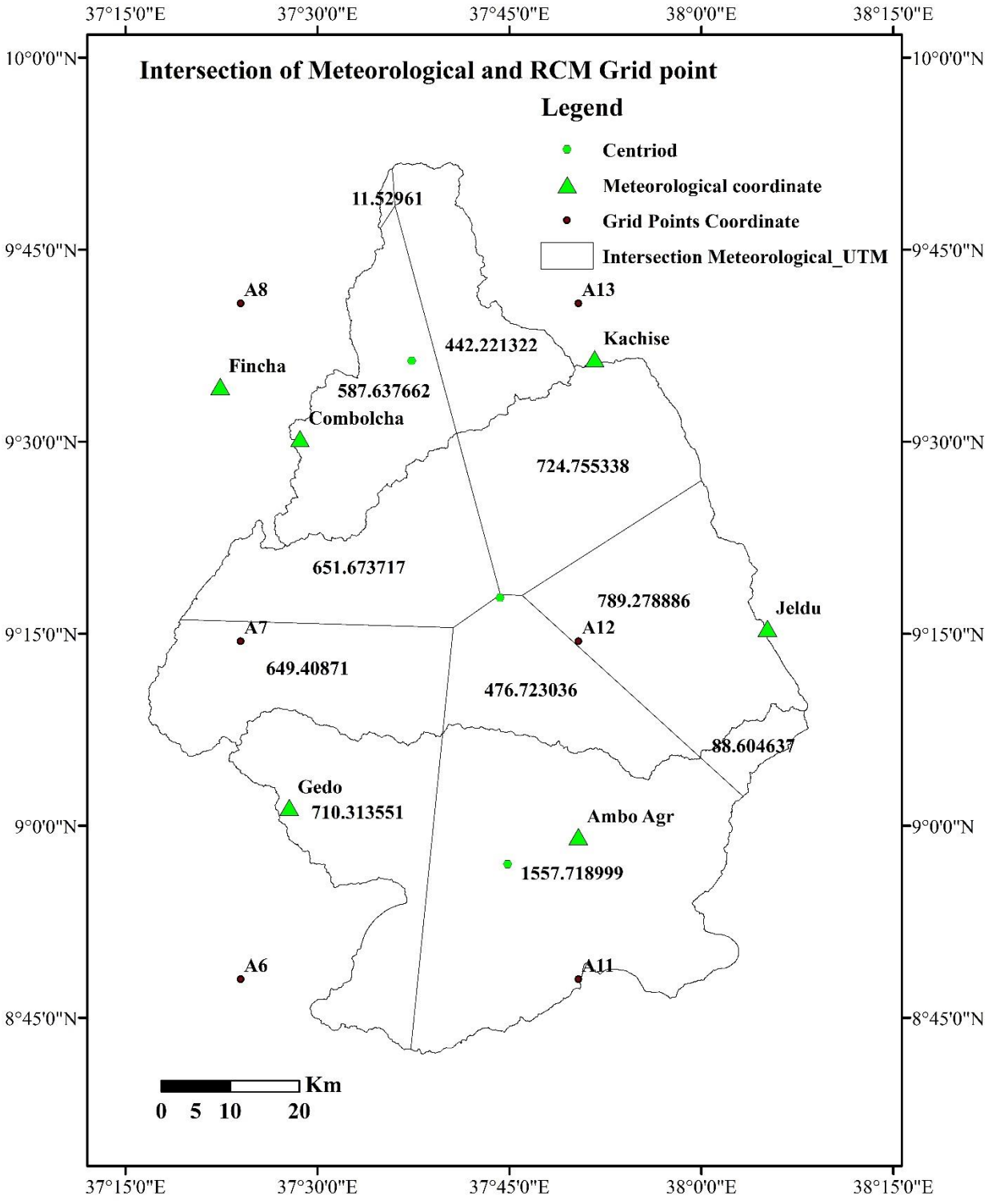

Figure 3. 8:Intersection of Meteorological and RCM Grid Points

3.8. Mann-Kendall (MK) Trend test analysis

MK-Trend test to identify trends in time series data for observed and future projected climate variables. The Mann-Kendall test gives interesting insight about annual precipitation and temperature data to understand climate change over time. For this study trend analysis has been computed by using non-parametric MK trend test since the purpose of a trend analysis is to determine if the values of a series of data have a general increase or decrease with time. Trend analysis of observed rainfall and temperature data of all used stations for this study were evaluated by using MK trend test in XLSTAT2021.Analyzing the long term series data for predicting the influence of potential climate change is an important application of statistics in recent researches.

3.9. Streamflow data transferring from gauged to ungauged watershed

Stream flow measurements are important for characterizing the hydrologic behavior of river basins within modeling frameworks, so that future assessments of hydrologic behavior in response to climate and/or land-use change can be obtained. The streamflow estimation at ungauged or poorly gauged basins are essential issue in growing economic countries like Ethiopia for Water resource management system and plan. The regional model developed for gauged catchments is used to estimate model parameters of ungauged catchments by respective Physical Catchment Characteristics (PCCs). But it needs more than two gauged stream flow around the target station or ungauged station. For this study Inverse Distance Similarity Weight of spatial were selected based on the physical catchment characteristic similarity correlation. In this study, the physical similarities between the donor and the target station were taken into account when selecting the appropriate donor station for the target station.

Table 3. 3:Physical characteristics of Upper Guder watershed or donor Station

Station	Elevation (m)	Latitude (m)	Longitude (m)	Area (Km^2)	Basin Slope (%)	Channel Length(Km)	AM Temp.	A.M.total Precip
Bello	2509	8.8667	37.7167	290	35.23	45	17.71	2.25
Fatto	2551	8.8667	37.6670	96	35.23	47	17.71	2.25
Guder	2518	8.9500	37.7500	524	20.23	62	17.71	2.25
Indris	2520	8.9333	37.7500	111	20.23	58	17.71	2.25

Table 3. 4: Physical characteristics used in Donor or upstream of Guder watershed

Physical Characteristics	Maximum	Minimum	Mean
Drainage Area (Km^2)	524	96	310
Elevation (m)	3221	1984	2602.5
AMTP(mm)	2.25	0	1.125
AMT(^0C)	24.44	10.98	17.71
Basin Slope (%)	35.23	20.23	27.73
Channel Length	62	45	52.5
Latitude	8.95	8.667	8.8085
Longitude	37.75	37.667	37.7085

Table 3. 5:Physical Characteristics of Downstream of Guder or Target station (Outlet)

Station	Elev.	Lat.	Long.	Area	Slope	Channel L.	AMT Target	AMTP
Target	1209	9.605	37.623	6165.87	15	132	16.61	4.79

qtarget$= \sum_{i=1}^{n} wi * qdonor$ and Qtarget= qtarget*A target

Where qtarget is the area normalized streamflow ($m^3/s/km2$) at the target station and donor is the area normalized streamflow ($m^3/s/km^2$) at the donor station i. the weights based on physical similarity can be calculated for all donor station by using the following equation.

$$wi=\frac{1/_{Sip}}{\sum_{i=1}^{n}\frac{1}{Si^p}} \text{ and } \sum wi = 1 \quad \ldots\ldots(3)$$

Where si is the similarity coefficient between the target station and donor station i and where the Exponent p is called a power parameter (p > 0). The station with the lowest similarity coefficient was selected as the donor station. The similarity coefficient was used both to select the donor stations and to transfer streamflow from several donor stations as the weight.

$$Si= \sum_{i=1}^{n} \frac{|Xi^{donor}-Xi^{target}|}{\Delta Xi} \quad \ldots\ldots(4)$$

Where i indicates one of a total of k selected basin characteristics values of basin characteristic i for the donor station and the target station, ΔX is a range of values for Xi donor in the dataset. Lower Si indicates a higher similarity between basins which it means the best donor with decrease the distance between donor and target station, but the weight coefficient is increase.

3.10. Model Setup

The relationship between GIS, HEC-GeoHMS, and HEC-HMS is the preprocessing of required geospatial data computations. After computing the hydrological model for future conditions, the process starts with the availability of DEM and GIS tools, watershed properties can be extracted by using automated procedures. Then the data assembly is complete, HEC-GeoHMS with the help of Arc-Hydro starts terrain preprocessing, basin processing, hydrologic parameter estimation, and spatial information to generate many input files to HEC-HMS model. This helps to estimate hydrologic parameters from the stream, sub-basin characteristics, gaged RF and streamflow data. Then input files provided and facilitation of the HEC-HMS model to calculate streamflow simulation.

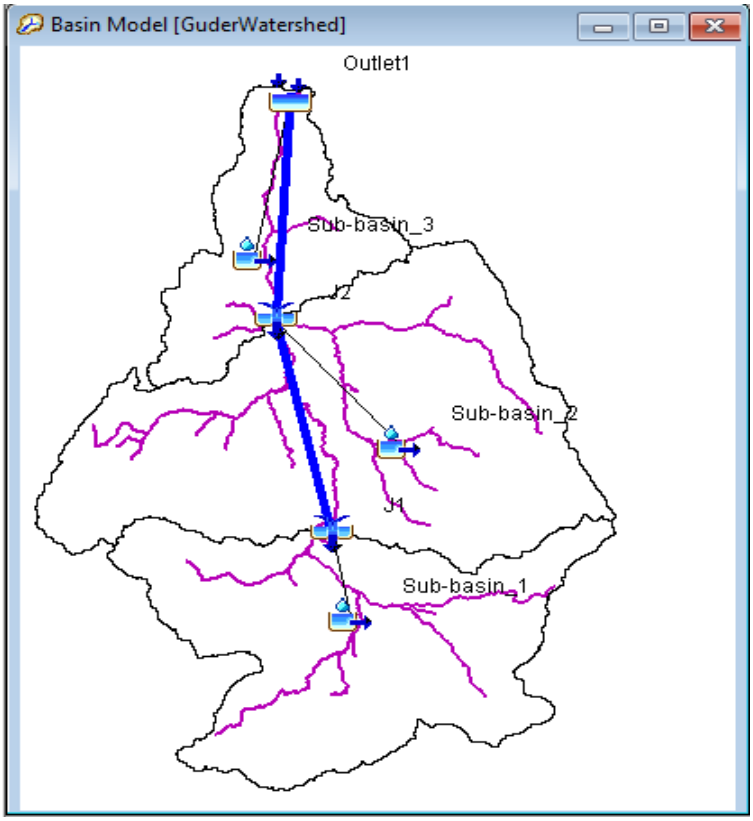

Figure 3. 9:Model setup and Sub-basins of Guder watershed

3.10.1. HEC-HMS Hydrological parameters used in basin model

The HEC model consists of three main model components; basin model, meteorological model, and control Specification. Among of them, the basin model consists different catchment characteristics such river reach, basin area, junction and outlets. This study basin model consists of sub-basin_1, sub-basin_2, sub-basin_3, J1, J2, R1, R2 and outlet where J and R stand for junction & reach respectively. There are different sub-basins elements for this study, the listed below are applied based on their purpose and suitability. To compute simulation, Loss (Curve number), Transform (SCS unit Hydrography), Base flow of recession and Routing (Muskingum) methods were employed.

i. Loss Method

The average curve number for sub-basins is computed using HEC- GeoHMS and this value is imported during the exporting of the Basin Model to HEC-HMS for initial parameter inputs before optimization**.** The curve number value of a certain land depends on infiltration characteristics of the soil and the land use/land cover conditions. The soil texture characteristics is one of the factor that determine infiltration of the soil. Soils of the study area are reclassified into hydrologic soil groups using their textural classes. The soil condition of the Guder watershed is dominated by type D soil (Clay loam, silty clay loam, sandy clay, silty clay, clay) that caused high runoff potential and low infiltration rates. The value of the CN varies from 100 (for waterlogged surfaces) to 30 for non-watertight surfaces with high infiltration values. The value of Initial Abstraction for the corresponding Curve Number value is calculated using the following formula.

$$Ia = 0.2 * S$$

$$S = \frac{25400 - 254 * CN}{CN}$$

Ia=Initial abstraction

S=Potential maximum retention value

ii. Transform

Transform methods is an approach for computing direct runoff at the outlet of watershed area from the excess precipitation falling over it and this is done based on principles of unit hydrograph. Unit hydrograph can be defined as the runoff hydrograph produced from excess rainfall of unit depth occurring over the watershed. The SCS unit hydrograph method was used for this study because the required parameter can simply be extracted from catchment characteristics using HEC-GeoHMS for initial estimations. The SCS unit hydrograph method requires only one parameter for each sub-basin: lag time between rainfall and runoff in the sub-basin to specified time to peak. The lag time is already computed in HEC- GeoHMS Model and imported with the Basin Model.

iii. Base Flow

Subsurface flow in the catchment is illustrated by base flow in HMS. Base flow comprises of interflow and flow in groundwater aquifer. There is insignificant contribution of base flow in case of short rainfall event, so it can be ignored. While in case of long rainfall event, the base-flow contributes to the recession limb of hydrograph and has a significant contribution in flood volume.

v. Routing-Muskingum

The Muskingum model seeks a method of parameter estimation to determine the values of the displacement time of the K wave and the mass coefficient of release x. Many methods or optimization techniques, including the trial-and-error method.

3.10.2. Model Calibration and validation

Model Calibration is a crucial step in any hydrological modeling study to reduce the uncertainty in the modeled discharge and systematic process of adjusting model parameter values until model results match acceptably the observed data. The quantitative measure of the match is described by the objective function. In the precipitation runoff models, this function measures the degree of variation between the observed and the computed hydrographs. The calibration process finds the optimal parameter values that minimize the objective function. Validation is essential to trust the model's performance to evaluate the model simulation outputs relative to the observed data (Muhammad Shahid Iqbal, 2018). The model performance will evaluate through visual inspection of the simulated and observed hydrographs and through a set of objective functions that measure the goodness-of-fit between simulated and observed values.

3.10.3. Model Performance Evaluation

The Model evaluation procedure include Calibration, Validation and Sensitivity analysis. The HEC-HMS uses the climate data and spatial data to calibration and validation of streamflow according to its own program parameters. For Model calibration and validation, daily measurements of flow Guder watershed for the period from 1986 to 2009 were used. The available hydro-meteorological data was divided into two (1989-2002) for model calibration and the other (2003-2009) for model validation. Then finally, the future streamflow simulations accomplished by running the HEC-HMS Model with the climate data under the CORDEX Project of both Scenarios RCP4.5 and RCP8.5. To evaluate the model simulation outputs relative to the observed data, model performance is determined by checking statistical parameters evaluation. For this study, the most common methods were employed.

1. Coefficient of determination (R^2)

The determination coefficient (R^2) describes the proportion of the variance measured in data by the model and R^2 values vary from 0 to 1, with values closer to 1 indicating better agreement between the data in comparison. It provides a measure of how well- observed outcomes observed desperation is explained by the prediction.

$$R^2 = \frac{\left[\sum_{i=1}^{n}(Q_S - \bar{Q}_S)(Q_O - \bar{Q}_O)\right]^2}{\sum_{i=1}^{n}(Q_S - \bar{Q}_S)^2 \sum_{i=1}^{n}(Q_O - \bar{Q}_O)^2} \quad \text{.......} \quad (5)$$

Where: Q_O Observed flow

$\bar{Q}_O$ The average of observed flow

Q_s The simulated flow and

$\bar{Q}_s$ The average simulated flow and n is umber of observed data points,

2. Nash-Sutcliffe coefficient (NSE)

Nash-Sutcliffe coefficient measures the efficiency of the model by relating the goodness of fit of the model to the variance of the measured data, range from $-\infty$ to 1. Efficiency values between 0 and 1 are considered acceptable for model performance, with an optimal value of indicates a perfect match of simulated discharge to the observed data. If NSE is equal to 0, the simulated results are as of accurate as the observed average; whereas an efficiency less than zero, ($-\infty <$ NSE < 0) the observed mean is more reliable in prediction than the simulated results.

$$\text{NSE} = 1 - \left[\frac{\Sigma_{i=1}^{n}[Q_0 - Q_s]^2}{\Sigma_{i=1}^{n}[Q_O - \bar{Q}_O]^2}\right] \quad \text{..... (6)}$$

3. Percent of Bias (PBIAS)

The PBIAS indicates the average tendency of the simulated to be larger or smaller than their observed values. The PBIAS can be utilized as the indicator of under or over-estimation which means negatives PBIAS indicates the under-estimation model generated values with respect to the measured values.

$$\text{PBIAS} = 100^* \ \frac{\sum_{i=1}^{n}(\text{Si} - \text{Oi})}{\sum_{i=1}^{n}(\text{Oi})}$$

Observations Standard Deviation Ratio (SDR)

Observations Standard Deviation Ratio (RSR), RSR is calculated as the ratio of the root mean square error and standard deviation of measured data, as shown in the following equation:

$$RSR = \frac{RMSE}{STDEVobs} = \left[\frac{\sqrt{\Sigma_{t=1}^{n}(Q_0 - Q_s)^2}}{\sqrt{\Sigma_{t=1}^{n}(Q_O - \bar{Q}_O)^2}}\right] \text{.....} \quad \text{..... (7)}$$

STDEVobs is the standard deviation of observed data of the constituent being evaluated, RSR varies from the optimal value of 0, which indicates zero RMSE or residual variation and therefore perfect model simulation, to a large positive value.

3.11. Flood Frequency Analysis Methods

The data analysis often requires the estimation of parameters for a probability distribution. Before the analysis can be done, the parameter for each selected distribution needs to be estimated first, even if an acceptable distribution is selected, a proper estimation of parameters is important. Hydrologic systems are sometimes impacted by extreme events, such as floods. The magnitude of the flood is inversely proportional to its frequency of occurrence. When the magnitude of flood predicted accurately it reduces the risk of hazard. To avoid the problem of data dependency, the annual maximum flow series model was selected. In addition to this, AM series is widely and universally used model by different researchers for the purpose of FFA result, to keep away from the concern of requirement on data, AMF series model was chosen for this study.

3.12. Goodness of- fit test and selection Probability Distribution

GOF tests are used to assist in finding the distribution that best fits the given data. These tests describe the differences between the observed data values and the expected values calculated from the specific distribution in case of parameter estimation. Statistical Software (Easy Fit5.6) trial version was used to select the best fit probability distribution with its method of parameter estimations, a goodness of fit tests and to check the estimation accuracy of each RCMs and observed data. In this study, Distributions fit tests were employed like Anderson-Darling (A-D), Kolmogorov-Smirnov (K-S) and Chi-Squared (x^2) tests were used for the goodness-of-fit tests. These selected distributions have been checked by using the Easy Fit software application weather the distribution has goodness of fit test or not for flood series data.

3.12.1. Probability Distribution and Parameter estimation

A fundamental step in flood frequency analysis is the selection of an appropriate probability distribution model that can accurately simulate the observed flood series. To do this, in this study distributions are selected based on best fits of goodness. The selected distribution was Generalized Extreme Value method for AM data series. The maximum likelihood estimation (MLE) technique generally show less bias and provides a more consistent approach to parameter estimation problems. It provides the smallest variance of the estimated parameters, most accurate method, especially for large datasets since it leads to efficient parameter estimate distribution.

3.12.2. Generalized Extreme Value (GEV) Distribution

The GEV distribution was used to fit the annual maximum discharges using the method of maximum likelihood parameter, and estimate changes in the flood levels and has three parameters distribution; shape (k), location (μ), and scale σ). GEV distribution is a combination of three different distributions according to the shape parameter, when the k=0, the GEV distribution reduces to Gumbel (EV1) distribution, when K < 0), we have Extreme Value type II (Fetchet), when K > 0, GEV becomes Extreme Value Type

$$\mathrm{QT} = \mu + \frac{\sigma}{k}\left(1 - (\ln\left(1 - \frac{1}{T}\right) \wedge k\right) \quad \text{.....(8)}$$

k=Shape parameter

μ=Location parameter

σ=Scale parameter

3.13. Evaluating flood frequency analysis under climate change

To evaluate flood magnitude and frequency under climate change after calibrating the hydrological model for the study area is extremely crucial. First, for RCM outputs, going to extract climate data for RCP 4.5 and RCP8.5 scenarios. The next step, flood frequency scenarios that can represent the effect of climate change on flood extremes from acceptable ranges of climate scenario known from dynamically downscaled RCM outputs and continuous simulation modeling is developed. The downscaled climate scenario consists of maximum temperature; minimum temperature and precipitation together was used as input to the hydrological model. The hydrological model was simulated a streamflow corresponding to future climate conditions for bias corrected precipitation and temperature data under the RCP 4.5 and RCP8.5 scenarios. The baseline period (1971-2000) used to define the observe climate with which climate change information is usually combined to create a climate scenario while the periods (2041- 2070) and (2071- 2100) were employed for future scenarios analysis.

3.13.1. Flood magnitude under climate change

The flood magnitude of future period was compare with baseline flood magnitude at time horizons under dominant RCP4.5 and RCP8.5 changes in flood magnitude will be estimated for each ensemble under climate scenarios. The quantile estimations for the time horizons (2041-2070) and (2071-2100) were used to calculate for the 2, 5, 10, 25, 50,100,200,500 and 1000 recurrence intervals under the RCP 4.5 and RCP8.5 scenarios comparison carried out.

3.14. Conceptual Frame work

The study required different materials and methods to arrive at the stated objectives. Regionally downscaled climate, meteorological, hydrological, digital elevation model, land use and land cover and soil data were required. Regionally Downscaled Climate change data derived from HadGEM2-ES Global climate model outputs that are dynamically downscaled by the CORDEX-Africa program using RCA4 regional model for the Representative Concentration Pathway scenario, RCP4.5 & RCP8.5 scenarios. Those data were selected to the local impact based on the grid points which are fitted to the study area by using bias correction method. The data input is bias-corrected by Delta-change and Scaling variance method were used to estimate the future climate change for hydrological model and its impact on hydrology of the catchment.

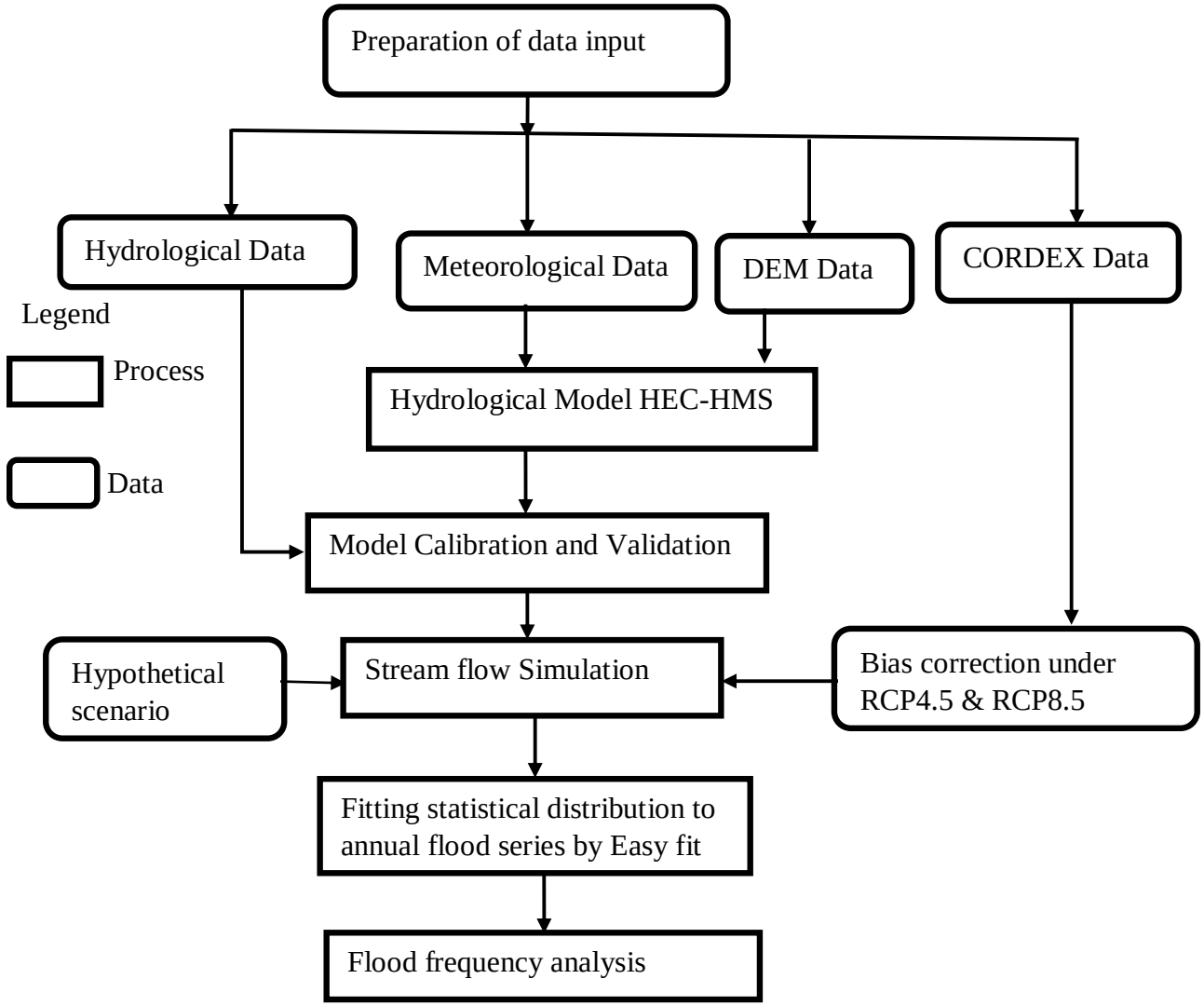

Figure 3. 10: General frame work of the study

4. RESULTS AND DISCUSSIONS

The analysis of climate change trends in relation to the derivation of climate change scenarios by disrupting the observed series with increments deduced from the HadGEM2-ES climate model simulations. The spatial resolution of Africa CORDEX-RCMs grid data size is at 50km*50km and aggregate metrics for Rainfall, T_{Min} and T_{Max} for the six grid cells spanning of Guder catchment. The potential Evapotranspiration is calculated for three sub-basins based on areal temperature by Thiessen polygon using T_{Max} and T_{Min} of observed and RCM data. The hydrological studies are used to assess the potential consequences of climate change on streamflow in the Guder Watershed. The future streamflow data was generated by using RF and temperature data based on the calibrated and validation HEC-HMS model. Lastly, analyzing the flood frequency of generated streamflow under climate change requires employing the AMS data.

4.1. Performance evaluation of regional climate model output

The performance of the model simulation outputs was evaluated by comparing observed and RCMs Rainfall extracted to understand in replicating or capturing observed average annual rainfall. The comparison was performed to determine the capability of CORDEX RCMs to simulate the annual cycles. When comparing the gauged mean annual rainfall to model counterparts there have differences, that all the models underestimated the observed Guder watershed annual rainfall amount. The mean annual precipitation of overlapped period for Bias correction (1986-2000) of Guder watershed which computed by Thiessen polygon, areal RF (SB_1, SB_2& SB_3) was 1305.5mm and 1069.51mm for observed and models respectively.

The performance of the CORDEX rainfall simulations assessed under the basis of the time-series based evaluation metrics. Mean annual rainfall amount of Guder watershed compared as obtained from gauging data and climate model. Three Stastical model performance evaluation criteria BIAS, RMSE and R^2 were used to evaluate how the RCMs perform in simulating the rainfall as shown in table 4.1. RMSE is the absolute error the climate models in simulating the climate variables. The smaller the absolute value of BIAS and the smaller RMSE indicates the better is the model performance and the vice versa. In terms of BIAS, and RMSE (Root Mean Square) the RCA4 model performed best whereas the CCLM4-8 model performed poorest.

Table 4. 1:Performance of the CORDEX-RCMs mean annual RF of Guder watershed

Stastical Evaluation	Observed	CCLM4-8	RACMO22T	RCA4	Ensemble
Annual RF(mm)	1305.5	1001.5	1066.68	1140.35	1069.51
Mean	3.57	2.74	2.92	3.12	2.93
Bias	….	-23.279	-18.287	-12.645	-18.07
RMSE	….	0.838	0.653	0.552	0.761
R^2	….	0.014	0.019	0.174	0.102

Table 4. 2:Annual mean Rainfall of Guder sub-basins (1986-2000)

Stations	Observed	CCLM4-8	RACMO22T	RCA4
Sub-basin_1	886.65	1256.65	1122.61	2157.10
Sub-basin_2	1329.290	935.19	1041.96	600.99
Sub-basin_3	1700.46	812.67	1035.48	662.96

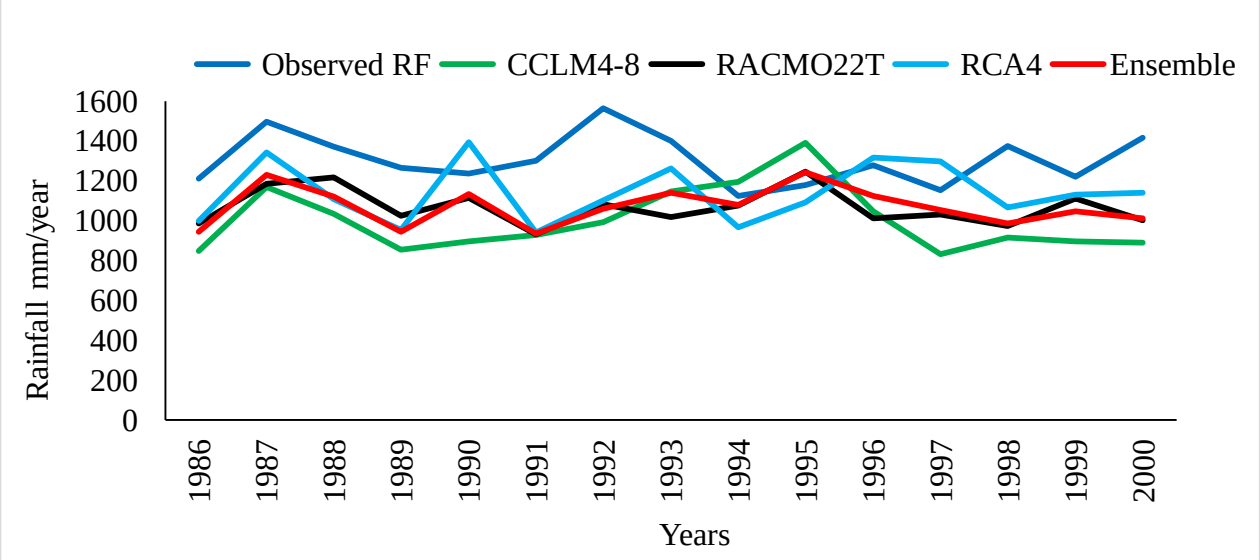

Figure 4. 1: The Comparison of Annual rainfall of Observed and RCM baseline

4.2. Evaluation of Bias Corrected Precipitation and Temperature

The daily bias corrections between the observed and simulated variables during the control period for each RCM models were applied. The output RCP precipitation, maximum and minimum data temperature is not directly used for climate change impact assessment. To remove and correct uncertainty of between downscaled RCM daily data and the observed climate variables, the bias correction is being carried out for Rainfall, T_{Max} and T_{Min} for Guder Watershed. The selected method for this study was Delta Change Correction (multiplicative) and Variance Scaling method significant corrects the bias raw RCMs respectively for precipitation and temperature.

The Projected future scenarios have been divided into two successive periods of 30 years based on WMO recommendations. The climate data for baseline period (1971-2000) data with observed climate variables for future different RCP's Scenarios for two horizon time of (2041-2070) and (2071-2100) climate data was bias corrected. The mean monthly precipitation, maximum temperature and minimum temperature of observed, RCPs uncorrected and RCPs corrected compared for the catchment. The RCPs output predictions of precipitation, maximum and minimum temperature resembled in producing the observed data for the base period. Therefore, it is plausible to use RCPs data output for future prediction for the catchment.

4.2.1. Bias corrected Precipitation

The daily bias corrections between the observed and simulated variables during the control period for each RCM models were applied. The outputs of the raw RCMs underestimate and overestimate the mean monthly rainfall and as compared to an Observed RF. At monthly level, as shown in figure 4.2, some months have overestimated RCP precipitation as compared to the observed precipitation (January, February, March, and April), while the rest months are underestimated especially the three months July, August and September which are found in the main rainy season. Areal precipitation has been computed under each scenario for general analysis of precipitation over the catchment. The values indicated that mean monthly RF of the area is monomodal, high RF relatively recorded in the main rainy season, and low RF recorded in dry season.

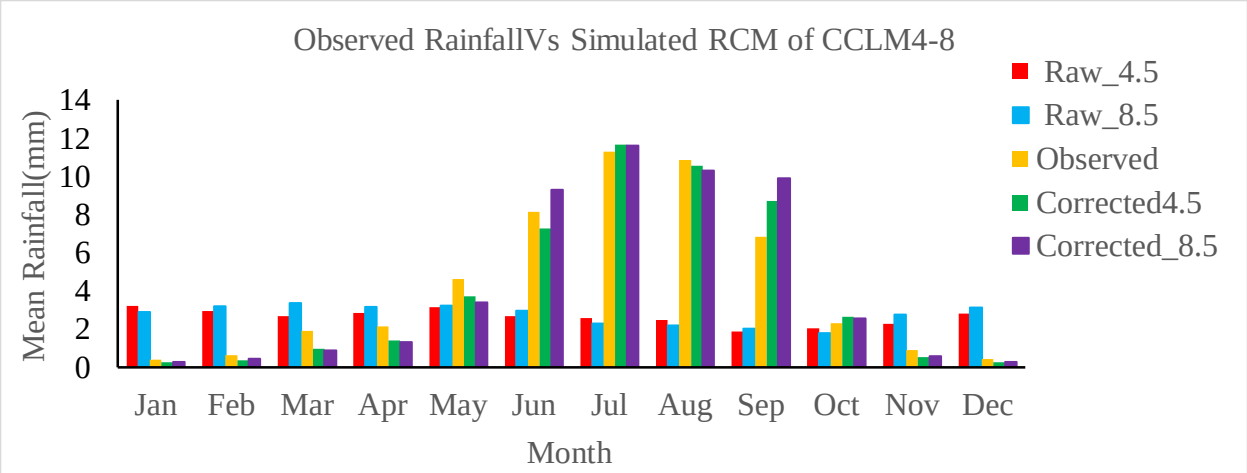

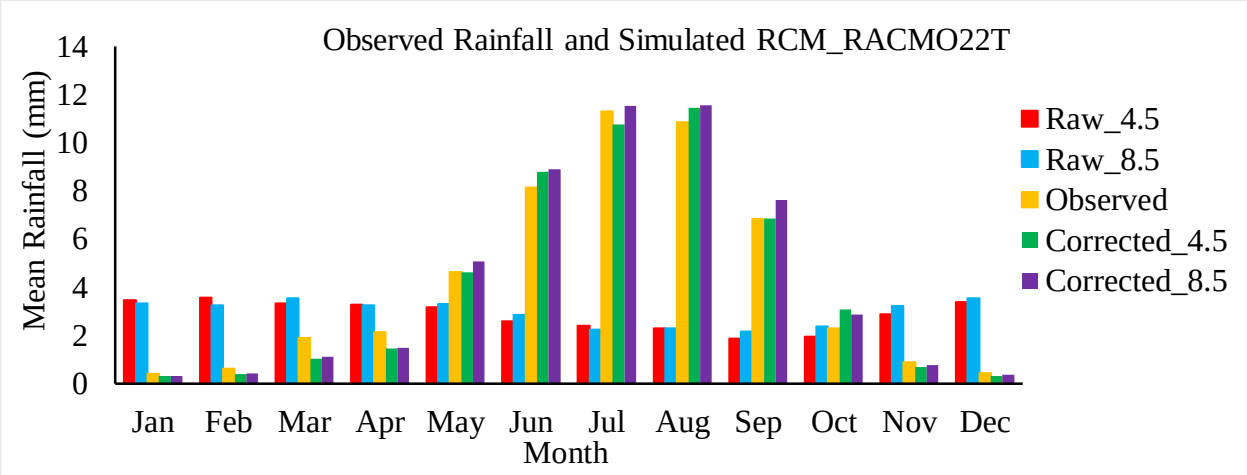

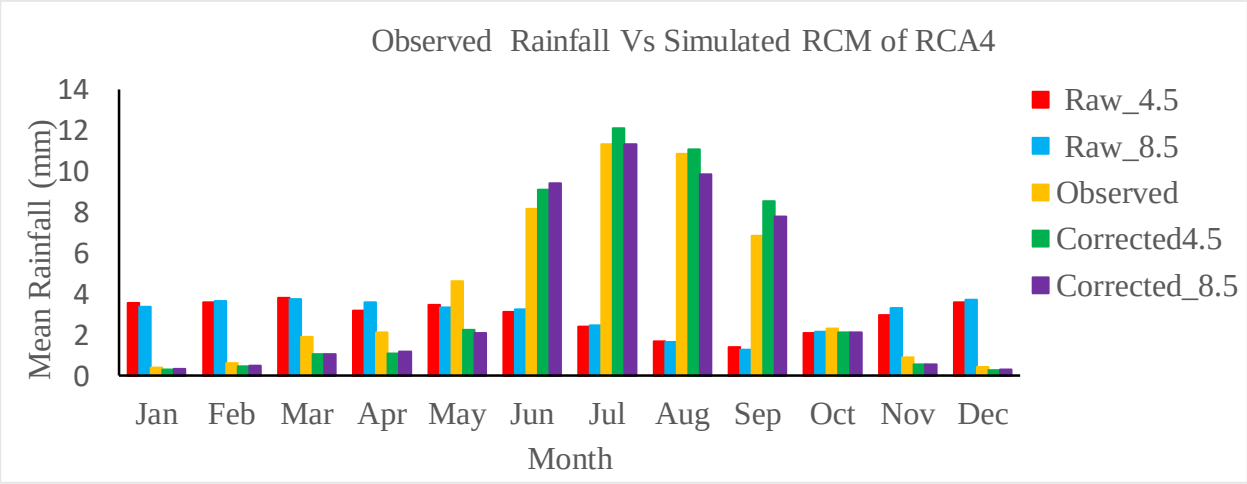

Figure 4. 2: Monthly Mean of Observed RF and Bias Corrected, Raw RCMs (2041-2100)

4.2.2. Bias Corrected RCMs Temperature

The bias corrected mean T_{Max} and TMin in the area shows a good agreement with controlled and observed period.

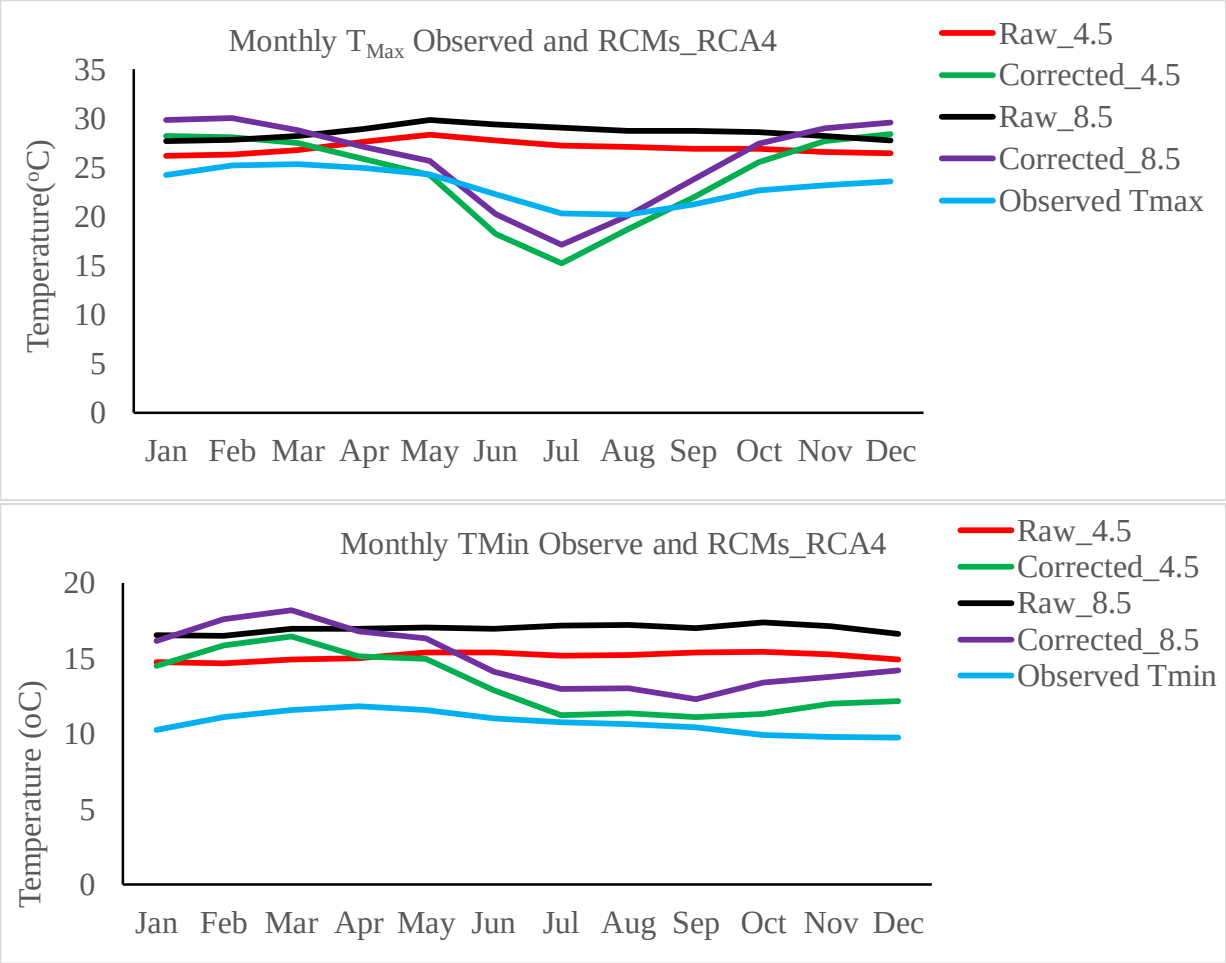

Figure 4. 3: Monthly mean of Observed, raw RCMs and Bias Corrected for TMax and TMin

4.3. Mann-Kendal(MK) Trend Analysis

The Mann-Kendall (MK) non-parametric test is frequently used to quantify the significance of time series trends and also employed to detect monotonic trends in time series of climate data, hydrological or environmental data. In this research Mann-Kendal trend analysis across Guder watershed and streamflow trend test based on the baseline period (1971-2000) future meteorological data from 2041 to 2100. Non-Parametric MK Stastical test was used to detect trends RF and Temperature in each three RCMs over the series aggregated to areal mean of catchment. If the p value is less than the significance level $\alpha = 0.05$ H_o, (there is trend), hence, the hypothesis is rejected. Rejecting Ho indicates that there is a trend in the time series while accepting Ho indicates no trend-detected hypothesis is accepted. Rejecting the null hypothesis implies that the result is said to be statistically significant at $\alpha = 0.05$ level of significance level and Vice versa.

4.3.1. Trend test of observed hydro-meteorological datasets

The MK test statistics was applied to the annual mean observed areal Rainfall pattern of Guder watershed. Areal annual mean of Observed, baseline and future RF of seven stations over Guder watershed is calculated by thiessen polygon method. The computed P-value is greater than significant confidence level (5%) and one cannot reject H_0. The result of Mk test showed that slightly increase trend in Annual Areal precipitation of Guder watershed. Trend slope magnitude is increase by 0.991 mm/year, 0.065°C/year & 0.072°C/year for Precipitation, TMax & TMin respectively in observed data of Guder watershed. Depending on the computed p-values of Precipitation is greater than the significance level alpha =0.05 its accept the null hypothesis H_0, TMax & TMin are rejected because of p-values less than the significance level alpha.

Table 4. 3:MK statistical result of Observed Rainfall, TMax and TMin

Variables(1986-2018)	Kendall's tau	p-value	Sen's slope	S	Alpha(α)	Trend Type
Precipitation	0.032	0.808	0.991	16	0.05	AcceptH_0
TMax	0.569	<0.0001	0.065	282	0.05	RejectH_0
TMin	0.504	<0.0001	0.072	250	0.05	RejectH_0

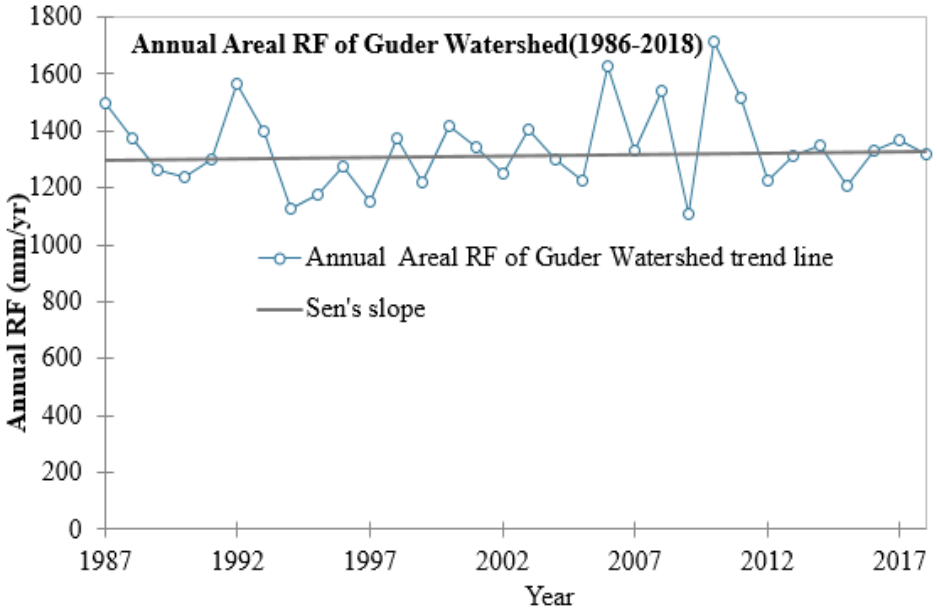

Figure 4. 4: Annual Areal observed RF of Guder Watershed

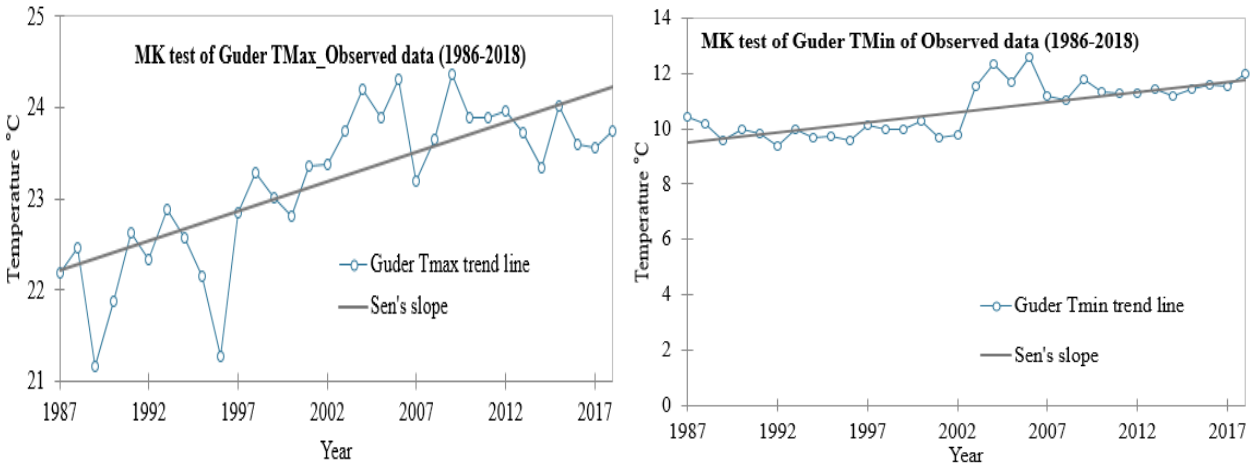

Figure 4. 5: MK test of Guder TMax and TMin Observed

4.3.2. Trend test of future hydro-meteorological datasets for RCP4.5 and RCP8.5

4.3.2.1. Precipitation Trend test (2041-2100)

MK trend test of Areal precipitation of Guder Watershed under two scenarios RCP4.5 and RCP8.5 are tested and their statistic illustrated below. The trend was done for entire period of two horizon time which test show that the change is non-significance over the catchment at the given 5% interval confidence level and slightly increase with 0.852mm/year ,0.825mm/year two scenarios of RCP4.5, RCP8.5 respectively. The computed p-values for RCP4.5 and RCP8.5 are less than the significance level α= 0.05, null hypothesis H_0 is rejected.

4.3.2.2. Temperature trend test

MK trend test of temperature has done under two RCPs scenarios for Maximum temperature and Minimum temperature of Guder watershed. Annual average temperature will increase non-significance for both RCP4.5, RCP8.5 of TMax and RCP8.5 of TMin 0.028ºC/year, 0.051 ºC/year and 0.045ºC/year respectively, that reject the null hypothesis H0, and accept the alternative hypothesis Ha for average TMin, 0.001ºC/year under RCP4.5 scenarios because of p-value 0.750 which is greater than alpha level.

Table 4. 4:MK Trend test of annual mean areal RF, TMax and TMin of RCP4.5 and RCP8.5

Variables	RCP's	Kendall's tau	p-value	Sen's slope	S	Alpha(α)	Trend Status
Precipitation	RCP4.5	0.543	<0.0001	0.852	836	0.050	RejectH_0
	RCP8.5	0.526	<0.0001	0.825	820	0.050	RejectH_0
T Max	RCP4.5	0.621	<0.0001	0.028	956	0.050	RejectH_0
	RCP8.5	0.809	<0.0001	0.051	1246	0.050	RejectH_0
TMin	RCP4.5	0.030	0.750	0.001	46	0.050	AcceptH_0
	RCP8.5	0.827	<0.0001	0.045	1274	0.050	RejectH0

XLSTAT sketches the graph of MK trend automatically for future mean areal RF, TMax and TMin show increasing trend over the catchment for the study area was analyzed using the MK test and the results in Fig 4.6 revealed that there has a significant increasing trend except for TMin of RCP4.5, indicates an increasing trend but not significant at 5% significant level since the p-value is greater than the significant level alpha = 0.05.

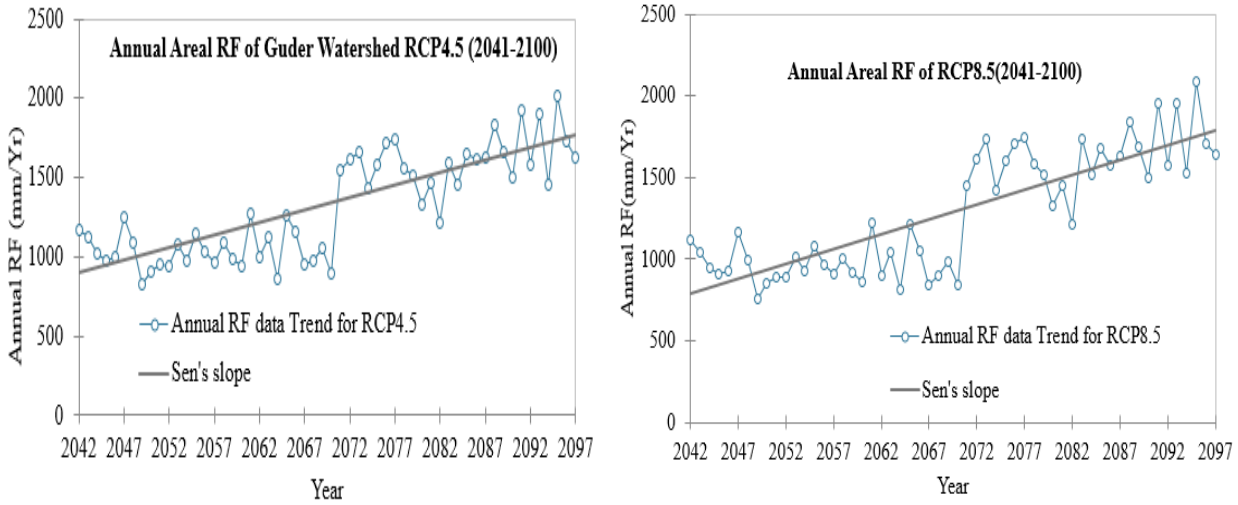

Figure 4. 6: MK Trend Test Annual Areal Rainfall of RCP4.5 and RCP8.5 (2041-2100)

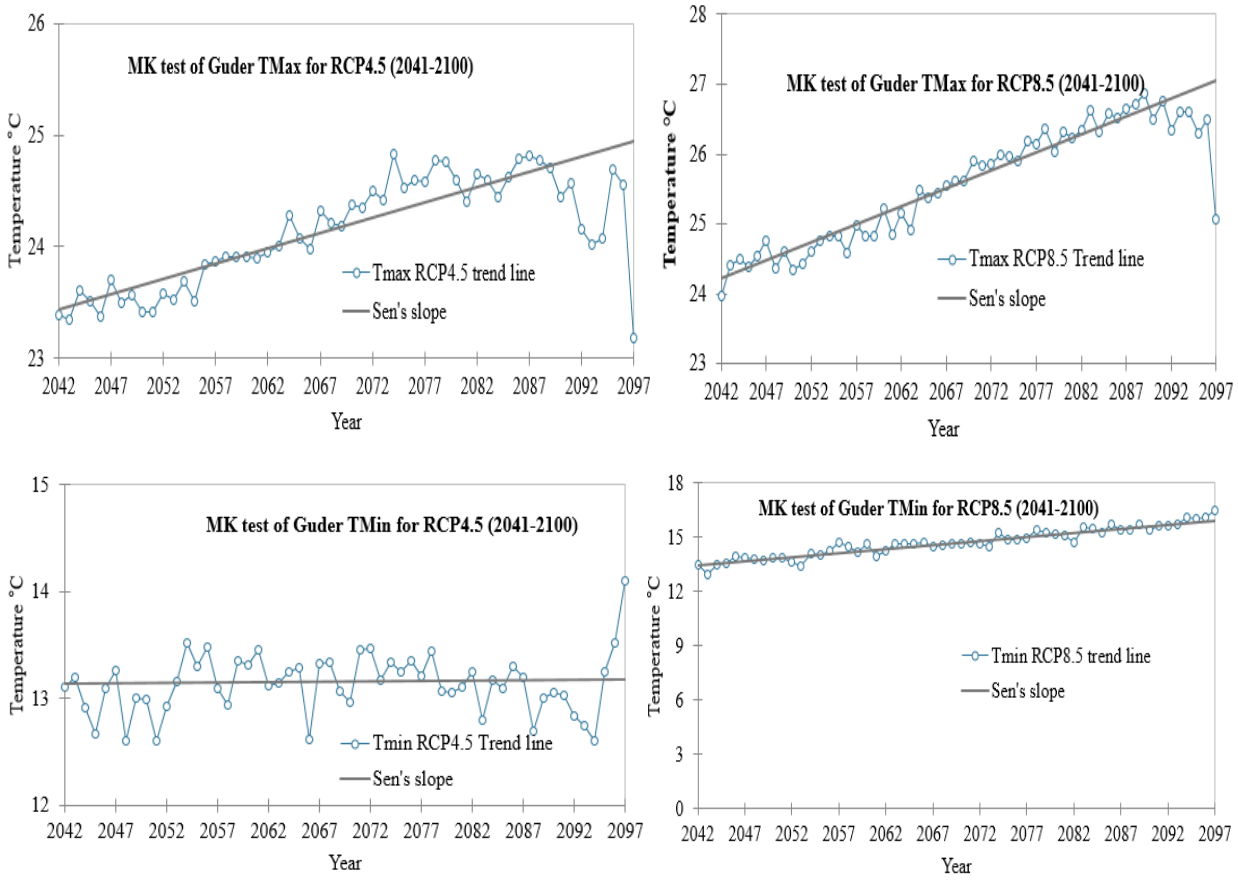

Figure 4. 7: MK Trend test for TMax & TMin of RCP4.5 and RCP8.5 (2041-2100)

4.4. Projected Future Climate Change variables for RCMs

4.4.1. Precipitation

The percent change of mean monthly, seasonal and annual RF results showed that the future RF variability on the catchment. The hydro-climate variable changes analysis was done between the baseline period and projected future data to know the positive or negative difference of change. All RCPs projected are decrease up to -1% in all seasonal and annual time except at mid-term (2041-2070) of RCP4.5, RCP8.5 and RCP4.5 of long-term (2071-2100) time horizon which increase 1-4.6% for CCLM4-8 RCM under Guder watershed. Under RACMO22T model the RF is decreased 1-1.5% for both RCP4.5 &RCP8.5 (2041-2100) in all Seasonal and Annual times, except RCP4.5 & RCP8.5 of long-term (2071-2100) is increase in Spring, Summer and annual 1-5% in magnitude. The precipitation changes of RCA4 model will increase by 1% in Spring, 4.5% in Summer and 2% in Annual time for RCP4.5 & RCP8.5 of long-term (2071-2100). But during the Winter and Autumn of two horizon time of RCP4.5 &RCP8.5 also at the mid-term of Spring,

Summer and Annual the RF is decrease by-1%. The Ensemble change RF of Guder watershed increase 1-6% in Spring, Summer and Annual at two horizons time of RCP4.5 & RCP8.5, except spring season of mid-term RCP8.5. But its decreases 1-2 % for Winter and Autumn under all RCPs.

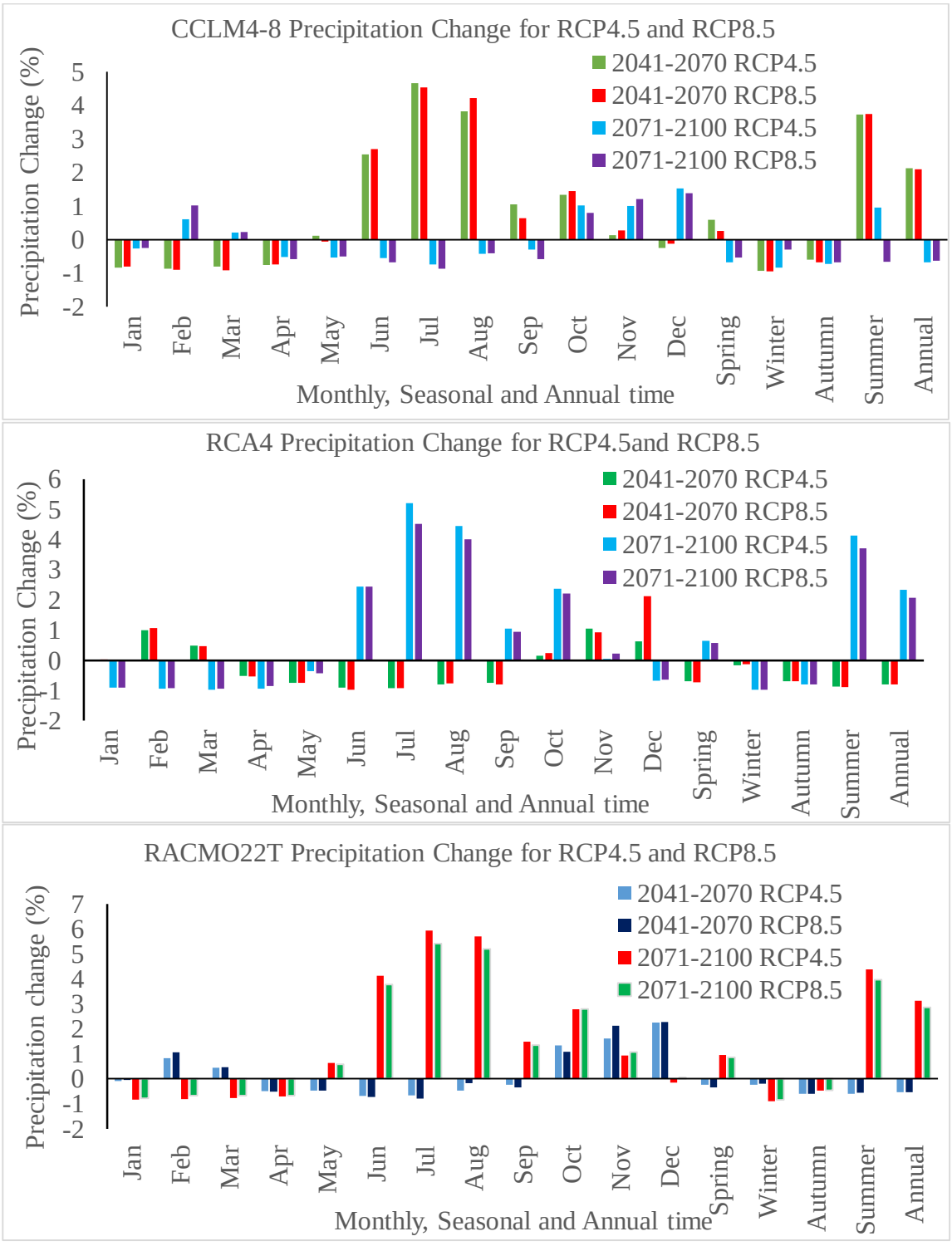

Figure 4. 8: Monthly, Seasonal and Annual Rainfall percent change of RCMs

4.4.2. Temperature Change

Future projected of Average minimum temperature of Guder watershed under all RCMs and RCPs scenarios will increase up to 0.7ºC for two horizons time at all seasons, Annual and Months except October for CCLM4-8 & RACMO22T. The average maximum temperature of all RCMs under RCP4.5 and RCP8.5 increase in Spring and Winter is 0.3 ºC, also in Annual 0.2ºC at mid-term & far term. But during Summer season average of TMax of all RCMs will decrease up to 0.2% for (2041-2070) and (2071-2100). TMax During the Autumn season for RCP4.5 & RCP8.5 of midterm the magnitude of temperature is decrease up to 0.2ºC and increase up to 0.2ºC at far term of RCP4.5 & RCP8.5 under all RCMs.

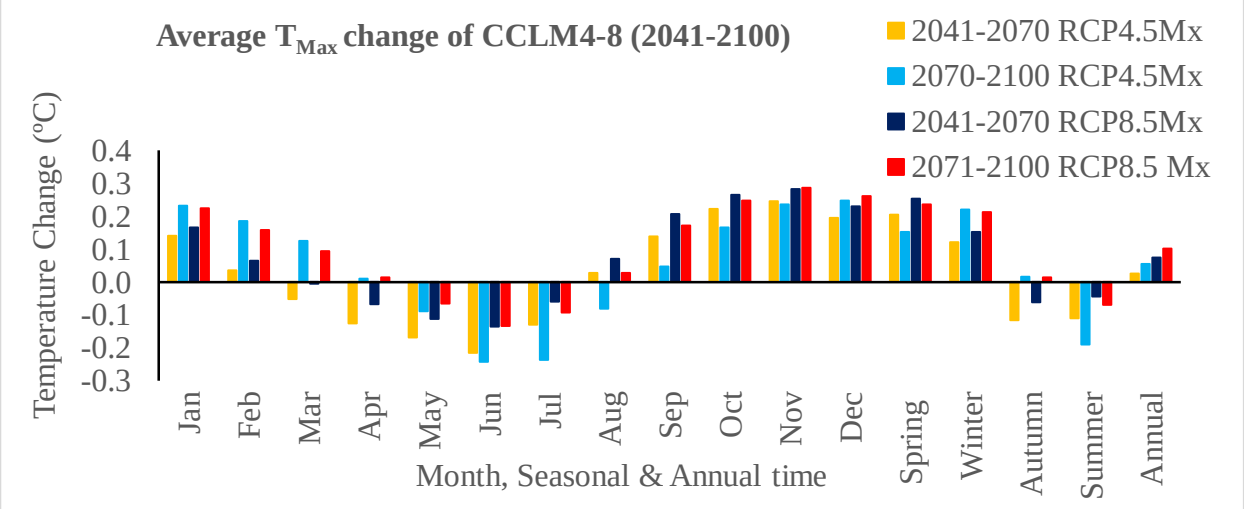

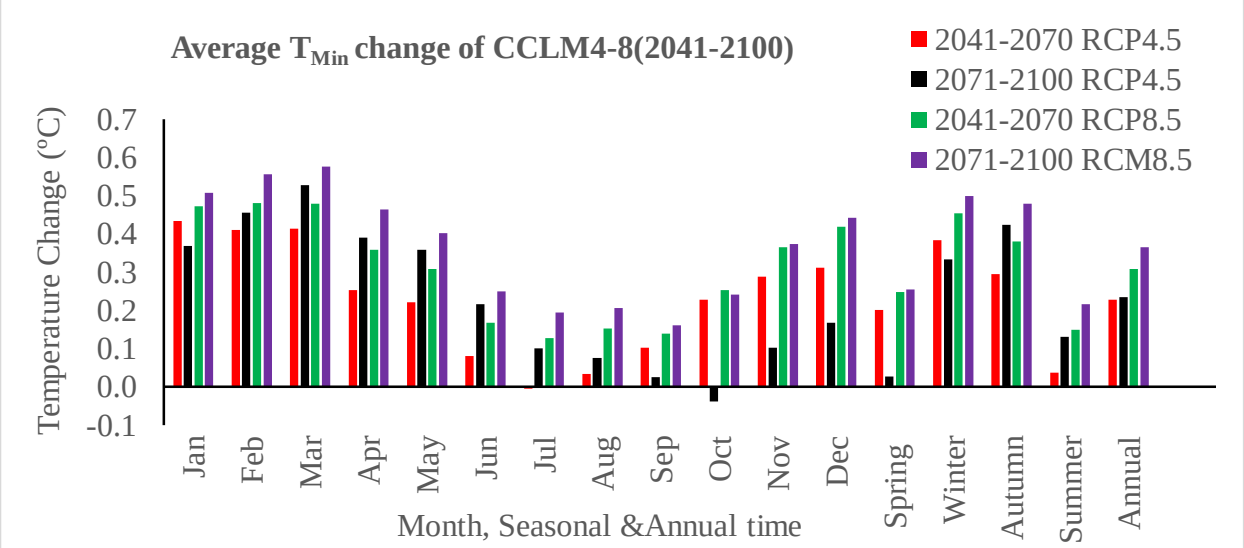

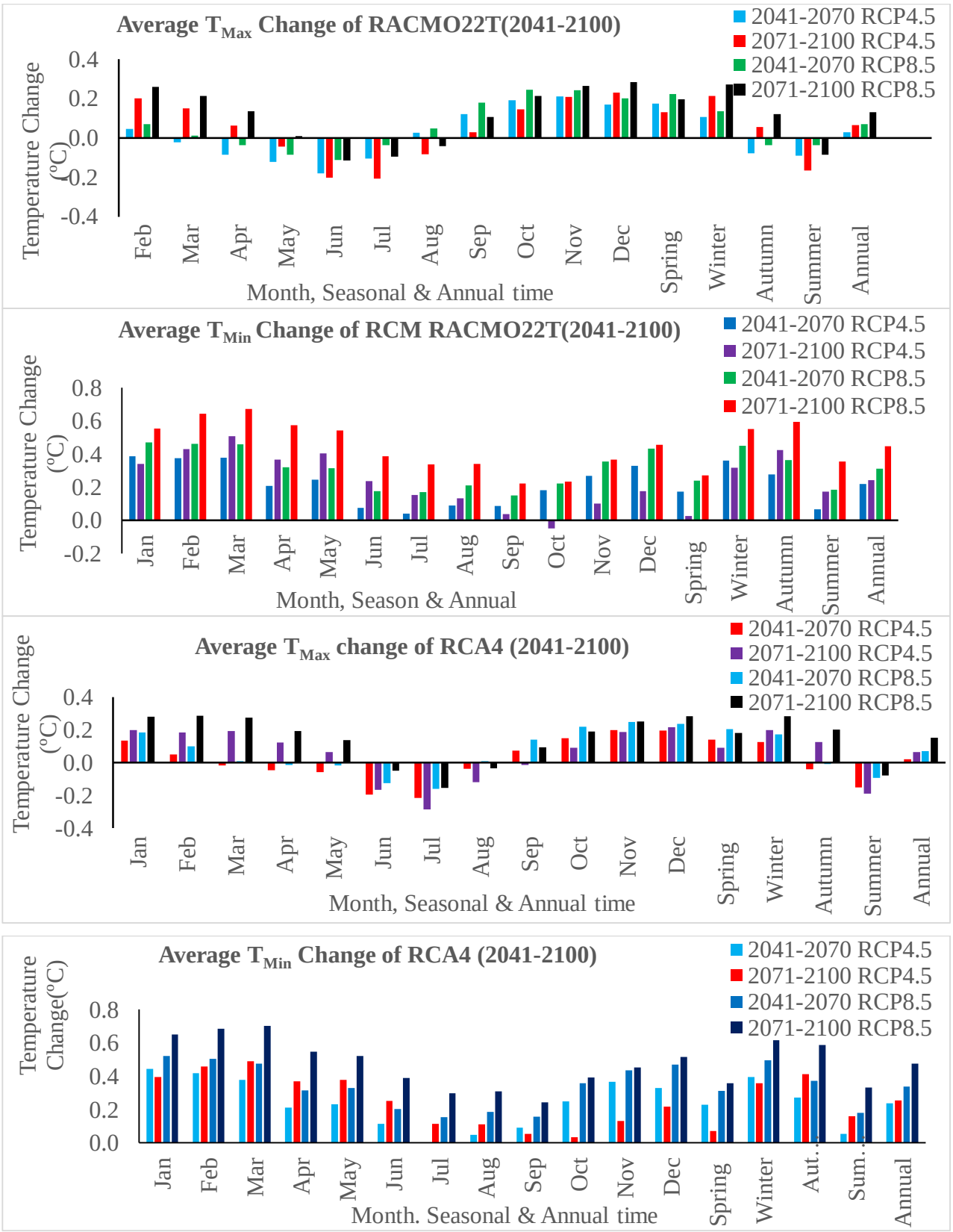

Figure 4. 9: RCMs average Temperature change

4.5. HEC-HMS Hydrological Model Results

The HEC-HMS program was selected for the current study due to its versatility, capability for flow generation, automatic parameter optimization, and its connection with GIS through HEC-Geo-HMS. The systematic search for the optimum parameter is carried out using automatic HEC-HMS Model parameter optimization from the model compute toolbar regarding observed flow of Guder watershed.

4.5.1 Model sensitivity Analysis

Sensitivity analysis is a process of selecting powerful parameters which can significantly affect model simulated result. To find the best value relate to observed and simulated streamflow of the catchment. Optimization of objective function needs changing of parameters to find the best value to relate observed and simulated daily streamflow. The sensitivity parameters are selected from the value of sensitivity function the results showed that with respect to peak flood magnitude, the event model was most sensitive the initial. In terms of peak discharge, the event model was most sensitive to the recession constant of base flow. Recession constant and ratio to peak were found to be the most sensitive parameters for the simulated stream flow for all the three sub basins. In this analysis sensitive analysis adopted for evaluating the model parameters were CN or loss, SCS Unit hydrograph (Transforming), Routing (Muskingum), Recession Constant, Ratio to peak.

4.5.2. Model Calibration and Validation

For this research, HEC-HMS model output results including Simulation, Calibration and Validation of flow data for observed period 1986-2009. The model was calibrated at the Guder watershed Outlet for the period of 1989 to 2002 daily data, where the three years (1986-1988) were used to “warm-up” the model. The period starting from 2003 to 2009 was used as validation period. The details for calibration and validation with their values of optimization criteria including model parameters are illustrated below. Model parameters were calibrated manually followed by HEC-HMS automatic optimization until the satisfactory agreement between simulated and observed flow was obtained. The model goodness of fit and the model performance was evaluated after adjusting the parameters. The optimization parameter value has taken for future simulation of the outflow using climate scenarios RCP4.5 and RCP8.5.

Table 4. 5:Calibrated initial value and Optimized Parameters of the sub-watershed

Element	Parameter	Initial Value	Optimized Value
Sub-basin_1	Curve Number(CN)	74.355	73.063
	Loss (Initial Abstraction)	9.3312	9.2999
	Peak to ratio	0.6954	0.7137
	Recession Constant	0.3920	0.3832
Sub-basin_2	Curve Number(CN)	79.358	78.936
	Loss (Initial Abstraction)	12.312	11.890
	Peak to ratio	0.3945	0.3743
	Recession Constant	0.89484	0.84517
	Routing (Muskingum K)	28.560	28.626
	Routing (Muskingum X)	0.3846	0.39698
Sub-basin_3	Curve Number(CN)	80.578	81.794
	Loss (Initial Abstraction)	13.256	14.622
	Peak to ratio	0.4264	0.4178
	Recession Constant	0.8360	0.8286
	Routing (Muskingum K)	32.645	33.202
	Routing (Muskingum X)	0.28642	0.26715

The model has been calibrated systematically and automatically to optimize for best possible option to identify and gives the trial of parameters depending on objective function. By rerunning the automatic calibration process used to minimize objective functions, like sum of the absolute error, sum of the squared error, percent error in peak, and peak weighted root mean square error by inspecting concurrently streamflow volume and peak flow depth. The model well-predicts streamflow depth and peak streamflow respectively values in the watershed with the optimized parameters. Since the goal of calibration scheme is to find reasonable parameters that yield the minimum value of the objective function. Hence for this study the peak-weighted root mean square error (RMS) objective function has been used.

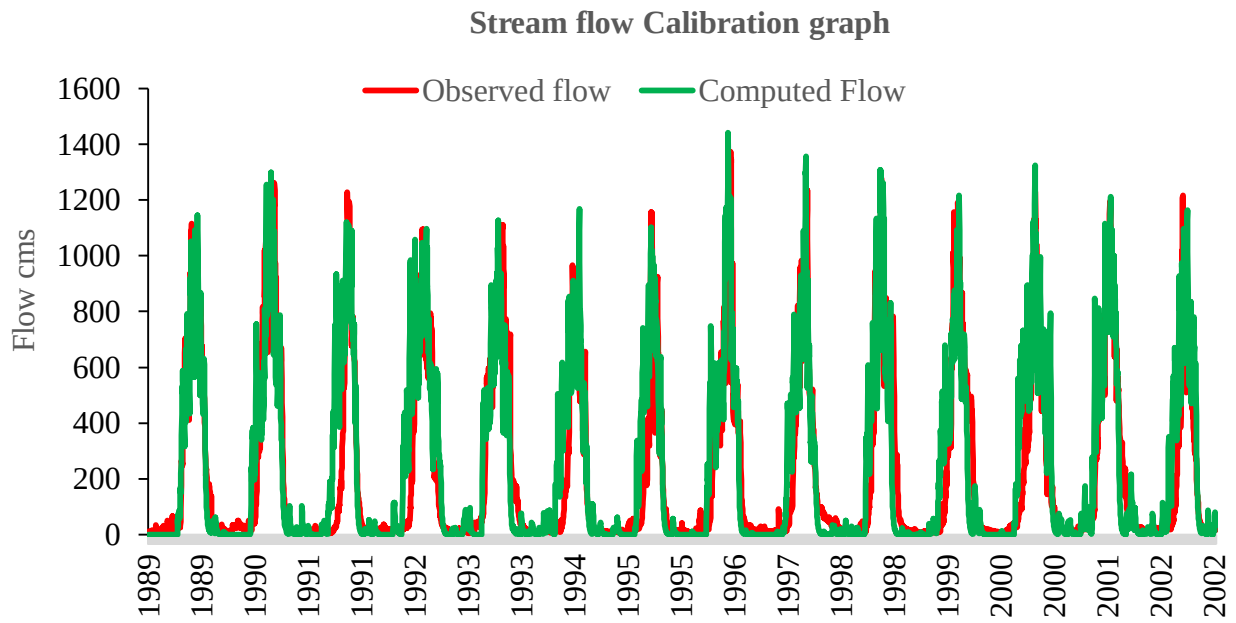

Figure 4. 10: Guder Stream Flow Calibration graph (1989-2002)

The process of assessing the performance of a hydrologic model requires both visual inspections and mathematical estimate of the error between the simulated and observed hydrologic variable. Different efficiency criteria are used to evaluate performance of hydrologic models; such as the Nash-Sutcliffe efficiency, coefficient of determination and volume difference are frequently used in hydrologic modeling. The performance evaluation measure of the model for the calibration period of the model showed in below table 6. Thus, the statistical test of error function value of RMSE and PBias as 0.7 and 10.22% respectively and also the values of R2 and NSE between the observed and simulated data obtained as 0.74 and 0.76 respectively. The model performed good during the calibration and validation period which is acceptable the efficiency criteria for model evaluation.

Table 4. 6:Statistical performance evaluation of HEC-HMS

	Performance evaluations			
Modeling type	RMSE	R^2	NSE	PBias
Calibration	0.7	0.76	0.73	10.22
Validation	0.7	0.79	0.76	11.78

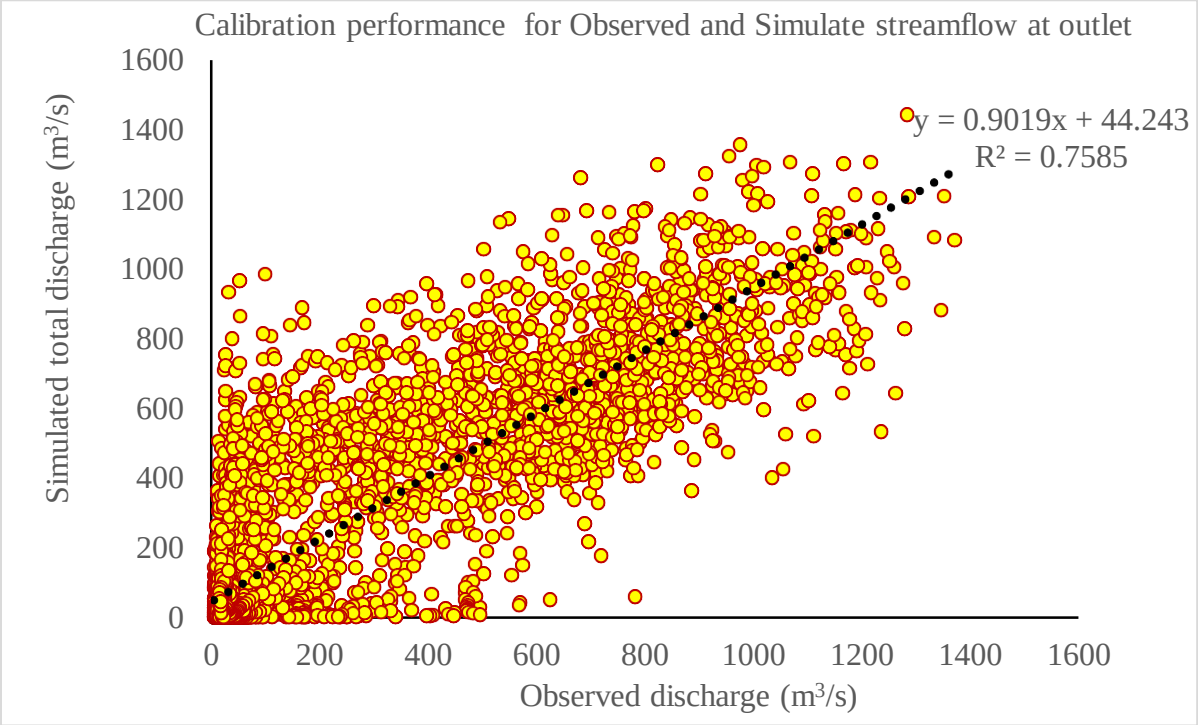

Figure 4. 11: HEC-HMS calibration performance of Guder streamflow

During the simulation process, the observed data of areal precipitation, areal evapotranspiration and observed streamflow at Guder station for Validation results show that there is good agreement between the observed and simulated daily flows. Fig:4.7 reveals that the simulated streamflow hydrograph is close to the observed one in the study watershed. The peak streamflow recorded at Guder river gages on 14 August 2006. As the values of statistical test error function are very small and Nash-Sutcliffe model efficiency (NSE) is greater than 0.5 then the model is validated. Thus, the validation result for the period 2003-2008 the value of RMSE and PBias are 0.7 and 11.78% respectively. Whereas the value of NSE 0.76 and R^2 0.79 and hence the result indicates that a close relationship between the observed and simulated streamflow.

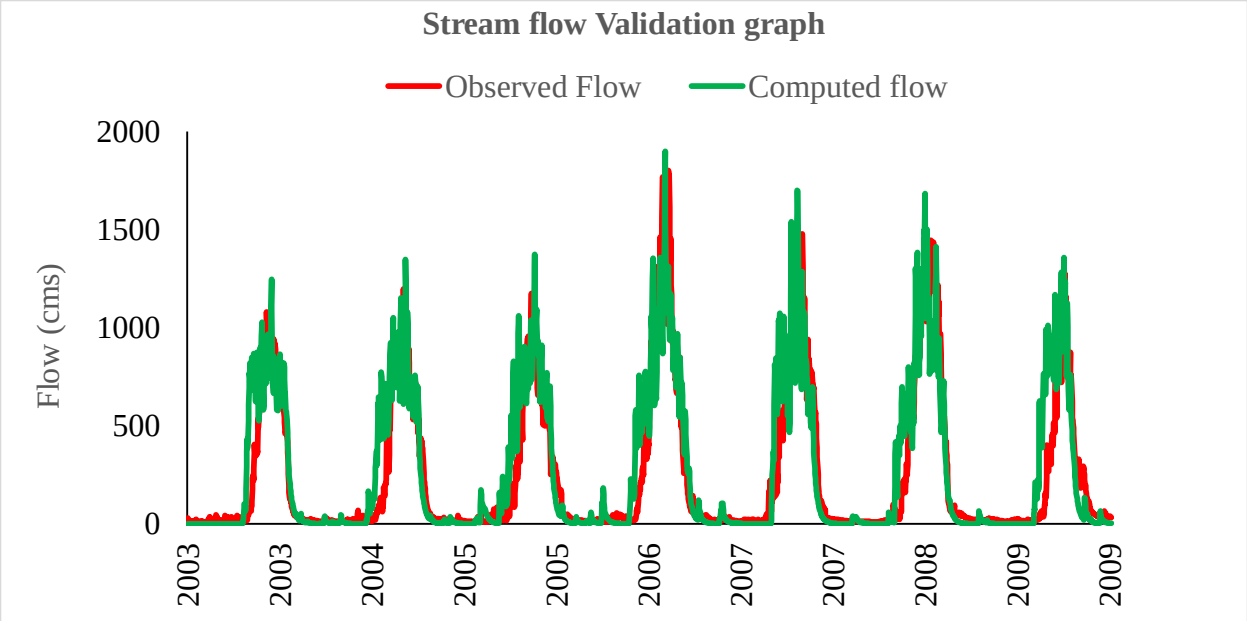

Figure 4. 12: Guder Stream flow Validation

Table 4. 7: Simulated and observed streamflow peak of calibration and validation

	Peak streamflow m^3/s		
Modeling type	Simulated	Observed	Percent difference
Calibration	1442.4	1371.8	5.2
Validation	1896.7	1812.9	4.6

4.6. RCP scenarios future simulated streamflow change

In this research, future climate projected precipitation and Temperature (T_{Max} and T_{Min}) HadGEM2-ES of three RCMs model data under two RCP's scenarios were used. HEC-HMS hydrological model is used to simulate the future streamflow for Mid-term (2041-2070) and far term (2071-2100) periods for Guder catchment. The RCMs RF bias corrected climate data for the period of 2041-2100 of two time horizons was used as input to HEC-HMS to simulate discharge at outlet of Guder watershed under RCP4.5 and RCP8.5. Observed streamflow for period of 1986-2009 and baseline period of 1971-2000 streamflow data was compared with simulated streamflow data under RCP4.5 & RCP8.5. Finally, the potential discharge changes were explored in these time horizons with respect to observed discharge data and simulated flow for the baseline period to

determine the future discharge changes. The model outputs analyzed in order to quantify the mean change of streamflow monthly, seasonal and annual in the study area of Guder watershed. Annual maximum streamflow simulated of all RCMs are in Appendix B.

4.6.1. Monthly Stream Flow Change Analysis

The mean Monthly streamflow change shows almost increase in all RCMs under RCP4.5 and RCP8.5 in both terms, a condition has shown increment in magnitude when compared with a baseline period. The maximum incremental value of both terms are 35% under RCP4.5 and RCP8.5 of all RCMs. This will happen because of the expectation in precipitation for future both periods under all RCP scenarios shows incremental change. Starting from April to Oct, the average streamflow will show increasing for mid-term and long-term periods under all RCP's scenarios. The minimum change of the streamflow happens in Jan and Feb months decrease (-1%) for RCP4.5 and RCP8.5 in mid-term and long-term periods of All RCMs except RACMO22 of mid-term. The mean stream flow decreased in the main rainy season (Jun- July) of RACMO22T for RCP4.5 and RCP8.5 scenarios, while mean annual stream flow will be increased Sept-Oct in mid-term.

The impact of climate change in precipitation and temperature has produced a significant change on stream flow. The CCLM4-8, RACMO22T and resulted different projection response to climate change over the basin. The result shows that, mean monthly and annual stream flow will increase for most months for both future periods of RCP4.5 and RCP8.5 scenarios. Maximum streamflow change projected during the month of July +35.15% under RCP 4.5 of RCA4 and the minimum change Jan to Feb -1% under RCP 4.5 and RCP8.5 of both term except RACMO22T. The average monthly streamflow at the watershed outlet from three climate models was projected to increase for all simulation periods (2041-2070), and 2071-2100) under two emission scenarios RCP 4.5 and RCP 8.5. The following figures shows monthly, seasonal and annual mean streamflow change for two periods under all RCP scenarios.

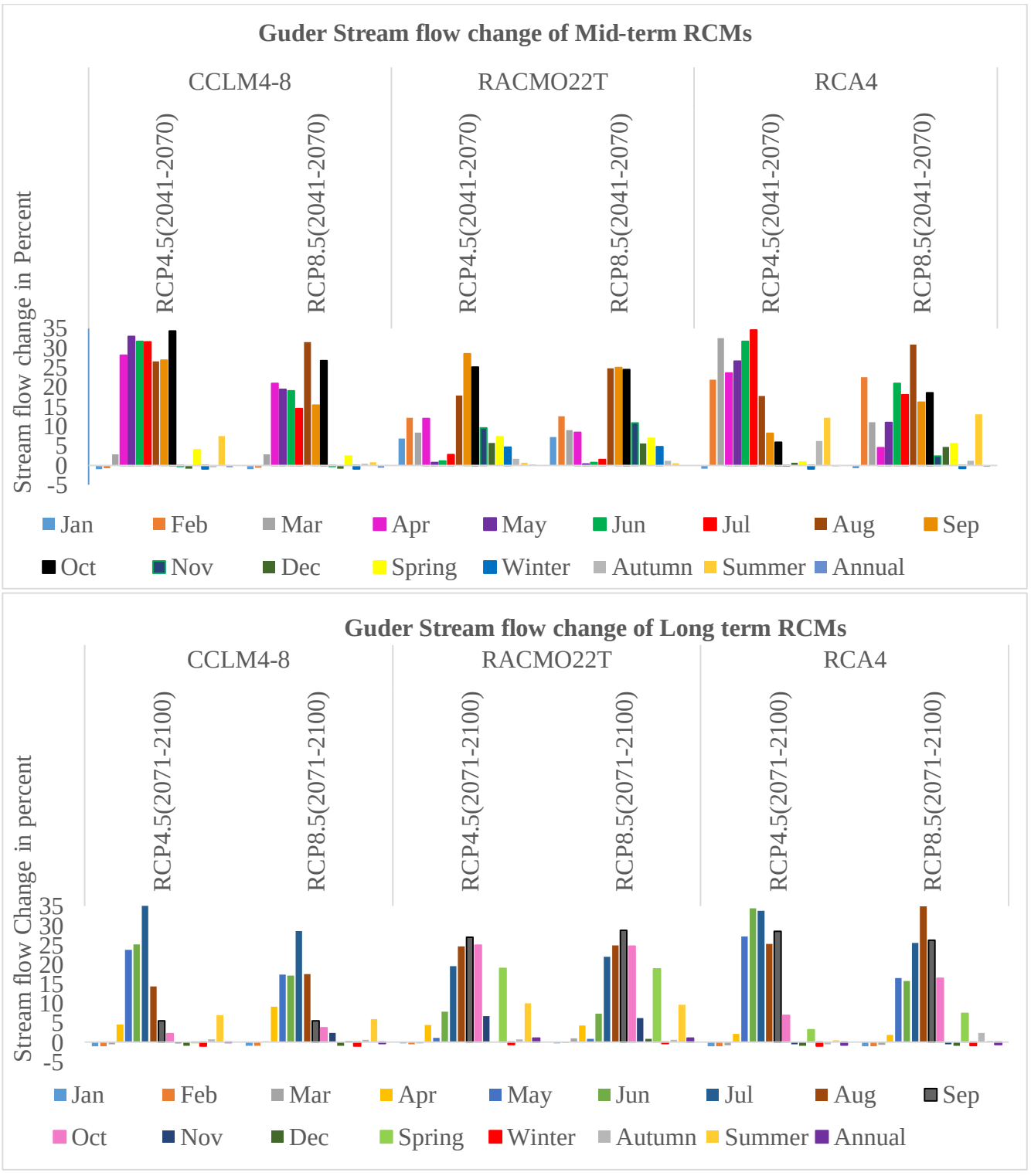

Figure 4. 13: Monthly, Seasonal and annual average stream flow change of RCMs

4.6.2. Seasonal stream flow change in the Long-term and Mid-term

Seasonal stream flow change showed an increase in Spring (2-19%), Autumn (0.44-6.2%) and Summer (0.48-13.11%) for all RCMs under RCP4.5 and RCP8.5 of both terms. The Winter season flow shows a considerable decrease (-1%) in average change in under RCP4.5 and RCP8.5 scenarios for both terms except mid-term of RACMO22T. The Annual result is decrease in all term except, long term of RACMO22T for RCP4.5 7 RCP8.5. The percentage change of projected streamflow Summer seasons all RCMs shows increment compared to baseline period.

Table 4. 8: Seasonal and Annual stream flow of RCMs under RCP4.5 and RCP8.5

Model	Horizon T.	RCPs	Spring	Winter	Autumn	Summer	Annual
CCLM4-8	Mid-term	RCP4.5	3.96	-0.90	-0.42	7.55	-0.52
		RCP8.5	2.39	-0.90	0.44	0.78	-0.64
	Long term	RCP4.5	-0.12	-0.99	0.69	7.02	-0.14
		RCP8.5	0.08	-0.99	0.62	5.93	-0.32
RACMO22T	Mid-term	RCP4.5	7.35	4.62	1.63	0.67	0.05
		RCP8.5	6.98	4.76	1.17	0.57	-0.09
	Long term	RCP4.5	18.96	-0.65	0.70	10.00	1.07
		RCP8.5	18.89	-0.38	0.60	9.58	1.00
RCA4	Mid-term	RCP4.5	0.88	-0.85	6.20	12.10	-0.24
		RCP8.5	5.52	-0.73	1.16	13.11	-0.34
	Long term	RCP4.5	3.23	-0.93	-0.53	0.48	-0.79
		RCP8.5	7.42	-0.92	2.41	0.35	-0.66

4.7. Flood Frequency Analysis

4.7.1. Probability Distribution

Frequency analyses of hydrologic and meteorological data use probability distributions to relate the magnitude of extreme events to their frequency of occurrence. In this research, Generalize Extreme value, Gumble Max, Log Pearson type III and Lognormal distribution were considered and the comparison was made based on Goodness of test result. Frequency analysis was done for observed and simulated future streamflow for Guder watershed under different RCP's scenarios. Flooding events with return periods 2, 5, 10, 25, 50, 100, 200, 500, and 1000 year were computed using the simulated streamflow at the basin outlet. Simulated flooding events from three RCMs under RCP 4.5 and RCP 8.5 were compared against observed flooding events and percentage change was computed.

The best fit distributions were checked by using Easy fit software. To obtain the best-fit distribution to the annual maximum flow series, and the most commonly adopted goodness-of-fit tests such as Kolmogorov-Smirnov, Anderson-Darling and Chi- squared and P-P and Q-Q plots were applied. The best-fit result of time data series was taken as the distribution with the lowest sum of the rank orders from each of the three test statistics. This GOFs at 5% level of significance was used to define the best-fit ranking using Easy Fit Statistical Software.

4.8. Goodness-of-Fit Test

The goodness of fit test was performed for all distributions using K-S, A-D and Chi-Squared methods AM time series data and the assessment of the best probability distribution was based on the total rank obtained from all the tests. The best-fit result was taken as the distribution with the lowest sum of the rank orders from each of the three test statistics. This GOFs at 5% level of significance was used to define the best-fit ranking using Easy Fit Statistical Software. The selection of distribution for the AM data series is based on the goodness of fit. The probability distribution having the first rank along with their test statistic was presented table below and Appendix-C. The results were summarized in table 4.8 and table 4.9 for CCLM4-8 of RCP4.5 mid and long term respectively using the three tests, it was detected that generalized extreme value distribution for both terms provides the best fit to the AMS data. Based on the overall analyses three test statistics the generalized extreme value distribution proved to be the robust distribution for flood frequency analysis over different spatial scales in the study area.

Table 4. 9: GOF test values for selected distributions of CCLM4-8_RCP4.5_Mid-term

	Distribution	K-S		A-D		Chi-Squared	
		Statistic	Rank	Statistic	Rank	Statistic	Rank
1	GEV	0.06871	1	0.23604	1	1.9945	5
4	Lognormal	0.07599	3	0.24253	2	1.1193	3
2	Gumbel Max	0.07298	2	0.24406	3	1.2887	4
5	Lognormal (3P)	0.08178	4	0.25284	4	1.1016	1
3	Log-Pearson 3	0.08403	5	0.25895	5	1.1107	2

Table 4. 10: GOF test values for selected distributions of CCLM4-8_RCP4.5_Long-term

	Distribution	K-S		A-D		Chi-Squared	
		Statistic	Rank	Statistic	Rank	Statistic	Rank
1	GEV	0.12908	2	0.35183	1	0.78399	1
2	Gumbel Max	0.13859	4	0.45827	5	0.82536	4
3	Log-Pearson 3	0.13382	3	0.3726	2	0.79429	3
4	Lognormal	0.13999	5	0.40436	4	0.8375	5
5	Lognormal (3P)	0.12365	1	0.3799	3	0.78492	2

Table 4. 11:Fitting results for probability distribution of annual flood CCLM4-8 of RCP4.5

		CCLM4-8_RCP4.5_Mid-term	CCLM4-8_RCP4.5 Long-term
	Distribution	Parameters	Parameters
1	GEV	k=0.03112 σ=276.1 μ=1208.7	k=0.05225 σ=449.64 μ=1538.5
2	Gumbel Max	σ=259.94 μ=1209.8	σ=404.49 μ=1542.3
3	Log-Pearson 3	α=359.4 β= 0.01285 γ=11.804	α=974.86 β=0.0093 γ=-1.6275
4	Lognormal	σ=0.23948 μ=7.1866	σ=0.28503 μ=7.4414
	Lognormal (3P)	σ=0.20561 μ=7.338 γ=-210.72	σ=0.39242 μ=7.1175 γ=446.31

Where; k = shape parameter, σ = scale parameter and μ = location parameter

4.9. Quantiles Estimation and Magnitude Change

Flooding events with return periods were computed using the simulated streamflow at the basin outlet. Simulated flooding events from Three climate models under RCP 4.5 and RCP 8.5 were compared against observed flooding events. Annual maximum discharge series were extracted for each hydrological was selected AM single value to each year. GEV distributions and Maximum Likelihood Estimation (MLE) was used to estimate magnitude of recurrent period.

After estimating parameters for the selected best-fit distributions, the extreme flow quantile (QT) corresponding to different return periods, T in years were computed from the statistics of the adopted distribution. An annual maximum event has a recurrence interval of T years if its magnitude is equaled or exceeded once on the average of every T year. The results of estimated extreme flow quantiles from observed and simulated AM discharge for three RCMs in both terms of Guder watershed shown in Table 4.12 for recurrence intervals of 2, 5, 10, 25, 50, 100, 200, 500 and 1000 years. The result indicated that RACMO22T for both terms of RCP4.5 and RCP8.5 revealed high quantile estimates.

Table 4. 12: Quantile Estimated in(m^3/s) and return period for mid-term

Return period	Observed	RCA4		CCLM4-8		RACMO22T	
		RCP4.5	RCP8.5	RCP4.5	RCP8.5	RCP4.5	RCP8.5
2	1290.484	1622.580	904.044	1310.463	1082.282	2669.477	2289.755
5	1492.533	1860.355	1119.476	1632.654	1418.618	2854.910	2668.572
10	1672.188	2053.670	1247.256	1852.283	1670.646	3002.936	2917.853
25	1767.321	2256.429	1393.547	2137.255	2026.927	3087.584	3122.810
50	1879.110	2506.457	1492.123	2354.089	2321.566	3226.003	3369.009
100	1995.513	2916.191	1582.311	2574.117	2642.367	3494.043	3626.872
200	2056.444	3198.289	1665.174	2798.227	2992.808	3819.509	4067.749
500	2271.260	3884.978	1764.729	3101.369	3507.115	4238.592	4597.474
1000	2533.782	4400.743	1833.230	3336.231	3939.380	4742.377	4744.485

Table 4. 13: Return period and flood magnitude in(m^3/s) for Long-term

Return Period	Observed	` RCA4		CCLM4-8		RACMO22T	
		RCP4.5	RCP8.5	RCP4.5	RCP8.5	RCP4.5	RCP8.5
2	1290.484	1696.645	1568.871	1704.845	1989.683	2778.583	2623.627
5	1492.533	1863.543	1796.753	2240.024	2321.050	3123.188	2872.118
10	1672.188	1981.399	1985.979	2612.240	2672.159	3481.831	3044.291
25	1767.321	2139.419	2279.944	3111.990	2983.396	3864.693	3398.545
50	1879.110	2263.604	2546.074	3484.611	3375.628	4056.311	3607.013
100	1995.513	2393.052	2859.126	3876.628	3541.506	4668.043	4010.569
200	2056.444	2528.457	3228.417	4281.760	3865.486	5090.307	4482.312
500	2271.260	2717.470	3623.425	4839.245	4179.877	5270.441	5321.198
1000	2533.782	2868.580	4233.638	5278.696	4467.226	5504.207	5558.596

The flood quantile obtained using generalized extreme value distribution for AM flood data series with all goodness of fit tests used globally for flood forecasting. The results in both tables show the change of flood magnitude for different future stream flow data under RCP scenarios in different return periods to the observed stream flow. In the future, the change of flood magnitude from CCLM4-8 and RACMO22T in AM series show increasing in all return periods for RCP4.5 and RCP8.5 of both terms by 1.2 %and 1.4% respectively. But RCA4_RCP8.5 mid-term of return period shows decrease changes in all return periods with magnitude of -0.3%. while RCA4_RCP4.5 long-term is increased. Flood magnitude of RCMs for long term will be increase under RCP4.5 and RCP8.5. The result of magnitude change analysis shows increasing future stream flow in dominant RCP scenarios for both near-term and mid-term periods.

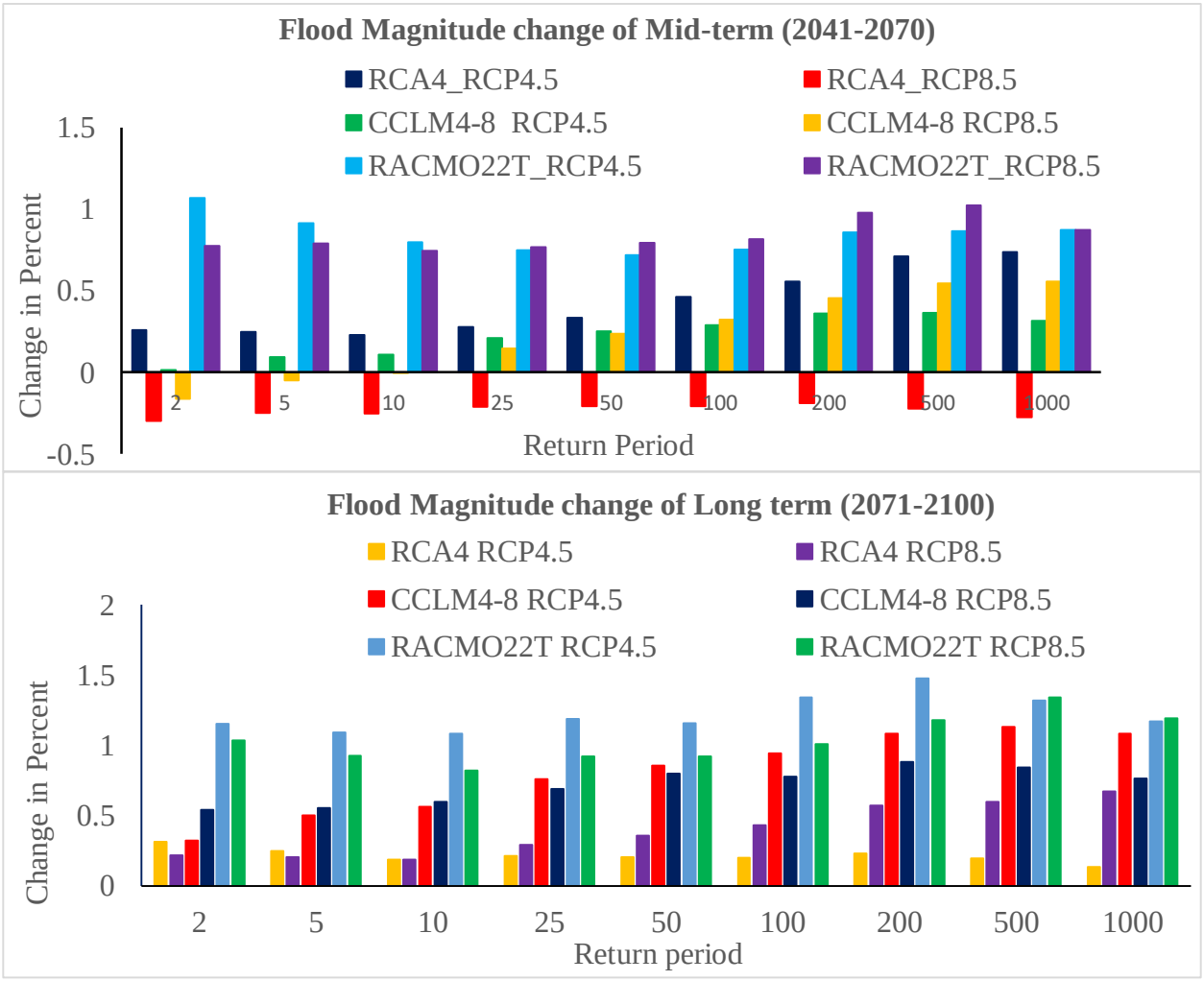

Figure 4. 14: Flood Magnitude change for RCP4.5 and RCP8.5 of both terms

4.10. Flood Frequency Curves

Flood frequency curves were developed by drawing for each RCM return period T versus the estimated extreme flood quantile Q_T smooth curve to provide an estimate of the intensity of a flood event and point on a stream shows how often flood discharges magnitudes equaled or exceeded.

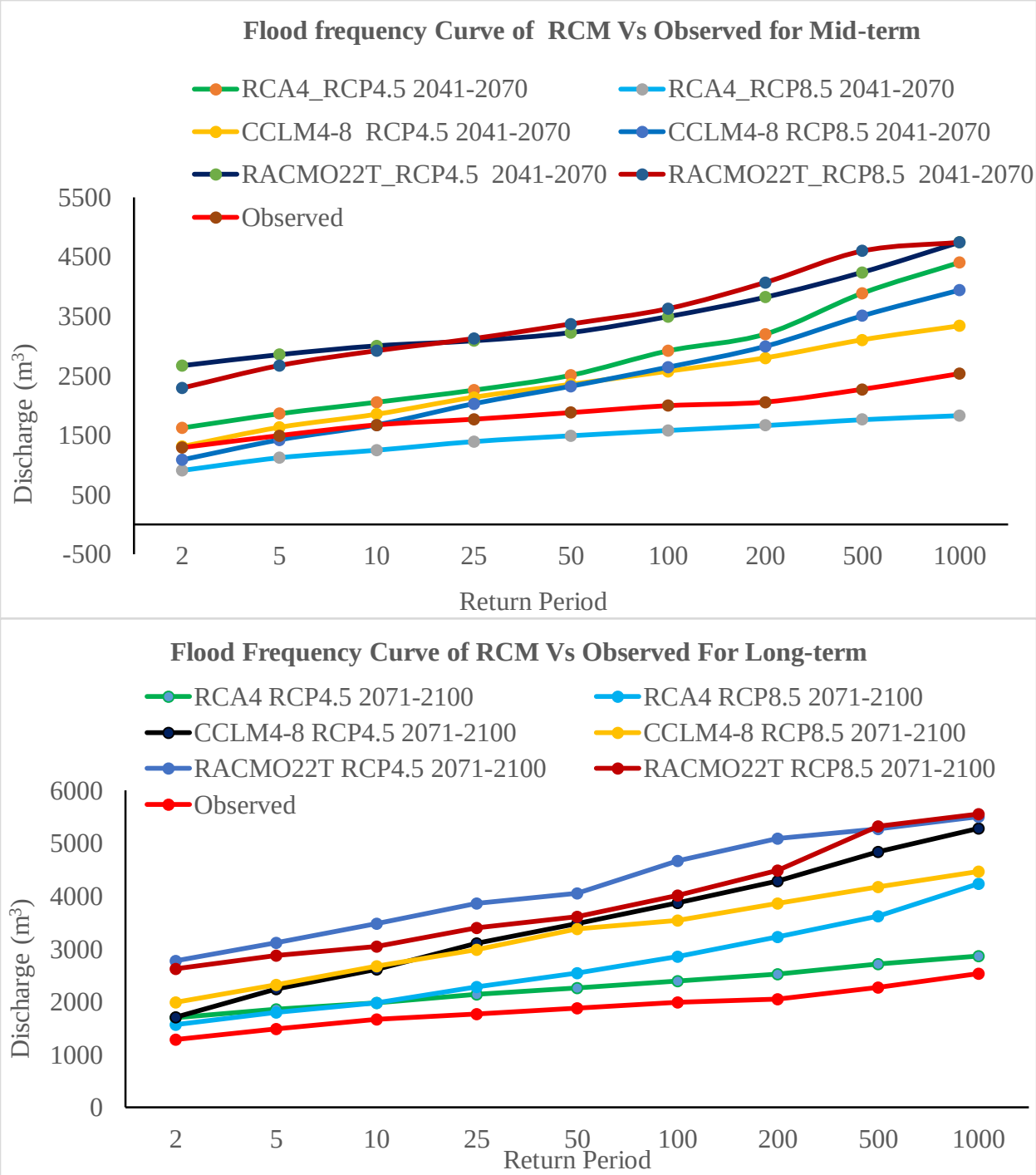

Figure 4. 15: Flood Frequency Curve of Observed and RCMs Quantiles estimated

5. CONCLUSIONS AND RECOMMENDATIONS

5.1. CONCLUSIONS

Impact of climate change is a major threat to world wide problem of natural global climatic phenomena and anthropogenic factors leading to more frequent flooding and a substantial loss of lives and properties. Hydrological modeling and flood frequency analyses have used together with climate scenario data to develop projections for the impact change on the flood flows. The impact climate change on flood frequency represents an important issue for water resources planning and design of various water resources projects, and flood risk mitigation, especially relevant for policy makers, those charged with the responsibility of selecting appropriate adaptation measures.

This study utilized the gridded bias-corrected climate scenarios data for the future (2041-2100), the observed climate data for 1986- 2018 and baseline (1971-2000). The future impact of climate change on hydro-meteorological characteristics of the catchment has been studied like: RF, T_{Max} and T_{Min} and Potential ET for (2041- 2070) and (2071-2100) using CORDEX data output, under RCP4.5 and RCP8.5 scenarios for future streamflow generation is by HEC-HMS. The values of performance efficiency of the HEC-HMS good agreement in both calibration and validation according to performance evaluation. The Regional climate models performances were evaluated for three climate models in terms of RMSE, R^2 PBIAS, show that RCA4 has best performance.

Man-Kendal(MK) trend test was done for observed and projected hydro climatic variables of precipitation, temperature (max and min) at 5% confidence level. Result of observed areal precipitation of Guder watershed shows slightly increase trend. Also, future precipitation under different RCP's scenarios for long-term period show non-significance over the catchment at the given 5% interval confidence level and slightly increase with 0.852mm/year ,0.825mm/year two scenarios of RCP4.5, RCP8.5 respectively both terms. The minimum and maximum temperature shows increasing trend for all RCP's.

Generally, the analysis was conducted to investigate the possible increase in the flood frequency in the future for various return periods including 2-, 5-, 10-, 50-, 100-, 200-, 500- and 1000 year compared to Observed flood frequency using GEV probability distribution and ML parameter estimation method.These long-term hydrologic predictions using projected climate data may provide the basis for the water resources managers or decision-makers to develop flood regulating strategies, especially when there is a likelihood of overflow of the flood regulating reservoir.

5.2. RECOMMENDATIONS

This research set target to analysis the impact of climate change on flood frequency of Guder watershed under RCP's scenarios. Based on the result of the study, the following points are recommended.

- For assessing climate change impact on this study, only three RCMs of the same family GCM model with different emission RCP's scenarios (RCP4.5 and RCP8.5) scenarios was used. But, the result may not be the same if different climate models were used. So, it is better to study further by including different climate models.
- In this study, only climate variable parameters (precipitation, maximum temperature and minimum temperature) were used for future climate change impact analysis. But, all other parameters assumed as constant. The future study must include other parameters like: ETo, change in land use, soil, management activity and other climate parameters to get better results. Because, they have direct and indirect impact on flood frequency.
- In this study, the impact of climate change was assessed on the assumption that land cover will remain the same going forward. But for the future, LULC must be consider because of urbanization expansion, deforestation and agricultural development change the volume of runoff will be increase which leads to flooding events.
- For simulation of observed and future stream flow in HEC-HMS, the daily stream flow data was used and it is the minimum requirement allowable data for simulation. But, for further model performance, it is better to use hourly and less time data depending on data availability to increase its accuracy.
- In last, as discussed under result part the future flood frequency expected to increase in the study area. Any regarding body, stockholders and development water planners must take into account the increment of summer and spring seasons precipitation and its causes on both seasons stream flow leads increasing frequent flood on rural livelihoods at downstream.

REFERENCES

A. N. Hilo et al. (2019). Impact of Climate Change on Water Resources of Dokan Dam Watershed. Engineering, 11, 464-474.

A. Rafiei Emam et al. (2016). Impact Assessment of Climate and Land-Use Changes on Flooding Behavior in the Upper Ciliwung River, Jakarta, Indonesia. Water 2016, 8(559). doi:10.3390/w8120559

A.L. Kay et al. (2021). Climate change impacts on peak river flows: Combining national-scale hydrological modelling and probabilistic projections. Climate Risk Management. Retrieved from https://doi.org/10.1016/j.crm.2020.100263

Abeba et al. (2017). Impact of Climate Change on the Development of Rainfall Intensity, Duration and Frequency Curves in Chiro and Hurso Stations of Eastern Ethiopia. Earth Sciences, 6(5), 97-105. doi:1 10.11648/j.earth.20170605.16

Ahmad I. et al. (2019). Regional Flood Frequency Analysis Using Linear Moments and Partial Linear Moments:. Applied Ecology and Environmental Research, 17(2), 3819-3836. Retrieved from http://dx.doi.org/10.15666/aeer/1702_38193836

Aicha Saad et al. (2019). Flood Frequency Analysis and Urban Flood Modelling of Sidi Ifni Basin, Southern Morocco. American Journal of Geographic Information System, 8(5), 206-212. doi:10.5923/j.ajgis.20190805.02

Ambrose M.et.al. (2021). Performance of rainfall–runoff models in reproducing hydrological extremes: a case of the River Malaba sub-catchment. SN Applied Sciences, 3(515). Retrieved from https://doi.org/10.1007/s42452-021-04514-7

Ashish Shrestha et al. (2017). Developing Intensity–Duration–Frequency (IDF) Curves under Climate Change Uncertainty: The Case of Bangkok, Thailand. Water, 9(145). doi:doi:10.3390/w9020145

B. Choubin, et al. (2019). Streamflow regionalization using a similarity approach in ungauged basins: Application of the geo-environmental signatures in the Karkheh River Basin,Iran. Catena 182 (2019) 104128, Elsevier. Retrieved from https://doi.org/10.1016/j.catena.2019.104128

Badri Bhakta Shrestha et al. (2019). Assessing flood disaster impacts in agriculture under climate change in the river basins of Southeast Asia. Natural Hazards, 97, 157-192.

Batablinle et al. (2018). Africa-Cordex Simulations Projection of Future Temperature, Precipitation, Frequency and Intensity Indices Over Mono Basin in West Africa. Journal of Earth Science & Climatic Change, 9(9). doi:10.4172/2157-7617.1000490

Belay & Getaneh. (2016). Climate Change in Ethiopia Variability, Impact, Mitigation, and Adaptation. International journal of Research & Development Orginazation, 2(4).

Biniyam Y. & Abdella K. (2017). The Impacts of Climate Change on Rainfall and Flood Frequency: The Case of Hare Watershed, Southern Rift Valley of Ethiopia. Journal of Earth Science & Climatic Change, 8(1). doi: 10.4172/2157-7617.1000383

C. Hu, et al. (2019). A modified regional L-moment method for regional extreme precipitation frequency analysis in the Songliao River Basin of China. Atmospheric Research. doi:https://doi.org/10.1016/j.atmosres.2019.104629

Cassalho F et al. (2019). Regional flood frequency analysis using L-moments for geographically defined regions : An assessment in Brazil. Journal of Flood Risk Management.

(2018). Climate Change Adaptation in Africa. nited Nations Development Programme.

(2018). Climate Change Profile: Ethiopia.

Dawit T. G & Hatim O. S. (2021). Development and Assessment of High-Resolution Radar-Based Precipitation Intensity-Duration-Curve (IDF) Curves for the State of Texas. Remote Sensing, 13(2890). Retrieved from https://doi.org/10.3390/ rs13152890

Demissie et al. (2016). Assessment of Climate Change Impact on Flood frequency of Bilate River Basin, Ethiopia. Civil and Environmental Research, 8(11).

Drissia T.K. al et. (2019). Flood Frequency Analysis Using L Moments: a Comparison between At-Site and Regional Approach. Water Resources Management. doi:https://doi.org/10.1007/s11269-018-2162-7

Enrique S. et al. (2018). Selection of Bias Correction Methods to Assess the Impact of Climate Change on Flood Frequency Curve. Preceedings 2019, 7(14).

Ery Suhartanto et al. (2018). Estimation of Design Flood with Four Frequency Analysis Distributions. Asian Journal of Applied Science and Technology (AJAST), 2(1), 1 3-27.

(2016). Ethiopia Climate Action Report.

(2019). Ethiopia's Climate Resilient Green Economy, NAP-ETH.

F. Mendonça dos Santos al et. (2018). Lumped verses distributed hydrological Modeling of the Jacaré-Guaçu Basin ,Brazil. Journal of Environmental Engineering, 144(8). doi: 10.1061/(ASCE)EE.1943-7870.0001397

F. Saka &H. T.Babacan. (2019). Discharge Estimation by Drainage Area Ratio Method at Some Specific Discharges for 2251 Stream Gauging Station in East Black Sea Basin, Turkey. Journal of Investigations on Engineering & Technology, 2(1).

Fevzi Onen and Tamer Bagatur. (2017). Prediction o f Flood Frequency Factor for Gumbel Distribution Using R egression and GEP Model. Arabian Journal of Science and Engineering, 3895–3906. doi:10.1007/s13369-017-2507-1

Fikru et al. (2018). a) Climate Change Impact on the Hydrology of Tekeze Basin, Ethiopia: Projection of Rainfall-Runoff for Future Water Resources Planning. Water Conservation Science and Engineering. doi: 10.1007/s41101-018-0057-3

Fikru et al. (2018). b) Impacts of Climate Change on the Water Resources of Guder Catchment, Upper Blue Nile, Ethiopia. International Technology and Science of Water, 16-29.

Firdaus M.H. et.al. (2021). A Comparative Flood Frequency Analysis of High-Flow between Annual Maximum and Partial Duration Series at Sungai Langat Basin. Sains Malaysiana, 50(7), 1843-1856. doi:doi.org/10.17576/jsm-2021-5007-02

G. D. Akpen et al. (2018). Rainfall Intensity-Duration-Frequency Models For Lokoja Metropolis, Nigeria. Global Journal of Pure and Applied Sciences, 24, 81-90. doi:https://dx.doi.org/10.4314/gjpas.v25i1.11

G. Gelete et al. (2019). Impact of climate change on the hydrology of Blue Nile basin, Ethiopia:. Journal of Water and Climate Change. doi:10.2166/wcc.2019.014/607040/jwc2019014

Gebreegziabher et al. (2016). Mapping Vulnerability to Climate Change of the Farming Sector in the Nile Basin of Ethiopia. Environment for Development.

Hasan, I. F. (2020). Flood Frequency Analysis of Annual Maximum Streamflows at Selected Rivers in Iraq. Jordan Journal of Civil Engineering, 14(4).

I. Kása et al. (2017). Evaluation of three semi-distributed hydrological models in simulating discharge from a small forest and arable dominated catchment. Biologia 72/9, 1002-1009.

Ibe Go & Amikuzuno J. (2019). Climate Change in Sub-Saharan Africa: A menace to Agricultural productivity and Ecological protection. Journal Applied Science and Environmental Management, 23(2), 329-335. doi:https://dx.doi.org/10.4314/jasem.v23i2.20

Igor Lešcešen and Dragan Dolinaj. (2019). Regional Flood Frequency Analysis of the Pannonian Basin. Water, 11(193). doi:10.3390/w11020193

Ionela Gabriela Bucse et al. (2019). Climate Change Impact on Water Resources in Mehedinţi County - Case Study. Advanced Engineering Forum, 34, 215-220. doi:10.4028/www.scientific.net/AEF.34.215

(2018). IPCC.

(2018). IPCC Special Report of Global Warming.

Ismail Elhassnaoui et al. (2019). Generation of Synthetic Design Storm Hyetograph and Hydrologic Modeling under HEC HMS for Ziz Watershed. International Journal of Innovative Technology and Exploring Engineering (IJITEE), 8(10).

J.B. Swain & K.C. Patra . (2017). Streamflow estimation in ungauged catchments using regionalization techniques. Journal of Hydrology, 420-433.

J.G. Duan et al. (2017). Framework for incorporating climate change on flood magnitude and frequency analysis in the upper Santa Cruz River. Journal of Hydrology, 194-207. doi:http://dx.doi.org/10.1016/j.jhydrol.2017.03.042

Jessie R.G. et.al. (n.d.). Economic growth, development and climate change in Africa.

Joonghyeok Hoe. (2018). The Impact of Climate Change on Hydrology with Geomorphology in Northeast Texas. Journal of Earth Science and Engineering, 1-7. doi:10.17265/2159-581X/2018.01.001

Kousar S et al. (2020). Some best-fit probability distributions for at-site flood frequency analysis of the Ume River. Journal Flood Risk Management. doi:DOI: 10.1111/jfr3.12640

Kundwa MJ et al. (2019). Development of Rainfall Intensity Duration Frequency (IDF) Curves for Hydraulic Design Aspect. Journal of Ecology & Natural Resources, 3(2).

L. Ammann et al. (2019). A likelihood framework for deterministic hydrological models and the importance of non-stationary autocorrelation. Hydrology and Earth System Sciences, 2147–2172.

Lauren M. Cook, et al. (2020). The effect of modeling choices on updating intensity-duration-frequency curves and stormwater infrastructure designs for climate change. Climatic Change, 159, 289– 308. doi:https://doi.org/10.1007/s10584-019-02649-6

Lauro C et al. (2018). Regional flood frequency analysi s in the central- western river basins of Argen tina. River Res Applic., 1-13. doi:DOI:10.1002/rra.3319

M. Caian et.al. (2021). Extreme flood modeling and mechanism over Crisul Alb basin in Romania. Catena. Retrieved from https://doi.org/10.1016/j.catena.2020.104923

M. Dal Molin et al. (2020). Understanding dominant controls on streamflow spatial variability to set up a semi-distributed hydrological model: the case study of the Thur catchment. Hydrology and Earth System Sciences, 1319–1345.

M. L. Kavvas, et al. (2017). Current issues in and an emerging method for flod frequency analysis under changing climate. Journal of Japan Society of Hydrology and Water Resources. doi: 10.3178/hrl.11.1

M.S. Bhat et al. (2019). Flood frequency analysis of river Jhelum in Kashmir basin. Quaternary International, 288–294.

Mahmood Azari et al. (2016). Climate change impacts on streamflow and sediment yield in the North of Iran. Hydrological Sciences Journal, 61(1), 123-133. doi:http://dx.doi.org/10.1080/02626667.2014.967695

Mahmood Ul Hassan et al. (2019). Selecting the best probability distribution for at-site food frequency analysis; a study of Torne River. SN Applied Sciences, 1(1629). doi:https://doi.org/10.1007/s42452-019-1584-z

Maikel et al. (2020). Performance Evaluation of Bias Correction Methods for Climate Change Monthly Precipitation Projections over Costa Rica. Water, 12(482). doi:10.3390/w12020482

Melke and Abegaz . (2017). Impact of climate change on hydrological responses of Gumara catchment, in the Lake Tana Basin - Upper Blue Nile Basin of Ethiopia. International Journal of Water Resources and Environmental Engineering, 9(1), 8-21. doi:DOI: 10.5897/IJWREE2016.0658

Mokhtari E.H. et al. (2016). Modelling of the rain–flow by hydrological modelling software system HEC-HMS – watershed's case of wadi Cheliff-Ghrib, Algeria. Journal of Water and Land Development, 87–100.

Muhammad Farooq elt al. (2018). Flood frequency analysis of river swat using Log Pearson type 3, Generalized Extreme Value, Normal, and Gumbel Max distribution methods. Arabian Journal of Geosciences. doi:https://doi.org/10.1007/s12517-018-3553-z

Muhammad Noor et al. (2018). Uncertainty in Rainfall Intensity Duration Frequency Curves of Peninsular Malaysia under Changing climate scenarios. Water, 1750. doi: DOI:10.3390/w10121750

Muhammad Rizwan et al. (2018). Evaluation of Various Probability Distributions for Deriving Design Flood Featuring Right-Tail Events in Pakistan. Water, 10(1603). doi:10.3390/w10111603

Muhammad Shahid Iqbal, Z. H. (2018). Impact of Climate Change on Flood Frequency and Intensity in the Kabul River Basin. Geosciences, 8(114). doi:10.3390/geosciences8040114

Mustafa U. Y. & Bihrat O. (2020). A Comparative Study of Statistical Methods for Daily Streamflow Estimation at Ungauged Basins in Turkey. Water, 12(459).

Myo, H. T. et al . (2020). Projecti ng the Impact of Climate Change on Temperature, Precipitation, and Discharge in the Bago River Basin. Journal of Disaster Research, 15(3).

Negash & Marie. (2016). Analysis of Rainfall Intensity-Duration-Frequency Relationship for Rwanda. Journal of Water Resource and Protection, 706-723.

Negash et.al. (2020). Modeling the Effects of Climate Change on Streamflow Using Climate and Hydrological Models: The case of the Kesem Sub-basin of the Awash River Basin, Ethiopia. International Journal of River Basin Management.

Nkululeko Simeon Dlamini et al. (2017). Modeling Potential Impacts of Climate Change on Streamflow Using Projections of the 5th Assessment Report for the Bernam River Basin, Malaysia. Water, 9(226).

Noor S. R & Zulkifli Y. (2017). Frequency Analysis of Annual Maximum Flood for Segamat River. MATEC Web of Conferences, 103. doi:10.1051/matecconf/20171030

Noora Veijalainen et al. (2017). Impacts of climate change on extreme floods in Finland –studies using bias corrected Regional Climate Model data. Hydrology and Earth System Sciences Discussions.

Oladayo N.A. and Jonathan T. (2017). The Impacts of Climate Change in Africa: A Review of the Scientific Literature. Journal of International Academic Research For Multidisciplinary, 5(11).

P. Ganguli & P. Coulibaly. (2019). Assessment of future changes in intensity-duration-frequency curves for Southern Ontario using North American (NA)-CORDEX models with nonstationary methods. Journal of Hydrology: Regional Studies. doi:https://doi.org/10.1016/j.ejrh.2018.12.007

Philip Kibet Langat et al. (2019). Identification of the Most Suitable Probability Distribution Models for Maximum, Minimum, and Mean Streamflow. Water, 11(734).

Proloy Deb et al. (2018). Multi-GCMs approach for assessing climate change impact on water resources in Thailand. Modeling Earth Systems and Environment. doi:https://doi.org/10.1007/s40808-018-0428-y

R. A .I. Wilcke and L.Barring. (2016). Selecting regio nal climate scenarios for impact mo delling studies. Environmental Modelling & Software, 78, 191-201. doi:http://dx.doi.org/10.1016/j.envsoft.2016.01.002

R.C.C. Puno, et al. (2019). Hydrologic responses of watershed assessment to land cover and climate change using soil and water assessment tool model. Global Journal of Environmental Science and Management, 5(1), 71-82. doi:10.22034/gjesm.2019.01.06

Rangecroft al et. (2018). Hydrological modelling as a tool for interdisciplinary workshops on future drought. Progress in Physical Geography, 42(2), 237- 256. doi:10.1177/0309133318766802

S.Malik & S.Chandra Pal. (2021). Potential flood frequency analysis and susceptibility mapping using CMIP5 of MIROC5 and HEC-RAS model: a case study of lower Dwarkeswar River, Eastern India. SN Applied Sciences, 3(31).

Schardong & Simonovic. (2019). Application of Regional Climate Models for Updating Intensity-duration-frequency Curves under Climate Change. International Journal of Environment and Climate Change, 9(5), 311-330. doi:10.9734/IJECC/201 9/v9i530117

Sharu, E. H. (2021). Development of HEC-HMS Model for Flow Simulation at Dungun River Basin Malaysia. Advances in Agricultural and Food Research Journal, 2(1).

Shimelis. (2017). Evaluation of Conceptual Hydrological Models in Data Scarce Region of the Upper Blue Nile Basin: Case of the Upper Guder Catchment. Hydrology, 4(59). doi:10.3390/hydrology4040059

Shrestha S & Sharma S. (2021). Assessment of climate change impact on high flows in a watershed characterized by flood regulating reservoirs. Int J Agric & Biol Eng,, 14(1), 178–191.

Singh R. et al. (2016). Potential Impact of Climate Change on Rainfall Intensity-Duration-Frequency Curves in Roorkee, India. Water Resource Management. doi:10.1007/s11269-016-1441-4

Sridhar V et al. (2019). Precipitation Extremes and Flood Frequency in a Changing Climate in Southeastern Virginia. Journal of the American Water Resources Association (JAWRA), 55(4), 780–799.

T. Alemu and A. Mengistu. (2019). Impacts of Climate Change on Food Security in Ethiopia: Adaptation and Mitigation Options: A Review. Climate Change-Resilient Agriculture and Agroforestry,Climate Change Management. doi: https://doi.org/10.1007/978-3-319-75004-0_23

T. Razavi and P. Coulibaly. (2016). An evaluation of regionalization and watershed classification schemes for continuous daily streamflow prediction in ungauged watersheds. Canadian Water Resources Journal. doi:10.1080/07011784.2016.1184590

T.T. Hailegeorgis & K. Alfredsen. (2017). Regional flood frequency analysis and prediction in ungauged basins including estimation of major uncertainties for mid-Norway. Journal ofHydrology: Regional Studies, 9, 104–126. doi:http://dx.doi.org/10.1016/j.ejrh.2016.11.004

Tegegne G.et.al. (2020). Flood Frequency Analyses over Different Basin Scales in the Blue Nile River Basin, Ethiopia. Hydrology, 7(44). doi:doi:10.3390/hydrology7030044

Tomohiro Tanaka et al. (2016). Frequency analysis of extreme floods in a highly developed river basin. Hydrology and Earth System Sciences.

Usman A. I. et.al. (2016). Flood Frequency Analysis at Hadejia River in Hadejia – Jama'are River Basin, Nigeria. Civil and Environmental Research, 8(9).

Vikas Kamal et al. (2017). lood frequency analysis of Ganga river at Haridwar and Garhmukteshwar. Applied Water Science, 7, 1979–1986. doi:DOI 10.1007/s13201-016-0378-3

Wan Husna Aini Wan Deraman et al. (2017). Determination of return period for flood frequency analysis using normal and related distributions. Journal of Physics: Conferences Series 890. doi:10.1088/1742-6596/890/1/012162

Wootten et al . (2017). Characterizing Sourc es of Uncertain ty from Global Climate Models and Downscaling Technique s. Journal of Applied Meteorology and Climatology, 56. doi:10.1175/JAMC-D-17-0087.1

X. Yang et al. (2018). Runoff Prediction in Ungauged catchments in Norway: Comparision of Regionalization approaches. Hydrology Research.

Xiao et al. (2017). A comparative study of the methods for estimating streamflow at ungauged sites. 22nd International Congress on Modelling and Simulation, Hobart, Tasmania, Australia.

Xin Yu et al. (2018). LP3 Flood Frequency Analysis Including Climate Change. World Environmental and Water Resources Congress 2018.

Y. Sane et al. (2018). Intensity–duration–frequency (IDF) rainfall curves in Senegal. Nattural Hazards and Earth System Sciences, 18, 1849–1866. doi:https://doi.org/10.5194/nhess-18-1849-2018

Yamamoto et al. (2021). Impact of Climate on Flood Indulation in a Tropical river basin in Indonesia. Progress in Earth and Planetary Science, 8(5).

Yanjuan Wu et al. (2021). Using Integrated Hydrological Models to Assess the Impacts of Climate Change on Discharges and Extreme Flood Events in the Upper Yangtze River Basin. Water, 13(299).

Ye Bai et al. (2019). Assessing the Impact of Climate Change on Flood Events Using HEC-HMS and CMIP5. Water Air Soil Pollution. doi:https://doi.org/10.1007/s11270-019-4159-0

Yèkambèssoun N'Tcha M'Po, et.al. (2016). Comparison of Daily Precipitation Bias Correction Methods Based on Four Regional Climate Model Outputs in Ouémé Basin, Benin. Hydrology, 4(6), 58-71. doi:doi: 10.11648/j.hyd.20160406.11

Zhanling Li et.al. (2016). Frequency Analysis of High Flow Extremes in the Yingluoxia Watershed in Northwest China. Water, 8(215). doi:doi:10.3390/w8050215

Zhe Yuan et al. (2018). Projection of Future Extreme Precipitation and Flood Changes of the Jinsha River Basin in China Based on CMIP5 Climate Models. International Journal of Environmental Research and Public Health. doi:10.3390/ijerph15112491

APPENDICES

Appendix A: Annual Rainfall data homogeneity tests of Meteorological stations.

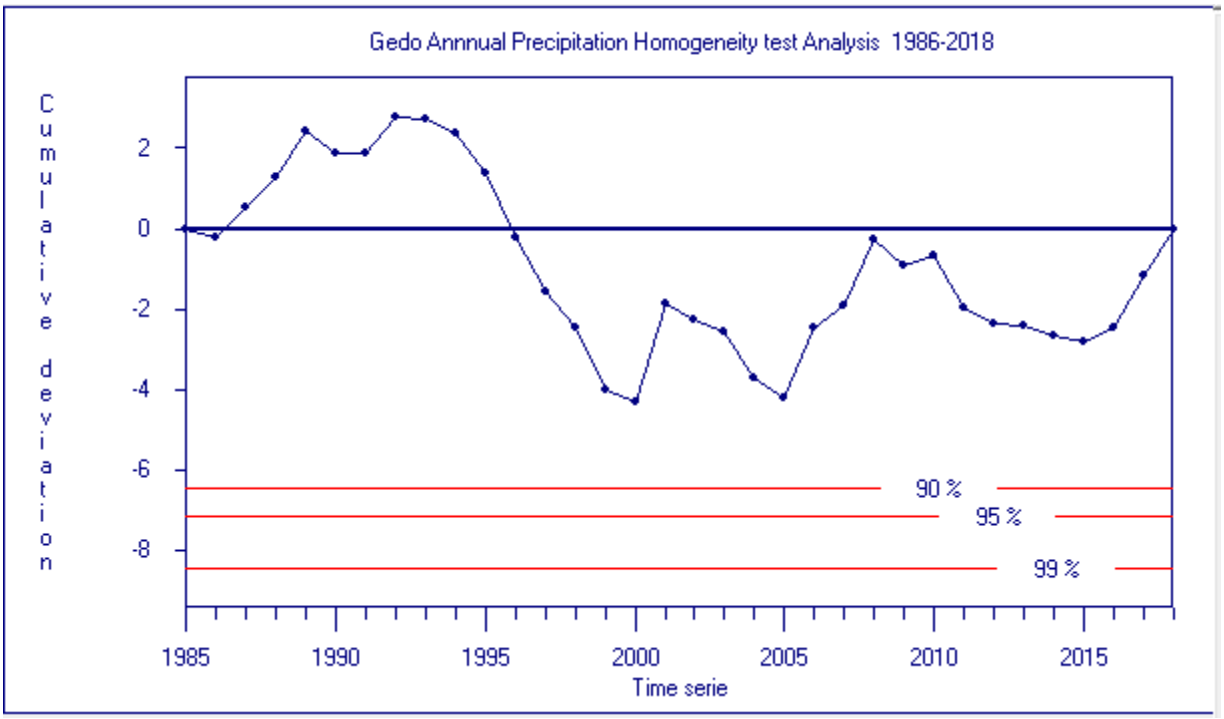

Description | Gedo Annnual Precipitation Homogeneity test Analysis 1986-201

Restrictions

Homogeneity test

Probability of rejecting homogeneity

statistic	rejected ?		
	90 %	95 %	99 %
Range of Cumulative deviation	No	No	No
Maximum of Cumulative deviation	No	No	No

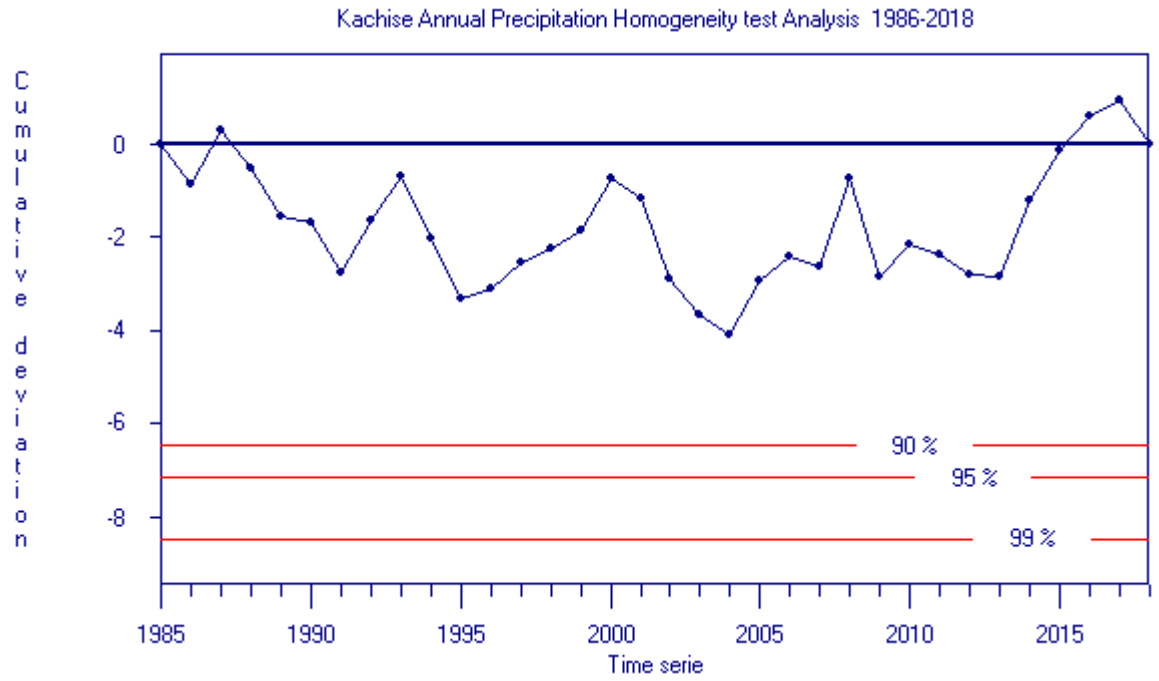

Description Kachise Annual Precipitation Homogeneity test Analysis 1986-20

Restrictions

Homogeneity test

Probability of rejecting homogeneity

statistic	rejected ?		
	90 %	95 %	99 %
Range of Cumulative deviation	No	No	No
Maximum of Cumulative deviation	No	No	No

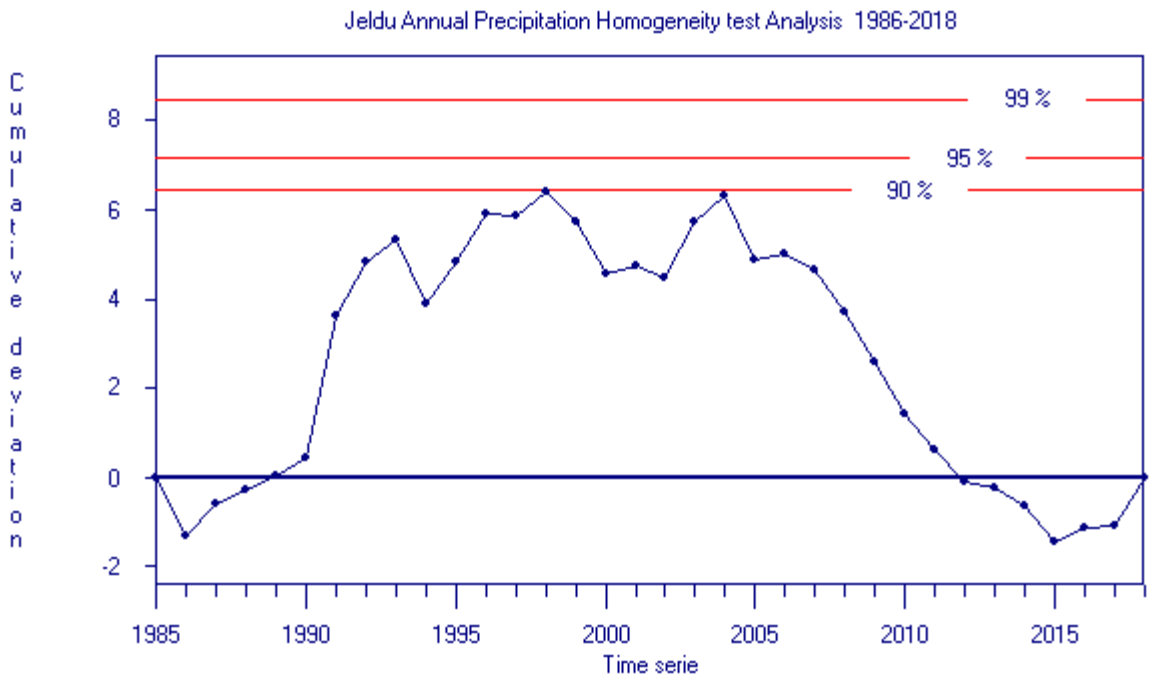

Description | Jeldu Annual Precipitation Homogeneity test Analysis 1986-2018

Restrictions

Homogeneity test

Probability of rejecting homogeneity

statistic	rejected ?		
	90 %	95 %	99 %
Range of Cumulative deviation	No	No	No
Maximum of Cumulative deviation	No	No	No

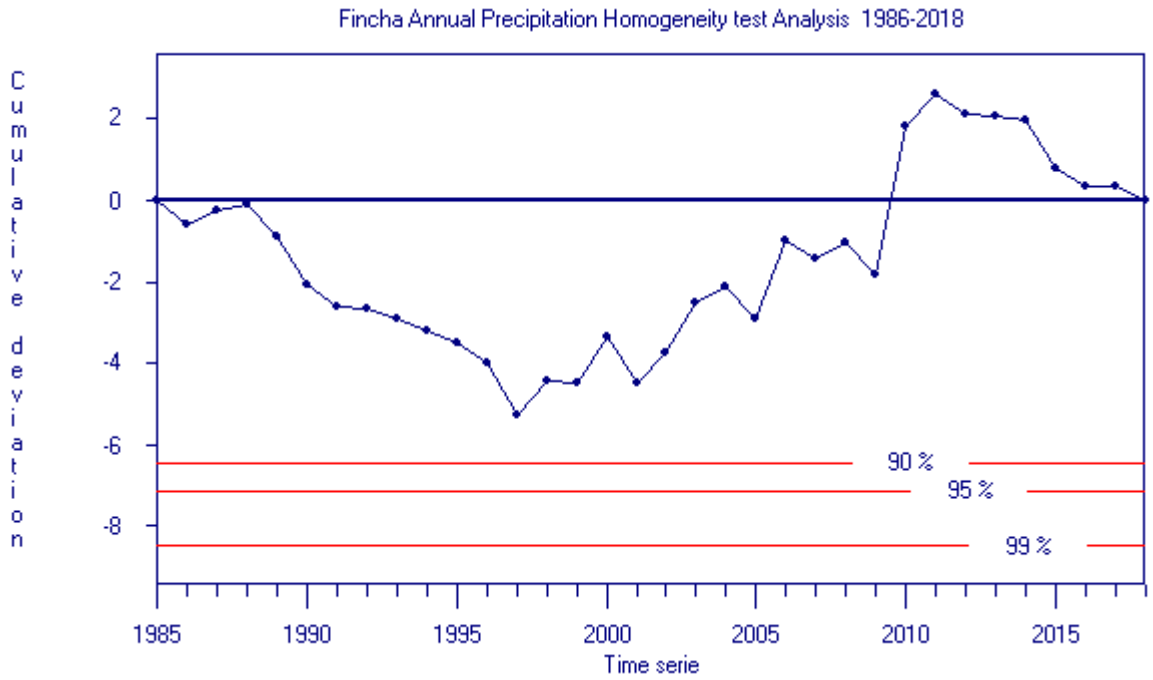

Description | Fincha Annual Precipitation Homogeneity test Analysis 1986-201

Restrictions

Homogeneity test

Probability of rejecting homogeneity

statistic	rejected ?		
	90 %	95 %	99 %
Range of Cumulative deviation	No	No	No
Maximum of Cumulative deviation	No	No	No

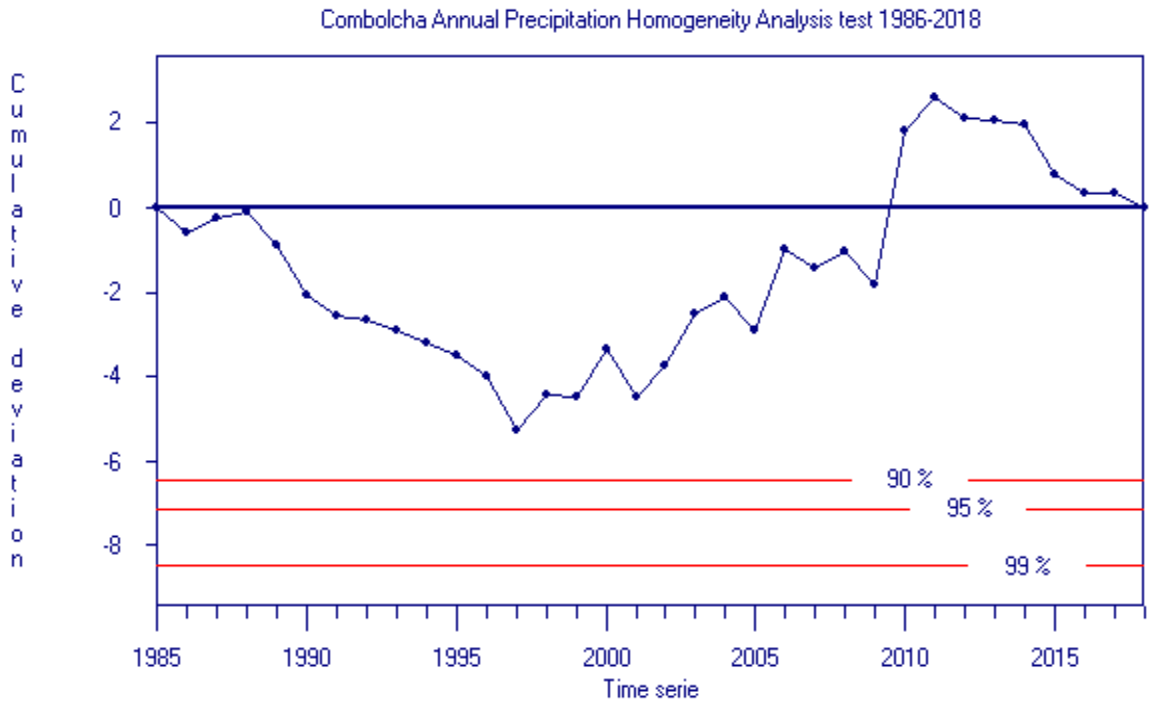

Description | Combolcha Annual Precipitation Homogeneity Analysis test 1986-

Restrictions

Homogeneity test

Probability of rejecting homogeneity

statistic	rejected ?		
	90 %	95 %	99 %
Range of Cumulative deviation	No	No	No
Maximum of Cumulative deviation	No	No	No

Appendix B: Annual maximum Simulated streamflow of all RCMs for Mid and Long term

CCLM4-8 Mid-term simulated Streamflow			CCLM4-8 Long-term simulated Streamflow		
Year	RCP4.5	RCP8.5	Year	RCP4.5	RCP8.5
2041	1358.3	1346.4	2071	1223.7	475.4
2042	1815	1771.9	2072	2452.2	2989.6
2043	1068.6	836.4	2073	1455.9	1551.1
2044	1240	1243.8	2074	1333.3	984.8
2045	1353.1	1348.7	2075	1196.9	977.7
2046	695.8	681.9	2076	1392.8	1704.7
2047	1660.7	1247.4	2077	1378.4	2280.4
2048	2289.5	1636.4	2078	2178.8	3311
2049	1222.6	895.1	2079	1688.9	808.5
2050	1921.2	1399.7	2080	1727.8	1211
2051	1391	1402.4	2081	2081.6	1533.3
2052	1609	1148.2	2082	1327.9	883.3
2053	1076.1	1035	2083	1957.9	1954.9
2054	1128.2	821.8	2084	2092.4	3275
2055	1318.4	942.2	2085	1725.8	1662.6
2056	1149.2	1067.4	2086	2235.3	1870.5
2057	1015.3	1000.3	2087	1367.2	1317.2
2058	1477.8	1133.6	2088	1399.1	2376.3
2059	1455.6	1442	2089	1100.8	2556.1
2060	1396.2	1366.5	2090	1777.3	3478.3
2061	1036.9	997.2	2091	2044.3	1488.6
2062	1151.6	666.3	2092	2318.8	1720.4
2063	1388.6	835.6	2093	2802	3173.1
2064	952.3	935.3	2094	985.5	3169.8
2065	1164.4	677.6	2095	2316.6	3001.3
2066	1631.1	1347.1	2096	2912	2768.6
2067	1192.5	885	2097	1473.8	1843.4
2068	1142.6	855.8			
2069	1737.1	1164.6			
2070	1756	1005.4			

Mid-term RACMO22T Simulated streamflow			Long term RACMO22T Simulated streamflow		
Year	RCP4.5	RCP8.5	Year	RCP4.5	RCP8.5
2041	3162.5	2711.8	2071	2090.1	2009.2
2042	3446.9	3144.8	2072	3189.7	2868.4
2043	2456.6	1783.4	2073	2420.5	2259.4
2044	2942.1	2569.1	2074	1754.4	1688.7
2045	2850.6	2784.5	2075	2144.2	2028.5
2046	1474.3	1434.9	2076	2952.2	2861.2
2047	3259.2	2663.9	2077	2501.2	2426.5
2048	3254.6	3437.7	2078	2822.1	2551.1
2049	2883.6	2047.1	2079	2312.3	2229
2050	3334.6	3074.7	2080	2241.8	1990.5
2051	2974.5	2917.1	2081	3155.5	3050.6
2052	2621.1	2461.7	2082	2040.6	1972.6
2053	2032.4	2003.4	2083	3323.1	3231.9
2054	2667.9	1885.7	2084	3037.5	2936.4
2055	3135.8	2183.3	2085	2731.5	2638.3
2056	2209.4	2148.8	2086	2847.5	2497.7
2057	2125.9	1976.5	2087	2879.8	2786.8
2058	3465	2550.4	2088	2978.1	2887.7
2059	3277	2810	2089	2377.8	2313.7
2060	2937.1	2862.8	2090	2622.6	2543.6
2061	2483.5	2144	2091	2640.3	2571.2
2062	1752	1224.8	2092	2940.6	2831
2063	2579.8	1866.1	2093	3392.6	3129.5
2064	1967	1924.4	2094	2028.3	1836.1
2065	1793.3	1380.2	2095	3023.5	2673.6
2066	3014.9	2700.6	2096	3345.3	2910.5
2067	2810.7	2006.6	2097	3155.2	3065.6
2068	2619	1897			
2069	3213.3	2355.3			
2070	1840.4	1489.7			

Mid-term RCA4 simulated Streamflow			Long term RCA4 simulated streamflow		
Year	RCP4.5	RCP8.5	Year	RCP4.5	RCP8.5
2041	2106.2	699.9	2071	1632.2	1402.4
2042	2342.4	1463.7	2072	1686.4	1337
2043	2764.7	1442.9	2073	1680.9	1340.7
2044	3175.3	947.5	2074	1574.8	1437.6
2045	3107.4	1233.2	2075	1576.8	1246.2
2046	1591.4	700.8	2076	1820.4	1727.7
2047	2044.1	826.4	2077	1951.9	1534.4
2048	2571.8	763.4	2078	1607.1	1705.8
2049	3175.2	611.7	2079	1580	1408.3
2050	3132.7	837.4	2080	1646.8	1412.6
2051	2261.6	1109.9	2081	1786.4	1624
2052	1863.4	1234.7	2082	1908.6	1680.9
2053	2425.6	840.7	2083	2069.1	1801.8
2054	2918	965.3	2084	1547	1514.5
2055	1977.3	843.8	2085	1703.2	1576.2
2056	2518.7	732.1	2086	1918.7	1591.3
2057	2386.1	647.9	2087	1518.5	1451.9
2058	1612.7	1412	2088	1895.4	1639.9
2059	2417.1	917.3	2089	1504.8	1574.4
2060	2206	1243.8	2090	1713.7	1606.9
2061	2712.1	1172.5	2091	1715.9	1601.1
2062	1837.2	728.3	2092	1820.3	1479.7
2063	2895.7	1678.5	2093	1735.5	1991.5
2064	2199	729.7	2094	1484.5	1553.9
2065	1904.8	799.9	2095	1946.8	1644.6
2066	2140.5	981.1	2096	1601.8	1698.3
2067	3124.7	763.6	2097	1712.1	1758.8
2068	2933.3	1487.1			
2069	2481.8	842.3			
2070	1557.9	670.5			

Appendix: C Goodness fit test results of Probability distribution for RCMs

	Distribution	CCLM4-8_RCP 8.5_Mid-term Parameters	CCLM4-8_RCP8.5 Long-term Parameters
1	GEV	k=0.13195 σ=262.12 μ=983.85	k=0.20179 σ=871.68 μ=1658.1
2	Gumbel Max	σ=221.2 μ=976.88	σ=692.85 μ=1613.7
3	Log-Pearson 3	α=587.35 β=0.01068 γ=13.25	α=7.8651 β=0.18209 γ=8.9283
4	Lognormal	σ=0.25458 μ=6.9751	σ=0.50113 μ=7.4961
5	Lognormal (3P)	σ=0.24684 μ=7.006 γ=-32.455	σ=0.15896 μ=8.6037 γ=-3507.1

	Distribution	RACMO22T RCP 4.5 Mid Parameters	RACMO22T RCP4.5 Long Parameters
1	GEV	k=0.57906 σ=634.62 μ=2567.1	k=0.46105 σ=508.09 μ=2575.7
2	Gumbel Max	σ=438.4 μ=2433.1	σ=357.91 μ=2495.2
3	Log-Pearson 3	α=5.0591 β=0.10236 γ=8.3897	α=10.673 β=0.05474 γ=8.471
4	Lognormal	σ=0.22636 μ=7.8719	σ=0.17548 μ=7.8868
5	Lognormal (3P)	σ=0.0316 μ=9.779 γ=-14983.0	σ=0.03782 μ=9.3988 γ=-9376.8

	Distribution	RACMO22T RCP 8.5 Mid Parameters	RACMO22T RCP8.5 Long Parameters
1	GEV	k=-0.25732 σ=566.3 μ=2072.1	k=0.47453 σ=476.19 μ=2433.0
2	Gumbel Max	σ=438.15 μ=2028.4	σ=334.69 μ=2354.6
3	Log-Pearson 3	α=18.252 β=-0.06074 γ=8.81	α=10.267 β=0.05539 γ=8.3971
4	Lognormal	σ=0.25515 μ=7.7013	σ=0.17418 μ=7.8283
5	Lognormal (3P)	σ=0.05107 μ=9.2909 γ=-8569.1	σ=0.03454 μ=9.4125 γ=-9693.8

	Distribution	RCA4 RCP 4.5 Mid-term Parameters	RCA4 RCP4.5 Long-term Parameters
1	GEV	k=-0.27833 σ=212.98 μ=1540.4	k=0.06984 σ=137.76 μ=1645.7
2	Gumbel Max	σ=389.37 μ=2188.1	σ=121.72 μ=1646.0
3	Log-Pearson 3	α=37.571 β=-0.03491 γ=9.0786	α=30.98 β=0.0161 γ=6.9451
4	Lognormal	σ=0.21039 μ=7.767	σ=0.08795 μ=7.444
5	Lognormal (3P)	σ=0.04638 μ=9.2677 γ=-8186.7	σ=0.36621 μ=5.9916 γ=1289.1

	Distribution	RCA4 RCP 8.5 Mid-term Parameters	RCA4 RCP8.5 Long-term Parameters
1	GEV	k=0.11627 σ=211.69 μ=828.1	k=0.24232 σ=159.86 μ=1507.6
2	Gumbel Max	σ=231.21 μ=844.14	σ=127.04 μ=1494.9
3	Log-Pearson 3	α=16.114 β=0.07135 γ=5.6943	α=16045.0 β=8.1875 γ=20.49
4	Lognormal	σ=0.28159 μ=6.844	σ=0.10177 μ=7.3525
5	Lognormal (3P)	σ=0.72464 μ=5.8227 γ=546.37	σ=0.09742 μ=7.3963 γ=-69.378